BIOMEDICAL PHOTONICS

BIOMEDICAL PHOTONICS –
research and practice, peer-reviewed, multidisciplinary journal.
The journal is issued 4 times per year.
The circulation – 1000 copies., on a quarterly basis.

The journal is included into the List of peer-reviewed science press of the State Commission for Academic Degrees and Titles of Russian Federation
The journal is indexed in the international abstract and citation database – Scopus.

The publisher «Agentstvo MORE».
Moscow, Khokhlovskiy lane., 9

Editorial staff:
Chief of the editorial staff Ivanova-Radkevich V.I.
Science editor professor Mamontov A.S.
Literary editor Moiseeva R.N.
Translators Urlova A.N.
Romanishkin I.D.
Computer design Kreneva E.I.
Desktop publishing Merkulova O.E.

The Address of Editorial Office:
Russia, Moscow, 2nd Botkinskiy proezd, 3
Tel. 8 (495) 945–86–60
www: PDT-journal.com
E-mail: PDT-journal@mail.ru

Corresponding to:
125284, Moscow, p/o box 13

Registration certificate ПИ № ФС 77–51995, issued on 29.11.2012 by the Federal Service for Supervision of Communications, Information Technology, and Mass Media of Russia

The subscription index of «Rospechat» agency – 70249

BIOMEDICAL PHOTONICS

BIOMEDICAL PHOTONICS –
научно-практический, рецензируемый, мультидисциплинарный журнал.
Выходит 4 раза в год.
Тираж – 1000 экз., ежеквартально.

Входит в Перечень ведущих рецензируемых научных журналов ВАК РФ.
Индексируется в международной реферативной базе данных Scopus.

Издательство «Агентство МОРЕ».
Москва, Хохловский пер., д. 9

Редакция:

Зав. редакцией	Иванова-Радкевич В.И.
Научный редактор	проф. Мамонтов А.С.
Литературный редактор	Моисеева Р.Н.
Переводчики	Урлова А.Н.
	Романишкин И.Д.
Компьютерный дизайн	Кренева Е.И.
Компьютерная верстка	Меркулова О.Е.

Адрес редакции:
Россия, Москва, 2-й Боткинский пр., д. 3
Тел. 8 (495) 945–86–60
www: PDT-journal.com
E-mail: PDT-journal@mail.ru

Адрес для корреспонденции:
125284, Москва, а/я 13

Свидетельство о регистрации ПИ № ФС 77–51995, выдано 29.11.2012 г. Федеральной службой по надзору в сфере связи, информационных технологий и массовых коммуникаций (Роскомнадзор)

Индекс по каталогу агентства «Роспечать» – 70249

ORIGINAL ARTICLES

REVIEWS OF LITERATURE

CASE REPORTS

ОРИГИНАЛЬНЫЕ СТАТЬИ

ОБЗОРЫ ЛИТЕРАТУРЫ

КЛИНИЧЕСКИЕ НАБЛЮДЕНИЯ

ORIGINAL ARTICLES

CLINICAL IMPLEMENTATION AND SCIENTIFIC DEVELOPMENT OF PHOTODYNAMIC THERAPY IN RUSSIA IN 2010-2020

Filonenko E.V.
P.A. Herzen Moscow Oncology Research Center – branch of FSBI NMRRC of the Ministry of Health of the Russian Federation, Moscow, Russia

Abstract

In recent years, the development of methods of photodynamic therapy (PDT) and fluorescence diagnostic (FD) in Russia is characterized by an intensive rise, steadily growing interest of specialists from various medical specialties in the method of specialists from various medical specialties, an increase in the level of equipment number of hospitals with the necessary equipment for performing FD and PDT, the and the emergence of new photosensitizers on the pharmaceutical market, and an increasing increase in the level of patients' confidence in these methods. This study analyzes the dynamics of the development of the clinical application and scientific developments of FD and PDT over the past decade in Russia in terms of the volume of public procurement of photosensitizers, as well as the activity of research work in the field of FD and PDT, the number of candidate and doctoral dissertations theses on this topic and the number of scientific publications in the RSCI. 688 contracts for the supply of photosensitizers for clinical use were analyzed. The analysis showed a stable annual growth in the volume of public procurement of photosensitizers, an increase in the number of subjects of the Russian Federation and clinical centers that purchase photosensitizers through the portal www.zakupki.gov.ru. From 2014 to 2020, the total volume of public procurement of all photosensitizers increased by 8 times (from 36.42 million rubles (3.58 thousand packages) to 307.37 million rubles (18.99 thousand packages)). The annual increase in the volume of public procurement in numerical terms over the previous 6 years ranged from 9.4% to 63.2% in different years. The main share of state purchases of photosensitizers falls on Moscow and St. Petersburg, h. However, in recent years there has been a noticeable trend towards an increase in sales of photosensitizers in the regions. Thus, in recent years, the share of purchases of photosensitizers in the constituent entities of the Russian Federation with a population of less than 1 million people has significantly increased (from 2.9% of the total number of purchases in 2014 to 25.3% in 2020). Also, in recent years, there has been a significant increase in the activity of research work activity in the field of FD and PDT. The number of defended candidate and doctoral dissertations theses defended in the field of FD and PDT photodynamic therapy and fluorescent diagnostics has been steadily high in recent years and, in some scientific specialties, reaches 2-3% of the total number of defended dissertations theses defended in these specialties. The increase in the total number of publications over 10 years according to the RSCI was 224% (from 218 publications in 2014 to 489 publications in 2019), according to the RSCI. The results obtained confirm the growing demand for photosensitizers for photodynamic therapy and fluorescence diagnostics in clinical practice, the expansion of the geography of the use of methods, as well and the stable interest in this topic in the research environment.

Keywords: photodynamic therapy, fluorescent diagnostics, public procurement, chlorin e6, aluminum phthalocyanine, 5-aminolevulinic acid, 5-aminolevulinic acid methyl ester.

For citations: Filonenko E.V. Clinical implementation and scientific development of photodynamic therapy in Russia in 2010-2020, *Biomedical Photonics*, 2021, vol. 10, no. 4, pp. 4–22. doi: 10.24931/2413–9432–2021–10-4-4-22

Contacts: Filonenko E.V., e-mail: derkul23@yandex.ru

КЛИНИЧЕСКОЕ ВНЕДРЕНИЕ И НАУЧНОЕ РАЗВИТИЕ ФОТОДИНАМИЧЕСКОЙ ТЕРАПИИ В РОССИИ В 2010-2020 ГГ.

Е.В. Филоненко
«Московский научно-исследовательский онкологический институт им. П.А. Герцена – филиал ФГБУ «Национальный медицинский исследовательский центр радиологии» Министерства здравоохранения Российской Федерации, Москва, Россия

Резюме

В последние годы развитие методов фотодинамической терапии (ФДТ) и флуоресцентной диагностики (ФД) в России характеризуется интенсивным подъемом, стабильно растущим интересом к методу специалистов различных медицинских специальностей, повышением уровня оснащенности больниц необходимым оборудованием для проведения ФД и ФДТ, появлением на фармацевтическом

рынке новых фотосенсибилизаторов, повышением уровня доверия пациентов к указанным методам. В настоящем исследовании проанализирована динамика развития клинического применения и научных разработок ФД и ФДТ в последнее десятилетие в России по объемам госзакупок фотосенсибилизаторов, а также по активности научно-исследовательской работы в области ФД и ФДТ по числу кандидатских и докторских диссертаций по данной тематике и по числу научных публикаций в РИНЦ. Проанализированы 688 договоров на поставку фотосенсибилизаторов для клинического применения. Анализ показал стабильный ежегодный рост объема госзакупок фотосенсибилизаторов, увеличение числа субъектов РФ и клинических центров, осуществляющих закупку фотосенсибилизаторов через портал www.zakupki.gov.ru. С 2014 по 2020 гг. общий объем госзакупок всех фотосенсибилизаторов увеличился в 8 раз (с 36,42 млн. руб. (3,58 тыс. упаковок) до 307,37 млн. руб. (18,99 тыс. упаковок)). Ежегодный прирост объема госзакупок в численном выражении за предыдущие 6 лет составил от 9,4% до 63,2% в разные годы. Основная доля госзакупок фотосенсибилизаторов приходится на Москву и Санкт-Петербург, однако в последние годы заметна тенденция увеличения объемов продаж фотосенсибилизаторов в регионах. Так, за последние годы значительно выросла доля закупок фотосенсибилизаторов в субъектах РФ с населением менее 1 млн человек (с 2,9% от общего числа закупок в 2014 г. до 25,3% в 2020 г.). Также в последние годы наблюдается значительный рост активности научно-исследовательской работы в области ФД и ФДТ. Число кандидатских и докторских диссертаций, защищенных по тематике фотодинамической терапии и флуоресцентной диагностики, в последние годы стабильно велико и, по некоторым научным специальностям, достигает 2-3% от общего числа диссертаций, защищенных по данным специальностям. Прирост общего числа публикаций за 10 лет по данным РИНЦ составил 224% (с 218 публикаций в 2014 г. до 489 публикаций в 2019 г.). Полученные результаты подтверждают растущий спрос на фотосенсибилизаторы для фотодинамической терапии и флуоресцентной диагностики в клинической практике, расширение географии использования методов, а также стабильный интерес к данной тематике в научно-исследовательской среде.

Ключевые слова: фотодинамическая терапия, флуоресцентная диагностика, государственные закупки, хлорин е6, фталоцианин алюминия, 5-аминолевулиновая кислота, метиловый эфир 5-аминолевулиновой кислоты

Для цитирования: Филоненко Е.В. Клиническое внедрение и научное развитие фотодинамической терапии в России в 2010-2020 гг. // Biomedical Photonics. – 2021. – Т. 10, № 4. – С. 4–22. doi: 10.24931/2413-9432-2021-10-4-4-22

Контакты: Филоненко Е.В., e-mail: derkul23@yandex.ru

The history of the use of photodynamic therapy (PDT) and fluorescence diagnostic (FD) in clinical practice has more than 100 years in the world and about 30 years in Russia [1,2,3,4]. The advantages of the PDT method are the focus of the impact on tumor foci and high efficiency in the absence of systemic toxicity. The method is successfully used in clinical oncology. In many oncological diseases, PDT makes it possible to achieve results that are not available with other methods of antitumor therapy. Thus, the method is effective even in a number of metastatic forms of malignant neoplasms, in cases where other methods are no longer applicable. Moreover, PDT makes it possible to avoid the appearance of rough cicatricial tissues in the treatment of precancer and early cancer, which is very important, for example, in gynecology during the treatment of patients of childbearing age; to achieve a good cosmetic effect, to minimally injure healthy tissues surrounding the tumor in the treatment of tumors on the face, etc. Conducting PDT of the surgical area after surgical removal of a tumor (localized, for example, in the bladder, brain, etc.) makes it possible to significantly reduce the risk of recurrence [5,6,7,8,9]. On the other hand, FD is successfully used for the purpose of early diagnosis of the disease, as well as to clarify the boundaries of an already detected neoplasm and identify additional foci during surgical treatment in order to more radically remove the tumor and reduce the likelihood of recurrences. The combination of FD and PDT is a recognized method of oncological theranostics [10,11,12,13,14,15].

As international experience shows, in addition to oncology, FD and PDT are widely used in various fields of medicine: in the treatment of infectious diseases, in dermatology, neurosurgery, ophthalmology, dentistry, etc.

In Russia, the beginning of the clinical application of FD and PDT methods dates back to 1992, when preclinical studies of the first domestically-produced photosensitizer photohem were completed. After obtaining permission from the Ministry of Health of Russia, the PDT method was first used in clinical practice in Russia, as part of the Phase I clinical trials of photohem at the Moscow Scientific and Research Oncological Institute named after P.A. Herzen (V.V. Sokolov, E.V. Filonenko) and at the Center for Laser Medicine (E.F. Stranadko) [1]. From 1992 to 2011, there was a stage of preclinical and clinical study of new domestically-produced photosensitizers, development of optimal FD and PDT methods and effective medical technologies based on them. This work was carried out with the active participation of a group of young scientists from the Moscow Scientific and Research Oncological Institute named after P.A. Herzen, who were able to combine the efforts of specialists from many other institutions – synthetic chemists, physicists, biologists, clinicians, and together go from the formation of an idea, through the development of new molecules of photosensitizers and experimental design samples of laser

equipment for FD and PDT, the development of industrial production of domestic drugs and laser equipment, to the widespread introduction of FD and PDT methods into clinical practice in the regions of Russia. This multistage and multi-directional work was evaluated by the award of the Russian Federation Government Prize in the field of science and technology in 2011. Over time, specialists united in the Russian Photodynamic Association (RPA) to develop and promote the method in Russia and popularize Russian experience abroad.

At present, after years of fruitful work of the RPA, FD and PDT methods are included in the oncological standards and clinical recommendations for a number of nosologies (since 2012), as well as to the program of state financing of treatment using these methods under the OMI system (since 2013). The result of the activities of the field-specific professional community of RPA was the creation of conditions, including economic ones, for the wide development of these methods in clinical practice. The key moment that influenced the beginning of the rapid introduction of the method into wide clinical practice in Russia was the inclusion of the methods in the list of therapeutic measures carried out within the framework of state guarantees in 2013. According to IMS Health, in the first half of 2014 the volume of the Russian market of drugs based on photosensitizers amounted to 33 million rubles, having increased by 90% compared to the same period in 2013, i.e. almost twice [16].

In recent years, the development of FD and PDT methods in Russia has been characterized by an intensive rise, a steadily growing interest in the method of specialists from various medical specialties, an increase in the equipping level of hospitals with the necessary equipment for FD and PDT, the emergence of new photosensitizers on the pharmaceutical market, and an increase in the level of patient confidence in these methods. Furthermore, traditionally, FD and PDT are those scientific areas that are in demand for the latest developments by scientists around the world, including Russia. One of the indicators of this is that in our country the number of dissertations defended in the field of FD and PDT is growing every year. Concurrently, the number of scientific studies in this area is also increasing. The growth of interest in FD and PDT in the regions has been especially evident in the last few years.

The aim of this study was to analyze the dynamics of the development of the clinical application and scientific developments of FD and PDT in the last decade in Russia. These indicators were assessed: by the volume of contracts (according to the website www.zakupki.gov.ru) in the framework of public procurement of photosensitizers in the constituent entities of the Russian Federation, for specific drugs and medical institutions in which this method is introduced into clinical practice; as well as by the activity of research work in the FD and PDT field, estimated by the number of candidate and doctoral dissertations on this topic and by the number of scientific publications in the RSCI.

Materials and methods

The activity of research work in the field of FD and PDT was assessed by the number of defended dissertations for the degree of candidate and doctor of science on the specified topic over the past 9 years (2012-2020). The dynamics of the number of defended dissertations over the years and the share of target dissertations from the total number of defended dissertations in individual specialties were assessed. The source of information about the defense of candidate's and doctoral dissertations was the official website of the State Commission for Academic Degrees and Titles under the Ministry of Science and Higher Education of the Russian Federation www.vak.minobrnauki.gov.ru. The sample of analyzed dissertations was limited to the period for which dissertations are presented in the State Commission for Academic Degrees and Titles archive on the website www.vak.minobrnauki.gov.ru – from 2012, there is no information on the website prior to this period.

The number of scientific publications in the RSCI database (www.elibrary.ru) for 2010-2019 was also analyzed. The dynamics of changes in the number of full-text scientific articles, abstracts of scientific reports and patents on the subject of FD and PDT by years was assessed. The analysis did not include publications of 2020 due to the fact that many periodicals post materials in the RSCI with a significant delay.

The breadth of clinical use of the methods in Russia was assessed by analyzing data on the volume of contracts in the framework of public procurement of photosensitizers intended for FD and PDT in clinical centers, implemented using the www.zakupki.gov.ru portal. Purchase volumes were analyzed in monetary and numerical terms (number of purchased packages of photosensitizers) and by the number of clinical institutions purchasing photosensitizers for PDT. For the analysis, we used data for 2014-2020 (prior to 2014 information on this issue is not available).

Results

Development of scientific research in the field of FD and PDT over the past decade

Analysis of the development of FD/PDT as a separate scientific area was carried out according to the number of defenses of candidate's and doctoral dissertations, data on which are published on the official website of the State Commission for Academic Degrees and Titles (vak.minobrnauki.gov.ru). The number of scientific publications in the RSCI database (www.elibrary.ru) was also analyzed. The dynamics of changes in the number of full-text scientific articles, abstracts of scientific reports

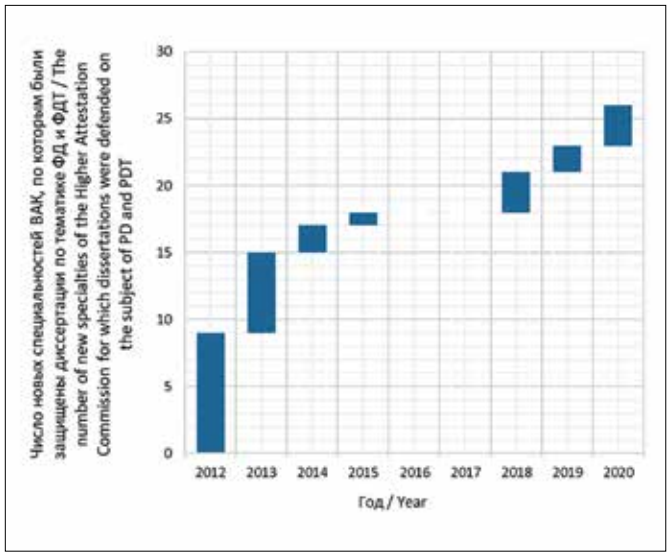

Рис. 1. Ежегодный прирост числа специальностей ВАК, по которым были защищены диссертации по тематике ФД и ФДТ и данные о которых были опубликованы на официальном сайте ВАК (vak.minobrnauki.gov.ru) в 2012-2020 гг.
Fig. 1. The annual increase in the number of specialties of the Higher Attestation Commission, for which theses on FD and PDT were defended and data on which were published on the official website of the Higher Attestation Commission (vak.minobrnauki.gov.ru) in 2012-2020.

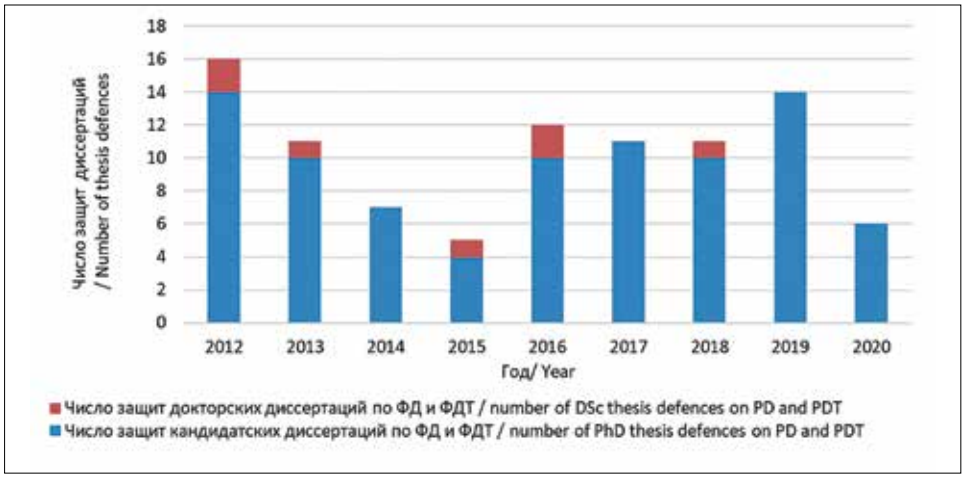

a

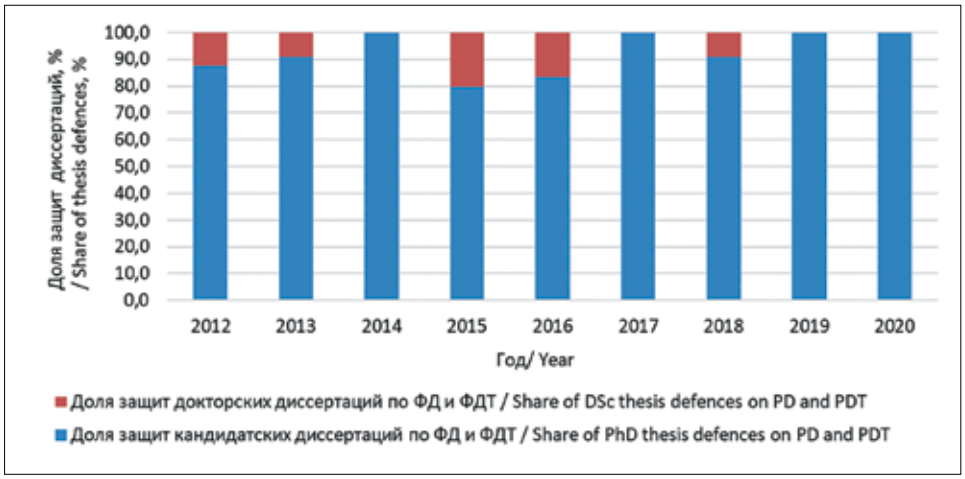

b

Рис. 2. Распределение защит кандидатских и докторских диссертаций по ФД и ФДТ по годам: a – в абсолютных числах; b – в процентном соотношении.
Fig. 2. Distribution of defenses of candidate and doctoral theses in FD and PDT by years: a – absolute values; b – relative values.

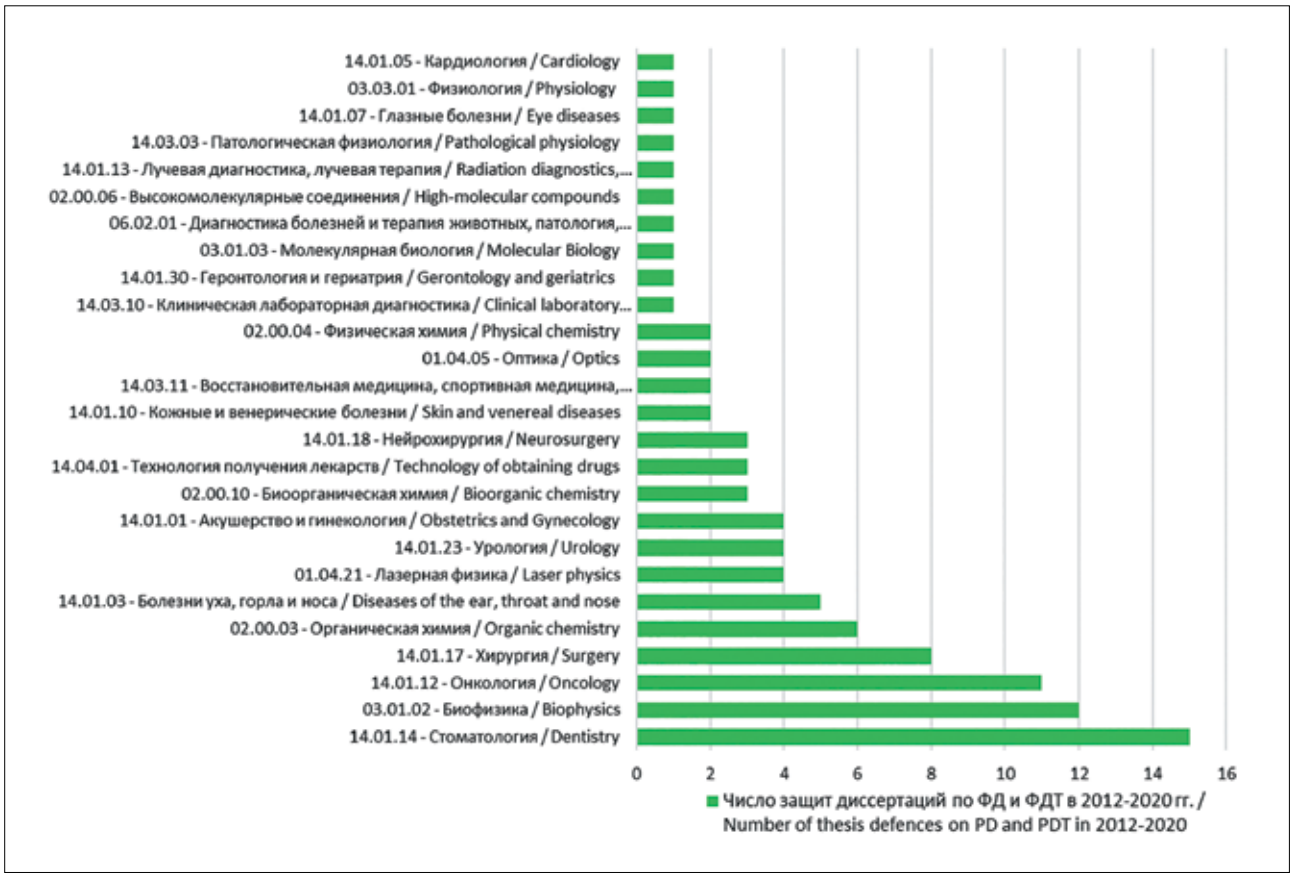

Рис. 3. Распределение диссертаций по ФД и ФДТ, защищенных в 2012-2020 гг., по специальностям.
Fig. 3. Distribution of theses on FD and PDT, defended in 2012-2020, by specialties.

and patents on the subject of FD and PDT by years was assessed.

The total number of candidate's and doctoral dissertations defended in 2012-2020 on the subject of FD and PDT, amounted to 93 dissertations in 26 scientific specialties out of 430 specialties represented in the State Commission for Academic Degrees and Titles. Of these, doctoral dissertations – 7, candidate's – 86. These figures do not exactly correspond to the real number of defenses on these topics, since the analysis only took into account those works in the title of which there was an indication of PD, PDT, as well as chemical and commercial names of photosensitizers. The real number of defenses on these topics is more than the figures given, since not all works have research and/or application of these methods in the title. Examples include the following works: Murshudova S. "Peculiarities of the clinical course and diagnosis of precancer and early vulvar cancer" (2013) – the paper presents a methodology and evaluates the results of fluorescent diagnostics in precancer and vulvar cancer. It is not possible to accurately estimate the number of works that were not included in this analysis for this reason, however, according to experts, they amount to about 25-30%.

The annual growth since 2012 of new scientific specialties in which candidate's and doctoral dissertations on the subject of FD and PDT were defended is shown in Fig. 1.

In 2012, the number of such specialties was 9 (14.01.12 Oncology, 14.01.14 Dentistry, 14.01.03 Diseases of the ear, nose and throat, 06.02.01 Diagnosis of diseases and therapy of animals, pathology, oncology and morphology of animals, 14.01.17 Surgery, 14.01.07 Eye diseases, 14.03.10 – Clinical laboratory diagnostics, 14.01.23 Urology, 14.01.01 Obstetrics and gynecology). By 2020, the number of specialties in which defenses were held on the topics of FD and PDT increased by 17 and the total number of specialties amounted to 26.

The distribution of the number of defenses of dissertations on FD and PDT by years is shown in Fig. 2.

As can be seen from Fig. 2a, in total, from 2012 to 2020 86 dissertations were defended for the degree of the candidate of medical sciences and 7 – the doctor of medical sciences. In those years when both candidate and doctoral dissertations were defended, the proportion of defending doctoral dissertations ranged from 9% to 20% (Fig. 2b). Despite the changes in the number of defenses of candidate's and doctoral dissertations for

Рис. 4. Распределение доли диссертаций по ФД и ФДТ от общего числа диссертаций, защищенных по данным специальностям в 2012-2020 гг.
Fig. 4. Distribution of the share of theses in FD and PDT from the total number of theses defended in the specialties in 2012-2020.

individual years, on average the number of defenses remains approximately at the same level with a tendency to some increase in recent years. So, over the past 3 years (2018-2020), the total number of defenses was 31 (30 candidate's and 1 doctoral), which is slightly more than in the previous similar period (2015-2017): 28 dissertations (25 candidate's and 3 doctoral), and close in terms of values to the previous three-year period (2012-2014): 34 dissertations (31 candidate's and 3 doctoral). The share of candidate's dissertations defended over the past 3 years has grown and in 2018-2020 averaged 96.8% compared to 91.2% and 89.3% in 2012-2014 and 2015-2017.

This fact indicates that research in this area does not stop and is relevant both in fundamental and applied areas. In different years of the analyzed period, the total number of dissertations defenses for the degree of a candidate and a doctor of medical sciences varied from 5 to 16 per year.

Fig. 3 shows the distribution of the number of dissertations on FD and PDT defended in 2012-2020 by individual scientific specialties.

The largest number of dissertations over 9 years was defended in three specialties: 14.01.14 Dentistry (15 dissertations, of which 14 are candidate's and 1 doctoral), 03.01.02 Biophysics (12 theses, of which 11 are candidate's and 1 doctoral) and 14.01.12 Oncology (11 dissertations, including 9 candidate's and 2 doctoral).

Fig. 4 shows the distribution of the share of dissertations in FD and PDT from the total number of dissertations defended in individual specialties for a total of 9 years.

From the data presented in Fig. 4, it can be seen that the largest share in the total number of dissertations defended in a particular specialty over 9 years are dissertations in the specialty 03.01.02 Biophysics – 3.46% of dissertations in this specialty were defended on the topics of FD and PDT. On the second and third places in this indicator are the specialties 02.00.10 Bioorganic Chemistry and 14.04.01 Formulation – 2.14% and 1.82%, respectively.

The number of publications on the subject of FD and PDT in the RSCI was analyzed. The analysis includes data on the number of scientific articles, abstracts of scientific conferences and patents for 2010-2019. The analysis did not include publications of 2020 due to the fact that many periodicals post materials in the RSCI with a significant delay.

Fig. 5 presents data on the annual increase in the number of journals in which articles and abstracts on the subject of FD/PDT were published according to the RSCI data.

As can be seen from the data presented in Fig. 5, in 2010, 94 journals published scientific materials on the subject of FD and PDT, in 2011, scientific materials on

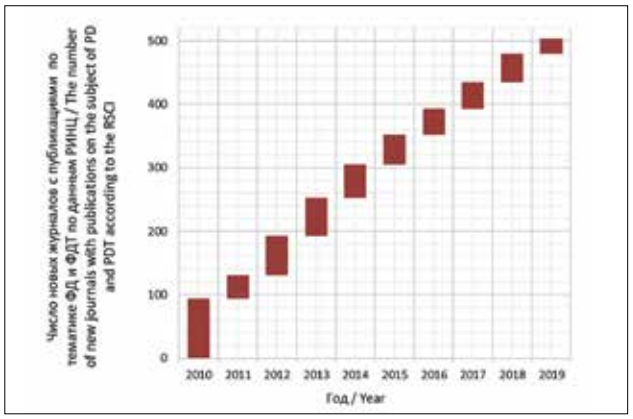

Рис. 5. Ежегодный прирост числа журналов, в которых были опубликованы научные материалы по тематике ФД и ФДТ по данным РИНЦ в 2010-2019 гг.
Fig. 5. An annual increase in the number of journals in which scientific materials on FD and PDT were published according to the RSCI data in 2010-2019.

the subject of FD and PDT were first published in 36 new journals, in 2012 – in 62, in 2013 – in 60, in 2014 – in 53, in 2015 – in 47, in 2016 in – in 41, in 2017 – in 42, in 2018 in 45 and in 2019 in 23 new magazines. The total number of journals in which, according to the RSCI data, scientific materials on the subject of FD and PDT were published during this period was 503.

In the period under review, the number of scientific publications on the subject of FD and PDT is steadily increasing. The total number of publications over 10 years increased by 2.6 times (218 publications in 2014, 565 publications in 2019), including the doubled number of scientific articles (152 articles in 2014, 306 articles in 2019 years), the number of conference abstracts – increased by 8 times (23 abstracts in 2014, 183 abstracts in 2019), the number of patents – by 1.8 times (43 patents in 2014, 76 patents in 2019). The dynamics of

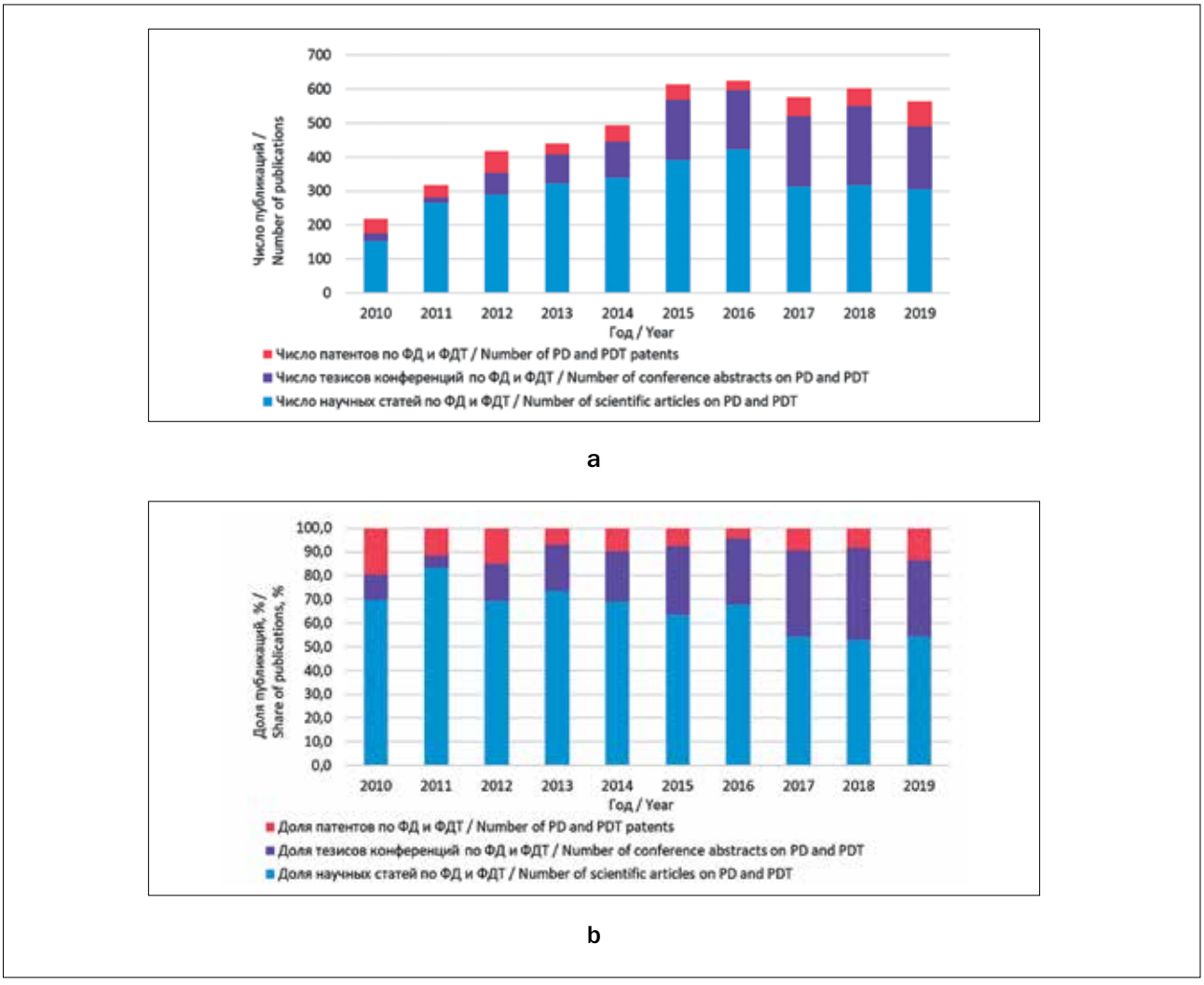

Рис. 6. Динамика числа публикаций в РИНЦ по тематике ФД и ФДТ за период 2010-2019 гг.: a – в абсолютных числах; b – в процентном соотношении.
Fig. 6. Dynamics of the number of publications in the RSCI on the subject of FD and PDT for the period of 2010-2019: a – absolute values; b – relative values.

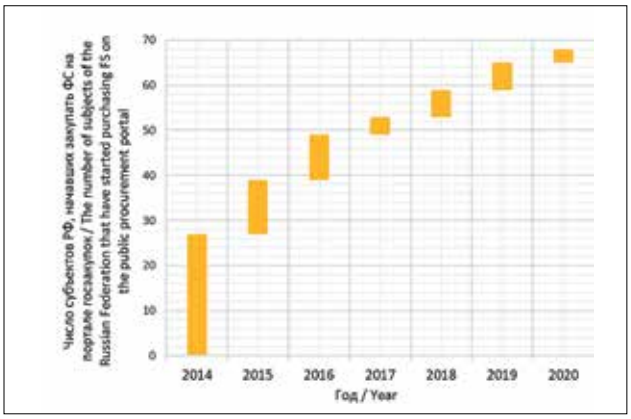

Рис. 7. Ежегодный прирост числа субъектов РФ, заключивших контракты на поставку фотосенсибилизаторов по данным сайта www.zakupki.gov.ru в 2014-2020 гг.
Fig. 7. An annual increase in the number of RF constituent entities that have entered into a contract for the supply of photosensitizers, according to the website www.zakupki.gov.ru in 2014-2020.

the number of publications for the analyzed period is shown in Fig. 6.

As shown by Fig. 6, in addition to an increase in the number of publications on the subject of FD and PDT, there is also a redistribution by the nature of publications. There is a trend towards an increase in the number of conference abstracts, which in 2012 accounted for 10.6% of the total number of publications, and in 2019 – 32.4%. This trend is associated with the active holding of schools, conferences and congresses, in particular, the RPA holds annually: "Winter School on FD and PDT" since 2013 and "International Congress on FD and PDT" since 2012. The Congress in 2012 was attended by 120 specialists from 32 organizations; after 5 years (in 2017), the number of participants increased by 5 times and amounted to more than 600 people from 53 organizations; by 2021, the number of participants exceeded 750 people from 85 organizations.

Introduction of FD and PDT methods into clinical oncological practice in the Russian Federation

An analysis of the dynamics of the introduction of FD and PDT methods into clinical oncological practice in Russia in recent years was carried out on the basis of the data on government purchases of photosensitizers published on the www.zakupki.gov.ru portal. It should be understood that, due to the fact that this resource reflects information only on purchases to federal medical institutions, the number of volumes of purchased photosensitizers, and, therefore, the number of patients treated in commercial clinics, is not taken into account in this analysis, which makes the data presented in the article not absolute. There may also be an error associated with the theoretical possibility of a situation where an already concluded contract has not been implemented.

Analysis of information on the portal www.zakupki.gov.ru revealed 688 contracts concluded for the purchase of photosensitizers for FD and PDT in clinical institutions in the Russian Federation in 2014-2020 (prior to 2014 information on this issue is not available).

During the analyzed period, the number of new constituent entities of the Russian Federation, in which the methods of FD and PDT were first applied, increased by 3-12 per year (Fig. 7).

In 2014, photosensitizers were purchased through the www.zakupki.gov.ru portal, and, accordingly, the FD and PDT methods were used in 27 constituent entities of the Russian Federation. In 2015, for the first time, purchases were made in 12 additional constituent entities of the Russian Federation, in 2016 – in 10, in 2017 – in 4, in 2018 – in 6, in 2019 – in 6 and in 2020 – in 3 constituent entities of the Russian Federation. Thus, by the end of 2020, the method has been implemented in 68 constituent entities of the Russian Federation. At the same time, in a number of the above constituent entities (13 constituent entities), purchases of photosensitizers through the portal www.zakupki.gov.ru are carried out annually, in others (43) – once every 2-3 years, there are also those where there were so far single purchases (12).

We did not find information on public procurement of photosensitizers in 17 constituent entities of the Russian Federation: the Republics of Adygea, Altai, Buryatia, Dagestan, Ingushetia, Kalmykia, Karelia, Tyva, Khakassia, the Udmurt Republic, Magadan, Oryol, Ryazan, Tambov regions, Nenets, Chukotka, Yamalo-Nenets Autonomous okrugs.

Distribution of total volumes of public procurement of photosensitizers by constituent entities of the Russian Federation in 2014-2020 in monetary and numerical terms is presented in Fig. 8 and 9, respectively.

Figs. 8 and 9 show that Moscow dominates in both indicators. In the analyzed period, 113 contracts for the purchase of photosensitizers for clinical practice were concluded in Moscow, while the volume of public procurement amounted to 176.36 million rubles (10.79 thousand packages). St. Petersburg city takes second place. The volume of public procurement of photosensitizers in the analyzed period in this constituent entity of the Russian Federation is comparable to the indicators of Moscow and amounted to 171.45 million rubles (10.61 thousand packages) within the framework of 107 concluded contracts. Chelyabinsk, Murmansk, Rostov and Sverdlovsk regions follow with a significant margin – 87.80 million rubles (5.82 thousand packages), 77.13 million rubles (4.51 thousand packages), 72.31 million rubles (4.09 thousand packages) and 66.54 million rubles (3.48 thousand packages), respectively. Fig. 8 and 9 also show the distribution of the volume of public procurement of photosensitizers in each constituent entity of the Russian Federation by years. In Moscow, the largest volume

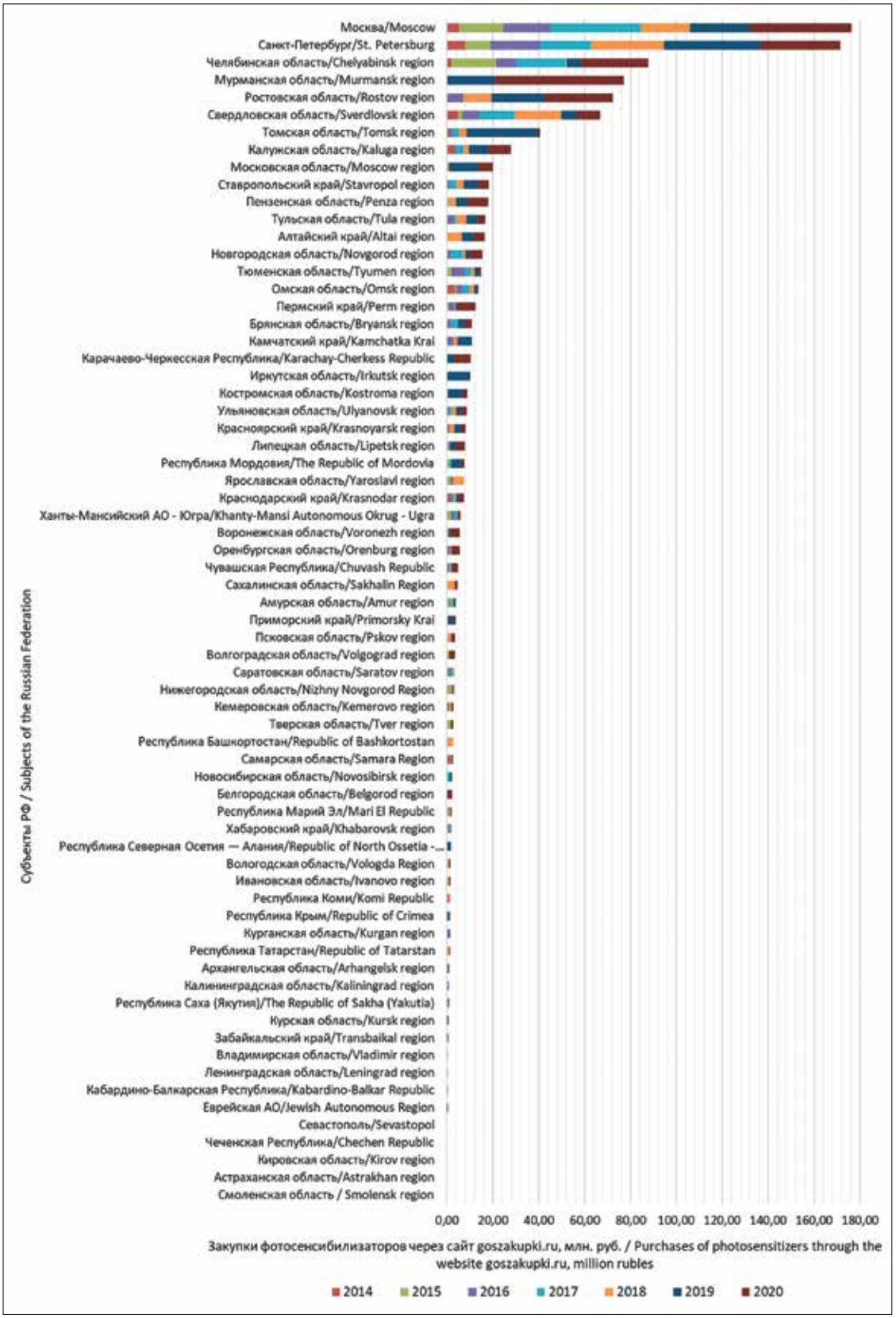

Рис. 8. Распределение ежегодных объемов госзакупок фотосенсибилизаторов по субъектам Российской Федерации в денежном выражении.
Fig. 8. Distribution of annual volumes of state purchases of photosensitizers by constituent entities of the Russian Federation in monetary terms.

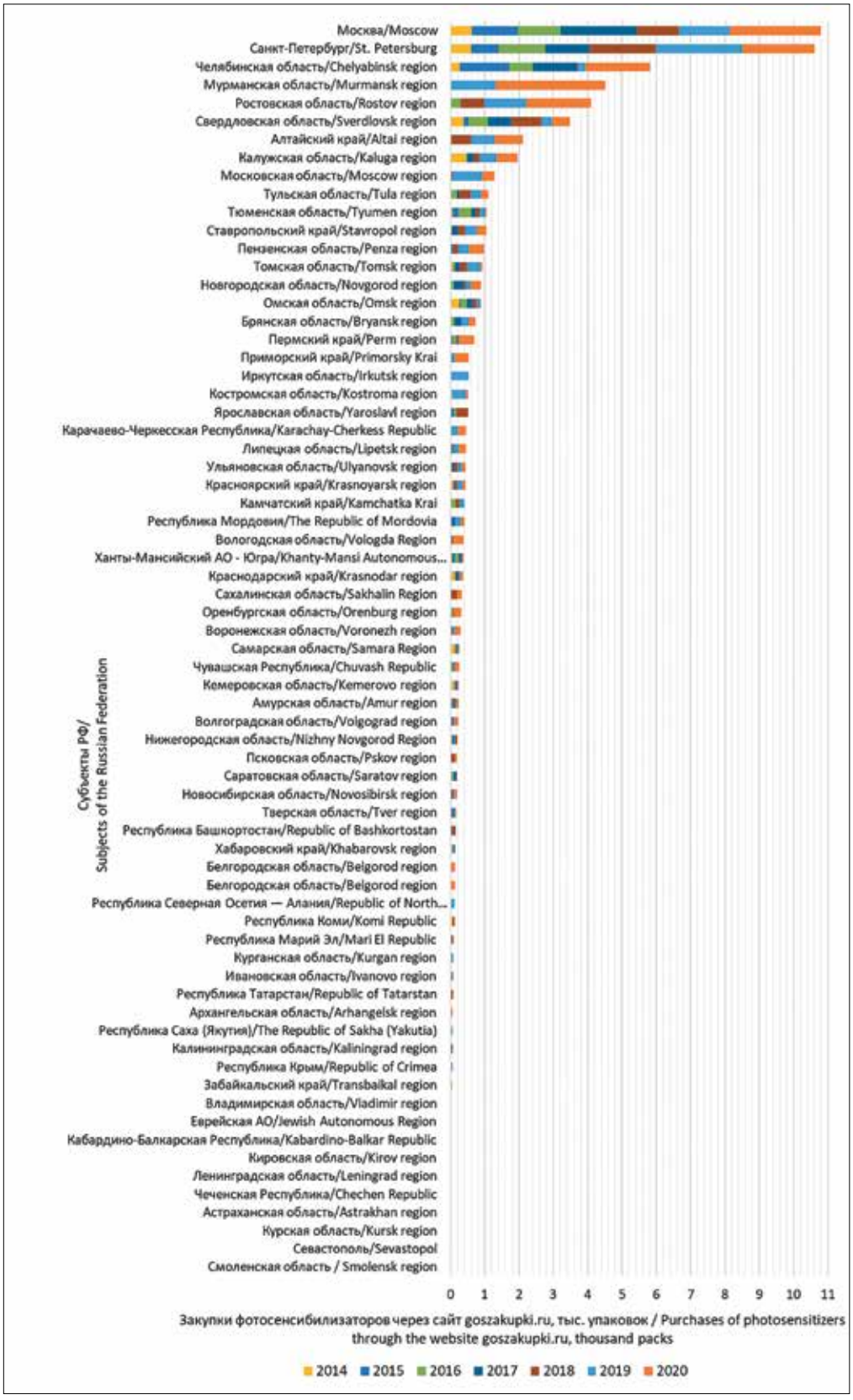

Рис. 9. Распределение ежегодных объемов госзакупок фотосенсибилизаторов по субъектам Российской Федерации в численном выражении.
Fig. 9. Distribution of annual volumes of state purchases of photosensitizers by constituent entities of the Russian Federation in quantitative terms.

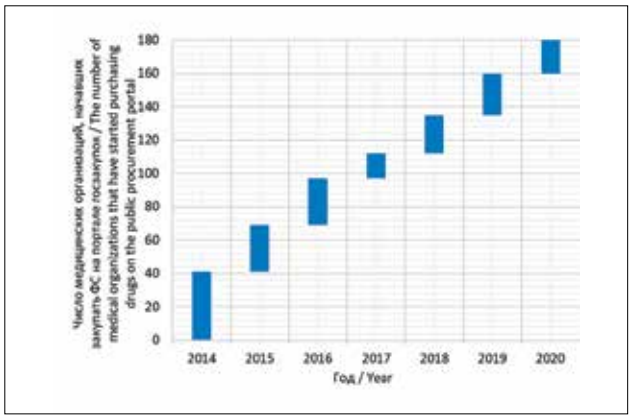

Рис. 10. Ежегодный прирост числа медицинских организаций, заключивших контракты на поставку фотосенсибилизаторов по данным сайта www.zakupki.gov.ru в 2014-2020 гг.
Fig. 10. An annual increase in the number of medical organizations that entered into contracts for the supply of photosensitizers according to the website www.zakupki.gov.ru in 2014-2020.

of procurement was noted in 2020 (44.77 million rubles, 2.63 thousand packages). In St. Petersburg, the largest volume of public procurement of photosensitizers was observed in 2019 (41.93 million rubles, 2.11 thousand packages).

Interestingly, in Murmansk region, information on the availability of public procurement of photosensitizers on the portal www.zakupki.gov.ru appeared only in 2019, while the volume of public procurement in 2019 amounted to 20.93 million rubles, and in 2020 – 56.20 million rubles, which is comparable to the figures for Moscow and St. Petersburg. These data confirm the trends in the development of FD and PDT methods in the regions. Thus, in 2014, the share of public procurement of photosensitizers in Moscow and St. Petersburg was 35.9% of the volume of public procurement of photosensitizers throughout Russia, in 2019 this figure dropped to 26.5%. The share of purchases of photosensitizers in the constituent entities of the Russian Federation with a population of less than 5 million people in 2014 was 60.4% of the total number of purchases of photosensitizers in Russia, and in 2020 it increased by more than 10%, and already amounted to 70.5% of the total number of purchases. Moreover, the share of purchases of photosensitizers in the constituent entities of the Russian Federation with a population of less than 1 million people from 2014 to 2020 increased by 9 times from 2.9% to 25.3% of the total number of purchases.

The number of medical organizations on the basis of which the methods of FD and PDT are introduced is also growing every year. At the same time, during the analyzed period, the number of new medical organizations in which the methods of FD and PDT were first applied, according to the portal www.zakupki.gov.ru, increased annually by 15-28 (Fig. 10).

In 2014, photosensitizers were purchased and, thereof, FD and PDT methods were used in 41 medical organizations; in 2015, for the first time, purchases were made in another 28 new medical organizations, in 2016 – in another 28, in 2017 – in another 15, in 2018 – in another 23, in 2019 – in another 25 and in 2020 – at 21. Thus, in general, during the analyzed period, FD and PDT methods were introduced in 181 oncological medical organizations.

In 2014, out of all constituent entities of the Russian Federation that used FD and PDT methods according to the portal www.zakupki.gov.ru, in 21 (77.8%) the method was used only in one medical organization, in 4 (14.8%) – in two, in 1 (3.7%) – in four and in 1 (3.7%) – in eight.

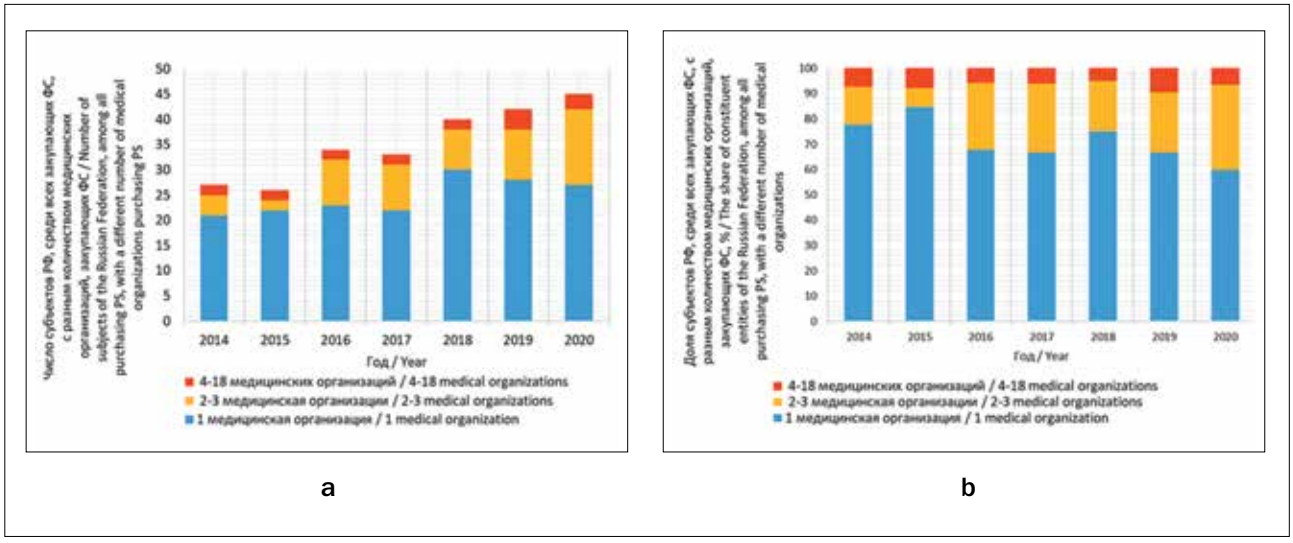

Рис. 11. Динамика числа организаций в отдельных субъектах Российской Федерации, закупавших фотосенсибилизаторы для ФД и ФДТ по данным портала www.zakupki.gov.ru: a – в абсолютных числах; b – в процентном соотношении.
Fig. 11. Dynamics of the number of organizations in individual constituent entities of the Russian Federation that purchased photosensitizers for FD and PDT according to the portal www.zakupki.gov.ru: a – absolute values; b – relative values.

In 2020, out of all constituent entities of the Russian Federation that used FD and PDT methods according to the portal www.zakupki.gov.ru, in 27 (60.0%) the method was used only in one medical organization, in 12 (26.7%) – in two, in 3 (6.7%) – in three, in 1 (2.2%) – in four, in 1 (2.2%) – in seven and in 1 (2.2%) – in thirteen (Fig. 11).

Fig. 11 shows that the number of constituent entities of the Russian Federation, where FD and PDT are used in 4 or more medical organizations, annually remains approximately at the same level (2-4 subjects, 5.0-9.5% of the total number of constituent entities of the Russian Federation using FD and PDT methods in a particular year), while the number of constituent entities in which FD and PDT were used in 4 or more medical organizations over the entire analyzed period was 5: Moscow city, St. Petersburg city, Rostov, Moscow and Tomsk regions.

The number of constituent entities of the Russian Federation, where medicinal products for FD and PDT were purchased from 2-3 medical organizations, is 2-15 (7.7-33.4%) annually, while the number of subjects in which medicinal products for FD and PDT were purchased from 2-3 medical organizations over the entire analyzed period was 23.

The number of constituent entities of the Russian Federation where medicinal products for FD and PDT were purchased from 1 medical organization is 21-30 (60.0-84.6%) annually, while the number of constituent entities in which FD and PDT were used in 1 medical organization for the entire analyzed period was 40.

During the analyzed period, the number of subjects in which FD and PDT are used in 4 or more medical organizations remains approximately the same, and the redistribution occurs due to a decrease in the number of subjects in which PDT is used only in 1 medical organization and an increase in the number of constituent entities in which PDT is used in 2-3 medical organizations. For instance, in 2014 PDT in one medical organization was presented in 21 constituent entities of the Russian Federation (77.8%), in 2-3 organizations – in 4 (14.8%); in 2020 – in 27 (60.0%) and 15 (33.4%), respectively.

The population size in different subjects of the Russian Federation varies greatly, so it was interesting to analyze the results obtained taking into account the population size. Figs. 12 and 13 show the total volume of public procurement of photosensitizers for 7 years in the constituent entities of the Russian Federation, taking into account the population in monetary and numerical terms, respectively.

The largest number of packages of photosensitizers per 100 thousand population was purchased under contracts, information about which is available on the public procurement portal, in Murmansk region – 608.7 packages per 100 thousand population in 2014-2020, which amounted to 10.40 million rubles per 100 thousand population. The second place in terms of the number of packages of photosensitizers per 100 thousand population – St. Petersburg (196.6 packages per 100 thousand population), then Kaluga (194.0 packages per 100 thousand population) and Chelyabinsk regions (167.8 packages per 100 thousand population), in fifth place is Novgorod region (147.5 packages per 100 thousand people).

At the same time, in terms of public procurement of photosensitizers (in monetary terms) per 100 thousand people, the second place after Murmansk region is occupied by Tomsk region (3.75 million rubles per 100 thousand of the population), the third – by Kamchatka Krai (3.44 million rubles per 100 thousand population) and St. Petersburg in fourth place (3.18 million rubles per 100 thousand population). Kaluga, Novgorod and Chelyabinsk regions are in fifth, sixth and seventh places (2.77, 2.57 and 2.30 million rubles per 100 thousand population), respectively.

Moscow ranks eleventh and tenth among the constituent entities of the Russian Federation in terms of public procurement of photosensitizers per 100,000 population in monetary (1.39 million rubles per 100,000 population) and numerical (85.1 packages per 100,000 population) terms, accordingly, yielding, in addition to the listed entities, also Rostov and Sverdlovsk regions and the Karachay-Cherkess Republic.

Figs. 14 and 15 show the distribution of the total volume of public procurement in 2014-2020 for individual photosensitizers in monetary and numerical terms, respectively.

Figs. 16 and 17 present data on the volume of public procurement of individual photosensitizers by years in monetary and numerical terms, respectively.

From the data presented in Figs. 16 and 17, it can be seen that in recent years there has been a steady increase in the volume of public procurement of photosensitizers. In 2014, the total volume of public procurement of all photosensitizers amounted to 36.42 million rubles (3.58 thousand packages), in 2015 – 67.52 million rubles (4.97 thousand packages), in 2016 – 98.18 million rubles (6.12 thousand packages), in 2017 – 134.25 million rubles (7.58 thousand packages), in 2018 – 143.59 million rubles (8.29 thousand packages), in 2019 – 255.46 million rubles (13.65 thousand packages), in 2020 – 307.37 million rubles (18.99 thousand packages).

It can be noted that since 2014, the volume of public procurement of medicinal products photoditazine, radachlorin and alasens has been proportionally increasing. Yearly, throughout the analyzed period, the largest volume of public procurement among photosensitizers falls on radachlorin: 34.1-55.7% in monetary terms and 37.7-49.3% in numerical terms. Thus, it should be noted that since 2014, the share of public procurement of radachlorin has slightly decreased: from 2014 to 2020, by 8.3% in monetary terms (from 55.7% to 47.4%) and by 2.1% in numerical terms (from 49.3% to 47.2%). A sig-

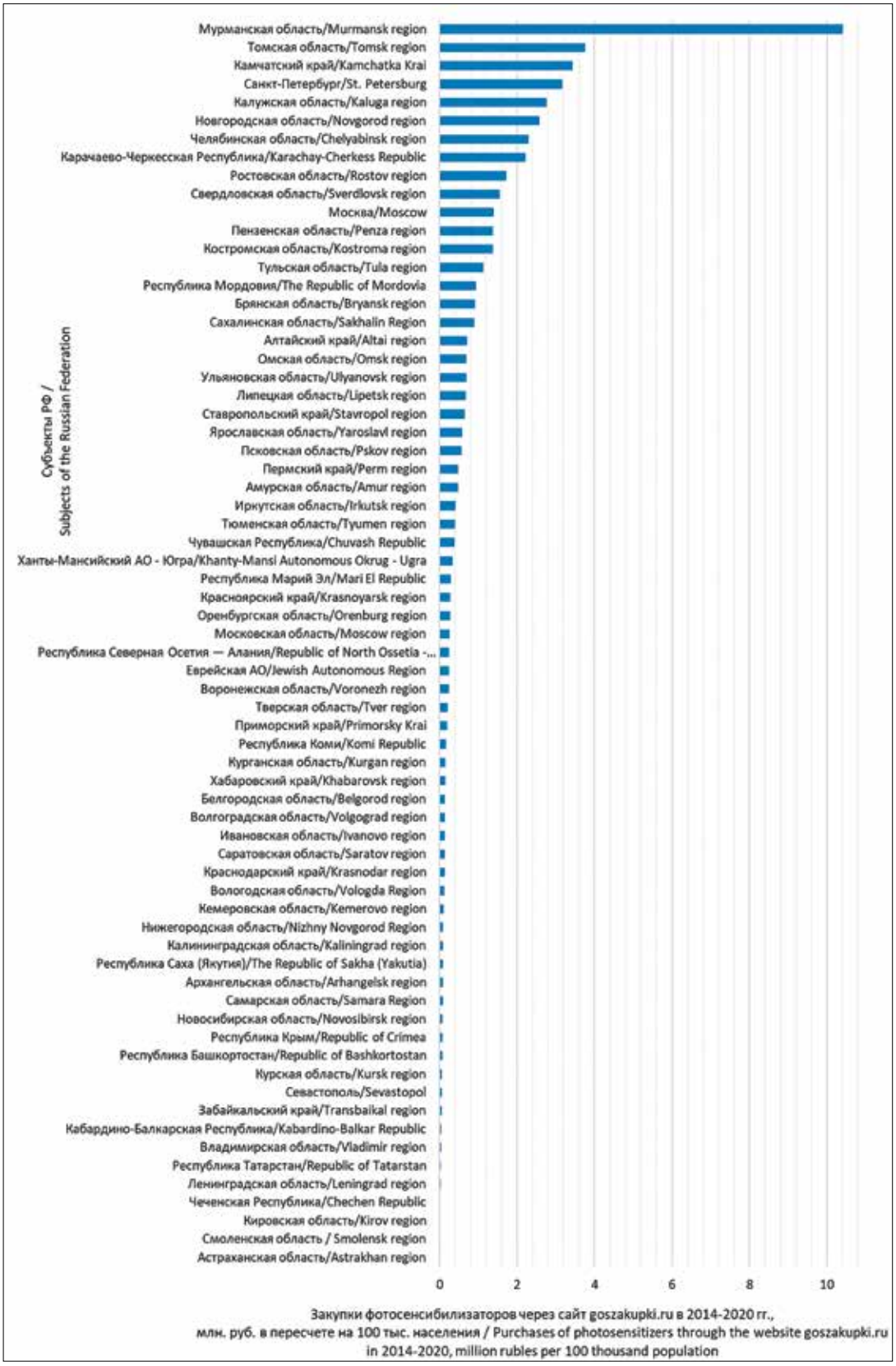

Рис. 12. Распределение объемов госзакупок фотосенсибилизаторов в 2014-2020 гг. в денежном выражении по субъектам Российской Федерации с учетом населения.
Fig. 12. Distribution of volumes of state purchases of photosensitizers in 2014-2020 in monetary terms by the constituent entities of the Russian Federation, taking into account the population.

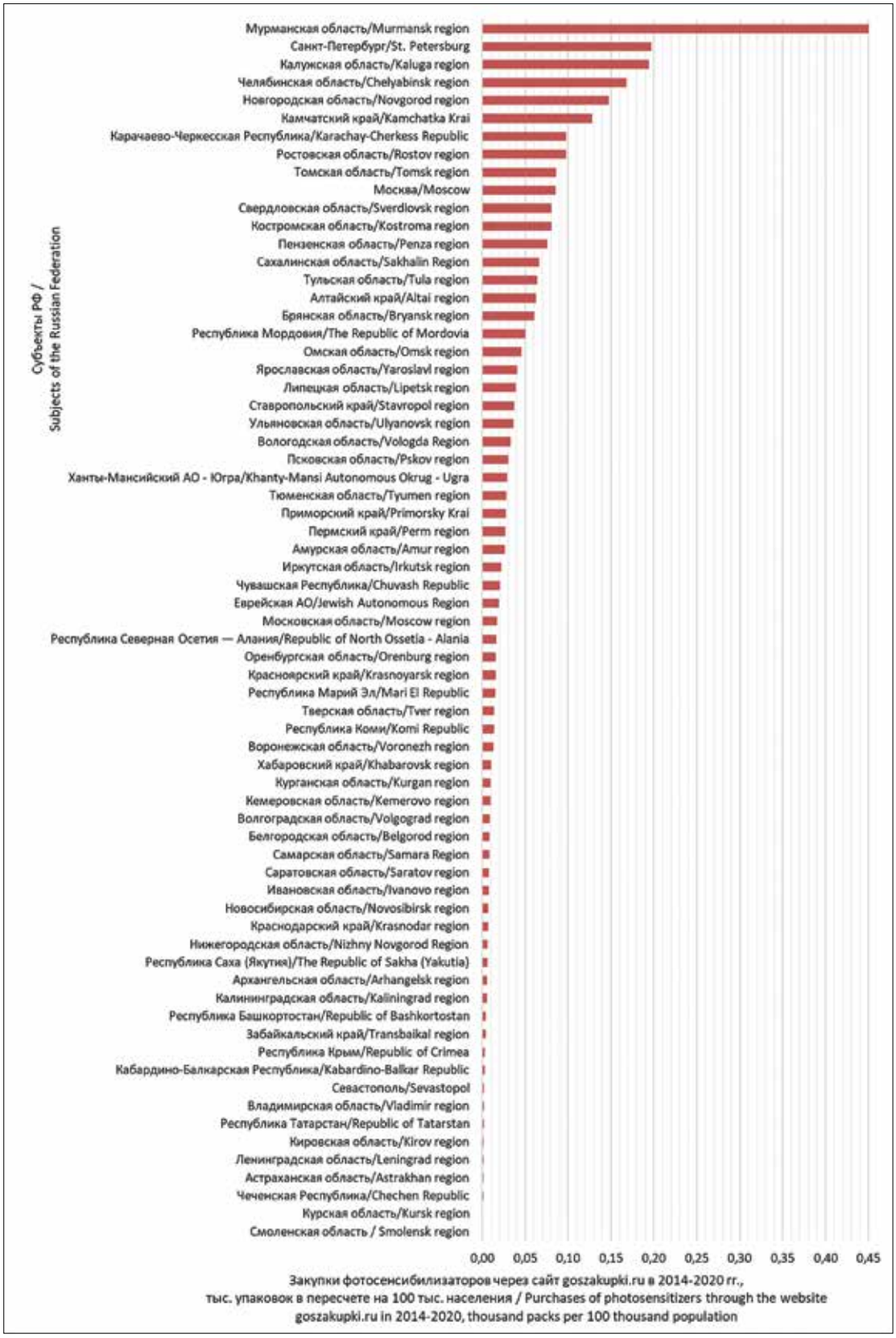

Рис. 13. Распределение объемов госзакупок фотосенсибилизаторов в 2014-2020 гг. в численном выражении по субъектам Российской Федерации с учетом населения.
Fig. 13. Distribution of volumes of state purchases of photosensitizers in 2014-2020 in quantitative terms by the constituent entities of the Russian Federation, taking into account the population.

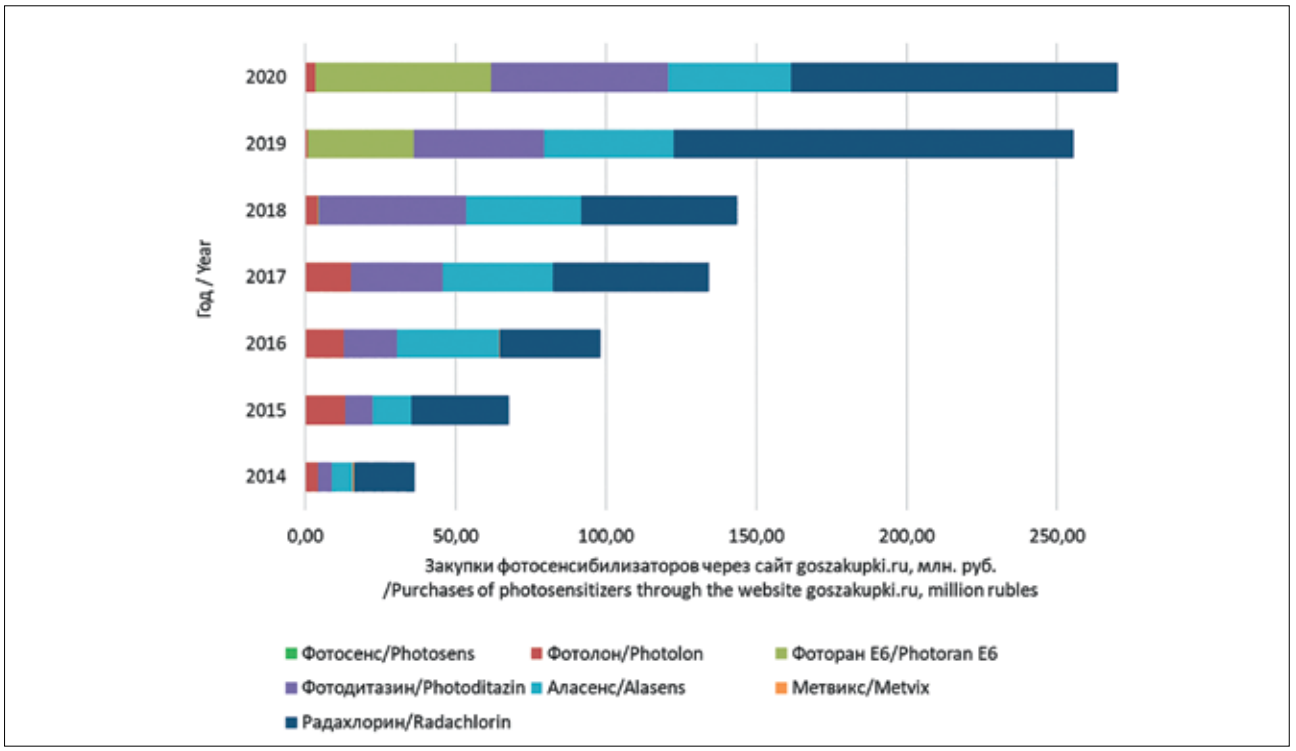

Рис. 14. Распределение ежегодных объемов госзакупок по фотосенсибилизаторам в денежном выражении.
Fig. 14. Distribution of annual volumes of public procurement of photosensitizers in monetary terms.

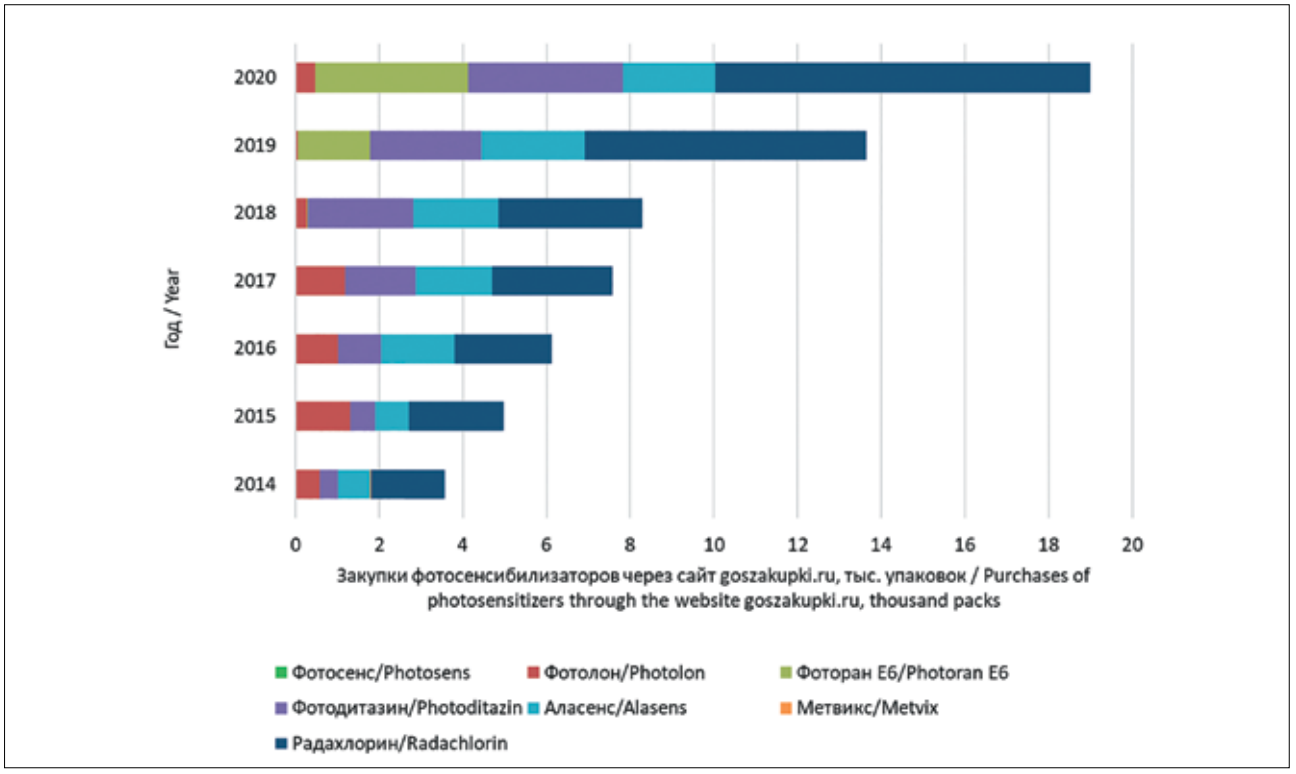

Рис. 15. Распределение ежегодных объемов госзакупок по фотосенсибилизаторам в численном выражении.
Fig. 15. Distribution of annual volumes of public procurement of photosensitizers in quantitative terms.

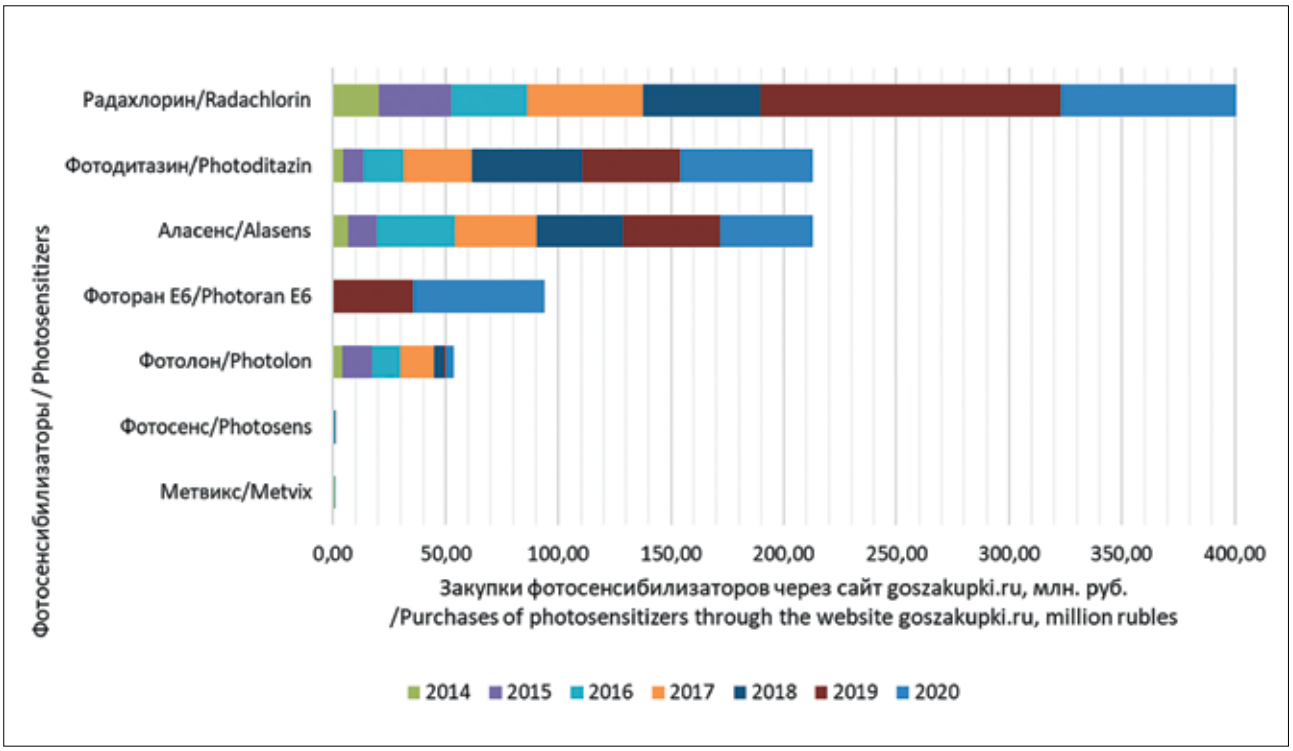

Рис. 16. Распределение госзакупок отдельных фотосенсибилизаторов по годам в денежном выражении.
Fig. 16. Distribution of state purchases of individual photosensitizers by year in monetary terms.

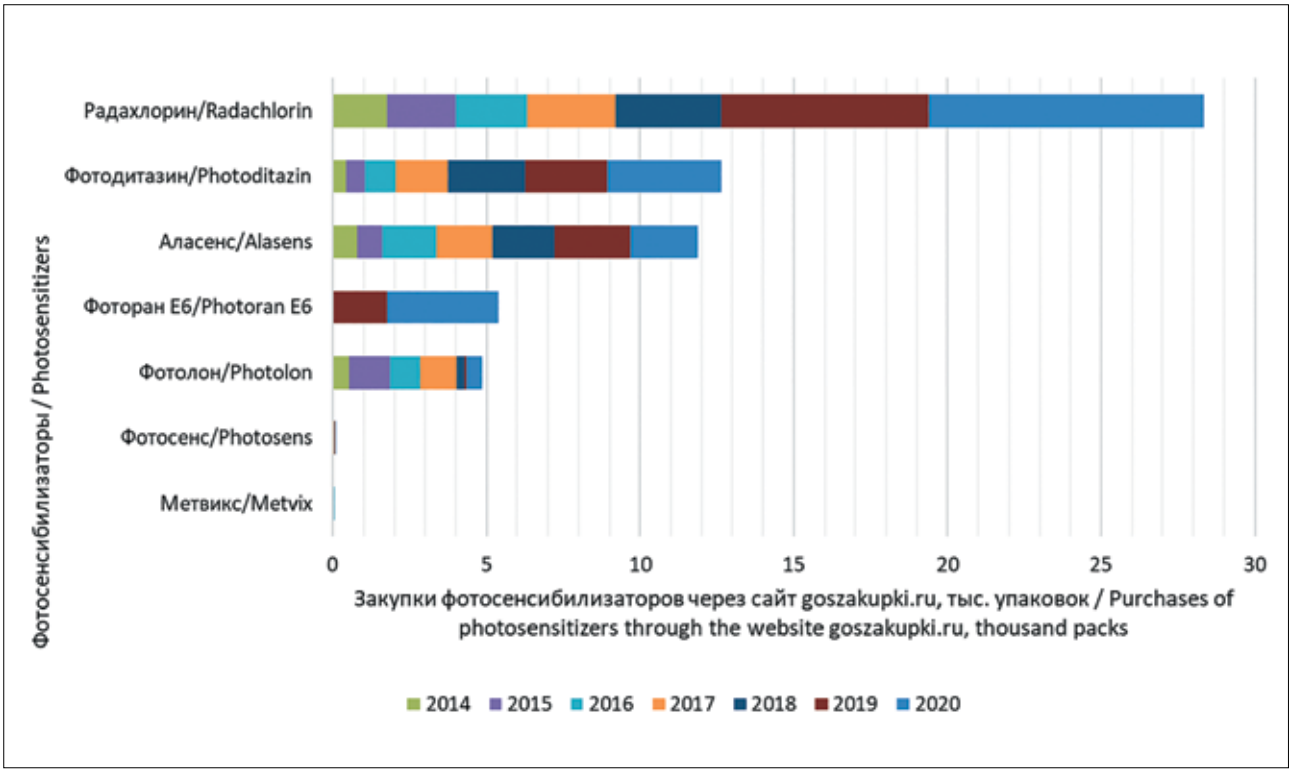

Рис. 17. Распределение госзакупок отдельных фотосенсибилизаторов по годам в численном выражении.
Fig. 17. Distribution of state purchases of individual photosensitizers by year in quantitative terms.

nificant increase in the volume of public procurement over the analyzed years is observed for photoditazine: the volume of public procurement in 2014 amounted to 4.46 million rubles (437 packages), in 2020 – 59.01 million rubles (3719 packages). The same trend is observed for alasens: the volume of public procurement in 2014 amounted to 6.85 million rubles (782 packages), in 2020 – 40.89 million rubles (2196 packages). Over the past three years, the volume of public procurement of photoran E6 has significantly increased: in 2018, the first contracts for the purchase of this medicinal product in the amount of 0.34 million rubles appear on the portal, in 2019, the volume of public procurement doubles and amounts to 35.23 million rubles, and in 2020 – gets to 58.29 million rubles.

From the data presented in Figs. 16 and 17, it can be seen that the total volume of public procurement of radachlorin significantly exceeds the volume of public procurement of other photosensitizers – the share of its procurement over the 7 analyzed years of the total procurement of all photosensitizers is 44.9% in monetary terms and 44.8% in numerical terms. As noted above, there is a trend towards a gradual decrease in the share of radachlorin purchases in the total procurement of photosensitizers: from 55.7% in 2014 to 47.3% in 2020 in monetary terms (from 49.3% in 2014 to 47.2% in 2020 in numerical terms). The shares of the total public procurement of alasens and photoditazine for 7 years are close and amount to 20.39% and 20.42% in monetary terms, and 18.8% and 20.0% in numerical terms, respectively. At the same time, the share of purchases of alasens is gradually falling: from 18.8% in 2014 to 13.3% in 2020 in monetary terms (from 21.9% in 2014 to 11.6% in 2020 in numerical terms). During the same period, the share of purchases of photoditazine almost doubled: from 12.2% in 2014 to 19.2% in 2020 in monetary terms (from 12.2% in 2014 to 19.6% in 2020 in numerical terms). The share of photoran E6 procurement has also grown significantly in recent years: in 2018 (when the first contracts for the supply of this photosensitizer appeared on the website www.zakupki.gov.ru), the share of its procurement was only 0.2% and 0.3% in monetary and numerical terms, respectively. In 2020, this share increased by almost 100 times and already stood at 19.0% and 19.2%, respectively. The total volume of public procurement of photosens and metvix for 2014-2018 (there were no public procurements of these two medical preparations in 2019-2020) is insignificant and amounts to 0.08% and 0.06% in monetary terms and 0.09% and 0.06% in numerical terms, respectively, of the total volume of public procurements of photosensitizers. In recent years, the share of public procurement of photolon has significantly decreased – from 11.2% in 2014 to 1.1% in 2020 in monetary terms (from 15.2% in 2014 to 2.5% in 2020 in numerical terms).

Discussion

Our analysis of information from available information sources in the Russian Federation does not allow us to determine the exact number of medical organizations and scientists who have been dealing with the problems of FD and PDT over the past decade, but it has made it possible to identify trends in the development of both the scientific and clinical components of these methods in Russia.

A systematic increase in both scientific products on this topic and the number of medical institutions and constituent entities of the Russian Federation that have applied the method has been registered.

As a rule, where the method is introduced into clinical practice, it continues to be used, as evidenced by the annual or systematic purchases of photosensitizers in 82.4% of Russian constituent entities that have introduced the method.

The number of patients who underwent FD sessions is growing, as evidenced by the increase in purchases of the drug for diagnostics – alasens. In 2014, 782 packages of alasens were purchased through the public procurement portal www.zakupki.gov.ru. By 2020, this number has increased almost 3 times – up to 2,196 packages.

The number of patients treated by PDT is growing, which is confirmed by the growth in purchases of photosensitizers intended for PDT: photoditazine, radachlorin, photoran E6, photolon. In 2014, the total volume of their purchases through the www.zakupki.gov.ru portal was 2,794 packages, and by 2020 it increased 6 times and amounted to 16,792 packages.

The change in the assortment and ratio of the volumes of purchased photosensitizers registered over the past decade indicates a trend in the introduction of methods into routine clinical practice in the regions of Russia. Thus, the greatest demand is for photosensitizers used mainly for those nosologies that occupy a leading position in the structure of morbidity in our country (drugs based on chlorin e6) and a drug used for diagnosis (alasens). On the contrary, photosensitizers that have a limited number of indications (photosens) or are used in secondary prevention programs (metvix) are becoming less popular or completely leaving the market, which is mainly due to unattractiveness for business.

Conclusion

The results obtained confirmed the growing demand for photosensitizers for photodynamic therapy and fluorescence diagnostics in clinical practice, the expansion of the geography of the photosensitizers use, as well as the stable interest in this topic in the research environment in the Russian Federation over the past decade.

REFERENCES

1. Filonenko E. V. The history of development of fluorescence diagnosis and photodynamic therapy and their capabilities in oncology, *Russian Journal of General Chemistry*, 2015, vol. 85 (1), pp. 211–216. doi: 10.1134/S1070363215010399
2. Sokolov V. V., Chissov V. I., Filonenko E. V. et al. Photodynamic therapy of cancer with the photosensitizer PHOTOGEM, *Proceedings of SPIE – The International Society for Optical Engineering*, 1995, vol. 2325, pp. 367–374. doi: 10.1117/12.199169
3. Sokolov V. V., Chissov V. I., Filonenko E. V. et al. First clinical results with a new drug for PDT, *Proceedings of SPIE – The International Society for Optical Engineering*, 1995, vol. 2325, pp. 364–366. doi: 10.1117/12.199168
4. Sokolov V. V., Chissov V. I., Yakubovskya R. I. et al. Photodynamic therapy (PDT) of malignant tumors by photosensitzer photosens: results of 45 clinical cases. *Proceedings of SPIE – The International Society for Optical Engineering,* 1996, vol. 2625, pp. 281–287.
5. Panova O. S., Dubensky V. V., Dubensky V. V. et al. Photodynamic reparative skin regeneration using application of photosensitizer gel based on chlorin e6, *Biomedical Photonics,* 2021, vol. 10, no. 3, pp. 4–11. (In Russ.) doi.org/10.24931/2413–9432–2021–10–3-4–11
6. Tseymakh A. E., Lazarev A. F., Sekerzhinskaya E. L., Kurtukov V. A., Mishchenko A. N., Teplukhin V. N., Shoikhet Ya. N. Palliative treatment with photodynamic therapy of patients with malignant neoplasms of the pancreatobiliary zone complicated by mechanical jaundice, *Biomedical photonics*, 2020, vol. 9, no. 1, pp. 4–12. doi: 10.24931/2413–9432–2020–9-1–4-12
7. Tzerkovsky D. A., Petrovskaya N. A., Mazurenko A. N. Photodynamic therapy in patients with skin metastases of disseminated melanoma, *Biomedical Photonics*, 2019, vol. 8, no. 1, pp. 24–28. (In Russ.) doi.org/10.24931/2413–9432–2019–8-1–24–28
8. Tumanina A. N., Polezhaev A. A., Filonenko E. V. et al. Experience of using photodynamic therapy in the treatment of esophageal cancer, *Biomedical Photonics*, 2019, vol. 8, no. 2, pp. 19–24. (In Russ.) doi.org/10.24931/2413–9432–2019–8-2–19–24
9. Tzerkovsky D. A., Protopovich Y. L., Kozlovsky D. I., Suslova V. A. Antitumor efficiency of contact radiotherapy in combination with a chlorin-based photosensitizer in experiment, *Biomedical Photonics*, 2021, vol. 10, no. 2, pp. 25–33. (In Russ.) doi.org/10.24931/2413–9432–2021–10–2-25–33
10. Pikin O., Filonenko E., Mironenko D. et al. Fluorescence thoracoscopy in the detection of pleural malignancy, *European Journal of Cardio-thoracic Surgery*, 2012, vol. 41 (3), pp. 649–652. doi: 10.1093/ejcts/ezr086
11. Zharkova N. N., Kozlov D. N., Smirnov V. V. et al. Fluorescence observations of patients in the course of photodynamic therapy of cancer with the photosensitizer PHOTOSENS, *Proceedings of SPIE – The International Society for Optical Engineering*, 1995, vol. 2325, pp. 400–403.
12. Sokolov V. V., Filonenko E. V., Telegina L. V. et al. Combination of fluorescence imaging and local spectrophotometry in fluorescence diagnostics of early cancer of larynx and bronchi, *Quantum Electronics*, 2002, vol. 32, no. 11, pp. 963–969. doi: 10.1070/QE2002v032n11ABEH002329
13. Sokolov V. V., Chissov V. I., Filonenko E. V. et al. Clinical fluorescence diagnostics in the course of photodynamic therapy of cancer with the photosensitizer PHOTOGEM, *Proceedings of SPIE – The International Society for Optical Engineering*, 1995, vol. 2325, pp. 375–380.
14. Rusakov I. G., Teplov A. A., Uljanov R. V., Filonenko E. V. Fluorescence cystoscopy in patients with non-muscle invasive bladder cancer, *Biomedical Photonics*, 2015, vol. 4, no. 3, pp. 29–35. (In Russ.) doi.org/10.24931/2413–9432–2015–4-3–29–35

ЛИТЕРАТУРА

1. Filonenko E. V. The history of development of fluorescence diagnosis and photodynamic therapy and their capabilities in oncology//Russian Journal of General Chemistry. – 2015. – Vol. 85 (1). – P. 211–216. doi: 10.1134/S1070363215010399
2. Sokolov V. V., Chissov V. I., Filonenko E. V., Kozlov D. N., Smirnov V. V. Photodynamic therapy of cancer with the photosensitizer PHOTOGEM//Proceedings of SPIE – The International Society for Optical Engineering. – 1995. – Vol. 2325. – P. 367–374. doi: 10.1117/12.199169
3. Sokolov V. V., Chissov V. I., Filonenko E. V., Kozlov D. N., Smirnov V. V. First clinical results with a new drug for PDT//Proceedings of SPIE – The International Society for Optical Engineering. – 1995. – Vol. 2325. – P. 364–366. doi: 10.1117/12.199168
4. Sokolov V. V., Chissov V. I., Yakubovskya R. I., Smirnov V. V., Zhitkova M. B. Photodynamic therapy (PDT) of malignant tumors by photosensitzer photosens: results of 45 clinical cases//Proceedings of SPIE – The International Society for Optical Engineering. – 1996. – Vol. 2625. – P. 281–287.
5. Панова О. С., Дубенский В. В., Дубенский В. В., Петунина В. В., Бейманова М. А., Санчес Э. А., Гельфонд М. Л., Шилов Б. В., Белхароева Р. Х. Фотодинамическая репаративная регенерация кожи с применением наружного геля-фотосенсибилизатора на основе хлорина е6//Biomedical photonics. – 2021. – Т. 10, № 3. – С. 4–11. doi.org/10.24931/2413–9432–2021–10–3-4–11
6. Цеймах А. Е., Лазарев А. Ф., Секержинская Е. Л., Куртуков В. А., Мищенко А. Н., Теплухин В. Н., Шойхет Я. Н. Паллиативное лечение с применением фотодинамической терапии пациентов со злокачественными новообразованиями панкреатобилиарной зоны, осложненными механической желтухой//Биомедицинская фотоника. – 2020. – Т. 9, № 1. – С. 4–12. doi: 10.24931/2413–9432–2020–9-1–4-12
7. Церковский Д. А., Петровская Н. А., Мазуренко А. Н. Фотодинамическая терапия пациентов с внутрикожными метастазами диссеминированной меланомы кожи//Biomedical photonics. – 2019. – Т. 8, № 1. – С. 24–28. doi.org/10.24931/2413–9432–2019–8-1–24–28
8. Туманина А. Н., Полежаев А. А., Апанасевич В. А., Гурина Л. И., Волков М. В., Тарасенко А. Ю., Филоненко Е. В. Опыт применения фотодинамической терапии в лечении рака пищевода//Biomedical Photonics. – 2019. – Т. 8, № 2. – С. 19–24. doi.org/10.24931/2413–9432–2019–8-2–19–24
9. Церковский Д. А., Протопович Е. Л., Козловский Д. И., Суслова В. А. Противоопухолевая эффективность контактной лучевой терапии в комбинации с фотосенсибилизатором хлоринового ряда в эксперименте//Biomedical Photonics. – 2021. – Т. 10, № 2. – С. 25–33. doi.org/10.24931/2413–9432–2021–10–2-25–33
10. Pikin O., Filonenko E., Mironenko D., Vursol D., Amiraliev A. Fluorescence thoracoscopy in the detection of pleural malignancy//European Journal of Cardio-thoracic Surgery. – 2012. – Vol. 41 (3). – P. 649–652. doi: 10.1093/ejcts/ezr086
11. Zharkova N. N., Kozlov D. N., Smirnov V. V., Galpern M. G., Vorozhtsov G. N. Fluorescence observations of patients in the course of photodynamic therapy of cancer with the photosensitizer PHOTOSENS//Proceedings of SPIE – The International Society for Optical Engineering. – 1995. – Vol. 2325. – P. 400–403.
12. Sokolov V. V., Filonenko E. V., Telegina L. V., Boulgakova N. N., Smirnov V. V. Combination of fluorescence imaging and local spectrophotometry in fluorescence diagnostics of early cancer of larynx and bronchi//Quantum Electronics. – 2002. – Vol. 32 (11). – P. 963–969. doi: 10.1070/QE2002v032n11ABEH002329
13. Sokolov V. V., Chissov V. I., Filonenko E. V., Kozlov D. N., Smirnov V. V. Clinical fluorescence diagnostics in the course

15. Filonenko E. V., Sokolov V. V., Menenkov V. D., Krylova G. P. Photodynamic therapy for early cancer of hollow organs, *Photodynamic therapy and photodyagnosis*, 2015, vol. 4, no. 1, pp. 22–25. (In Russ.) doi.org/10.24931/2413–9432–2015–4-1–22–25
16. *Pharmaceutical Bulletin*, 2014, vol. 37, pp. 782.

of photodynamic therapy of cancer with the photosensitizer PHOTOGEM//Proceedings of SPIE – The International Society for Optical Engineering. – 1995. – Vol. 2325. – P. 375–380.
14. Русаков И. Г., Теплов А. А., Ульянов Р. В., Филоненко Е. В. Флуоресцентная цистоскопия у больных немышечно-инвазивным раком мочевого пузыря//Biomedical Photonics. – 2015. – Т. 4, № 3. – С. 29–35. doi.org/10.24931/2413–9432–2015–4-3–29–35
15. Филоненко Е. В., Соколов В. В., Мененков В. Д., Крылова Г. П. Фотодинамическая терапия начального рака полых органов//Фотодинамическая терапия и фотодиагностика. – 2015. – Т. 4, № 1. – С. 22–25. doi.org/10.24931/2413–9432–2015–4-1–22–25
16. Фармацевтический вестник. – 2014. – № 37. – С. 782.

STUDY OF ENERGY TRANSFER PROCESSES BETWEEN RARE EARTH IONS AND PHOTOSENSITIZER MOLECULES FOR PHOTODYNAMIC THERAPY WITH IR-EXCITATION

Pominova D.V.[1,2], Bogatova A.S.[2], Proydakova V.Y.[1], Romanishkin I.D.[1], Akhlyustina E.V.[2], Kuznetsov S.V.[1], Saveleva T.A.[1,2], Lukyanets E.A.[3], Loschenov V.B.[1,2]
[1]Prokhorov General Physics Institute of the Russian Academy of Sciences, Moscow, Russia
[2]National research nuclear university MEPHI, Moscow, Russia
[3]Biospec, Moscow, Russia

Abstract

Today, photodynamic therapy is one of the most promising minimally invasive methods of treatment of various diseases, including cancer. The main limitation of this method is the insufficient penetration into the tissue of laser radiation used to activate photosensitizer molecules, which makes it difficult to carry out therapy in the treatment of large or deep-seated tumors. In this regard, there is a great interest in the development of new strategies for photodynamic therapy using infrared radiation for excitation, the wavelengths of which fall into the "transparency window" of biological tissues. In this work, it was proposed to use upconversion $NaGdF_4$:Yb:Er nanoparticles (UCNP), which absorb infrared excitation and serve as a donor that transfers energy to the photosensitizer. Photosens and phthalosens were chosen as the most promising photosensitizers for the study. The aim of this work was to study the energy transfer processes between upconversion nanoparticles doped with rare-earth ions and photosensitizer molecules. in order to excite photosensitizers with IR radiation and carry out photodynamic therapy of deep-seated neoplasms. Using spectroscopic and time-resolved methods, it has been demonstrated that there is an efficient energy transfer between upconversion particles and photosensitizers phthalosens and photosens. The calculated efficiency of energy transfer by the Foerster mechanism was 41% for the UCNP + photosens system and 69% for the UCNP + phthalosens system. It has been experimentally and theoretically proved that there is a binding of photosensitizer molecules with UCNP by means of surfactants, leading to a reduction in the distance between them, due to which effective nonradiative energy transfer is realized. The generation of singlet oxygen by the phthalosens photosensitizer upon excitation by means of energy transfer from UCNP, excited at 980 nm wavelength of, has been demonstrated.

Key words: photodynamic therapy, infrared range, upconversion nanoparticles, photosensitizer, rare earth ions, resonant energy transfer.

For citations: Pominova D.V., Bogatova A.S., Proydakova V.Y., Romanishkin I.D., Akhlyustina E.V., Kuznetsov S.V., Saveleva T.A., Lukyanets E.A., Loschenov V.B. Study of energy transfer processes between rare earth ions and photosensitizer molecules for photodynamic therapy with IR-excitation, *Biomedical Photonics*, 2021, vol. 10, no. 4, pp. 23–34. doi: 10.24931/2413–9432–2021–10-4-23-34

Contacts: Pominova D.V., e-mail: pominovadv@gmail.com

ИССЛЕДОВАНИЕ ПРОЦЕССОВ ПЕРЕДАЧИ ЭНЕРГИИ МЕЖДУ РЕДКОЗЕМЕЛЬНЫМИ ИОНАМИ И МОЛЕКУЛАМИ ФОТОСЕНСИБИЛИЗАТОРОВ ДЛЯ ЗАДАЧ ФОТОДИНАМИЧЕСКОЙ ТЕРАПИИ С ВОЗБУЖДЕНИЕМ В ИК-ДИАПАЗОНЕ

Д.В. Поминова[1,2], А.С. Богатова[2], В.Ю. Пройдакова[1], И.Д. Романишкин[1], Е.В. Ахлюстина[2], С.В. Кузнецов[1], Т.А. Савельева[1,2], Е.А. Лукьянец[3], В.Б. Лощенов[1,2]
[1]Институт общей физики им. А.М. Прохорова Российской академии наук, Москва, Россия
[2]НИЯУ МИФИ, Москва, Россия
[3]ООО «Биоспек», Москва, Россия

Резюме

На сегодняшний день фотодинамическая терапия (ФДТ) является одним из самых перспективных минимально инвазивных методов лечения различных заболеваний, включая злокачественные новообразования. Основным ограничением применения этой

методики является недостаточная проникающая способность в ткань лазерного излучения, используемого для активации молекул фотосенсибилизатора (ФС), что затрудняет проведение терапии при лечении объемных или глубокозалегающих опухолей. В связи с этим наблюдается большой интерес к разработке новых стратегий ФДТ с использованием для возбуждения инфракрасного (ИК) излучения, длины волн которого попадают в «окно прозрачности» биологических тканей. В работе было предложено использовать ап-конверсионные наночастицы (АКНЧ) $NaGdF_4$:Yb:Er, которые поглощают инфракрасное возбуждение и служат донором, передающим энергию ФС. В качестве наиболее перспективных ФС для исследования были выбраны фотосенс и фталосенс. Исследованы процессы передачи энергии между АКНЧ, легированными редкоземельными ионами, и молекулами ФС для верификации возможности возбуждения ФС ИК-излучением и проведения ФДТ глубокозалегающих новообразований. При помощи спектроскопических и время-разрешенных методов продемонстрировано, что наблюдается эффективная передача энергии между АКНЧ и ФС фталосенс и фотосенс. Расчётная эффективность передачи энергии по механизму Фёрстера составила 41% для системы АКНЧ + фотосенс и 69% для АКНЧ + фталосенс. Экспериментально и теоретически доказано, что наблюдается связывание молекул ФС с АКНЧ посредством поверхностно-активного вещества, приводящее к сокращению расстояния между ними, за счет чего реализуется эффективная безызлучательная передача энергии. Продемонстрирована генерация синглетного кислорода молекулами фталосенса при возбуждении посредством передачи энергии от АКНЧ, возбуждаемых длиной волны 980 нм.

Ключевые слова: фотодинамическая терапия, инфракрасный диапазон, ап-конверсионные наночастицы, фотосенсибилизатор, редкоземельные ионы, резонансный перенос энергии.

Для цитирования: Поминова Д.В., Богатова А.С., Пройдакова В.Ю., Романишкин И.Д., Ахлюстина Е.В., Кузнецов С.В., Савельева Т.А., Лукьянец Е.А., Лощенов В.Б. Исследование процессов передачи энергии между редкоземельными ионами и молекулами фотосенсибилизаторов для задач фотодинамической терапии с возбуждением в ИК-диапазоне // Biomedical Photonics. – 2021. – Т. 10, № 4. – С. 23–34. doi: 10.24931/2413–9432–2021–10-4-23-34

Контакты: Поминова Д.В., e-mail: pominovadv@gmail.com

Introduction

Today, high-tech methods of theranostics are actively being developed. One of the most promising areas is the development of laser spectral-fluorescent methods for diagnostics and therapy. Luminescent diagnostics is currently the only method that allows obtaining information both at the tissue and subcellular levels with high sensitivity. In the last few decades, photodynamic therapy (PDT) has been actively used as an alternative to chemotherapy and radiation therapy for the treatment of various diseases, including cancer [1-5]. A typical PDT process involves three key components: excitation light (laser radiation is most commonly used), photosensitizer (PS) molecules, and oxygen. After absorption of light, the PS passes from the ground state to an excited state, then energy is transferred to neighboring oxygen molecules, which leads to the formation of singlet ($^1O_2$) or other reactive oxygen species (ROS). ROS generated during PDT cause destruction of tumor tissues through multifactorial mechanisms, including necrosis and/or apoptosis of tumor cells [6] or destruction of blood vessels that supply the tumor [7]. PDT is considered a minimally invasive procedure compared to chemotherapy and radiotherapy [8, 9]. The advantages of PDT also include the possibility of its local application, high selectivity and minor toxic and side effects [10-13], as well as stimulation of the immune system to recognize and remove the remaining tumor cells [14].

Despite the aforementioned advantages of PDT, one of the main limitations of the applicability of this treatment technique in clinical applications is the insufficient penetration of laser radiation used to activate PS molecules into the tissue. The limited penetration depth of laser radiation into biological tissues [15, 16] makes it difficult to perform PDT in the treatment of bulk or deep-seated tumors [17]. Therefore, there is a need to search for and develop new PDT strategies based on the use of infrared (IR) radiation for excitation, the wavelengths of which fall into the "transparency window" of biological tissues. It is believed that IR radiation (in the spectral range of 700–1000 nm) not only has a greater penetration depth into biological tissues compared to visible light [18], but also has low phototoxicity for cells and tissues [19]. In addition, IR radiation scatters less and does not excite autofluorescence of biological tissues, which makes it possible to obtain images with high contrast [20, 21].

Among the promising approaches to the development of new PDT strategies that use IR radiation for excitation of PSs, it is worth highlighting PDT using two-photon excitation [22, 23] and the use of up-conversion nanoparticles (UCNPs) [24]. When using UCNPs to deliver light to deep layers of biological tissues, it is necessary to create such nanostructures with fluorophores, where UCNPs act as absorbers of IR radiation and transfers energy to the fluorophore (both PS and organic dye molecules or quantum dots can be used as a fluorophore) acting as an acceptor.

UCNPs are nanocrystals doped with rare earth ions (REIs), one of which is a sensitizer that absorbs excitation radiation (Yb^{3+} is most often used), and the other is an

activator (for example, Er^{3+}, Tm^{3+}, Ho^{3+}). In UCNP, the energy is transferred from the sensitizer to the activator and added up with the involvement of intermediate metastable energy states of the activator, as a result of which UCNPs emit high-energy photons when excited by low-energy IR radiation. UCNPs have low phototoxicity, high photostability, and good biocompatibility, and also exhibit narrow luminescence bands in the entire visible spectral range upon IR excitation [25]. Due to these unique properties, UCNPs have been widely studied in recent years as new nanoprobes for medical bioimaging [26-28], including multimodal luminescent diagnostics in combination with magnetic resonance imaging (MRI), positron emission tomography (PET), and computed tomography (CT) with additional introduction of boron and/or gadolinium ions into the UCNP composition [29, 30]. In addition, UCNPs are being actively studied as therapeutic agents, especially for PDT [31, 32]. When using UCNPs as PS carriers, it is possible to increase the selectivity of drug accumulation in tumor due to the different vascular permeability of normal tissues and tumors for nanoobjects [33]. The surface of the UCNPs can be functionalized by attaching hydrophilic molecules and targeting agents for selective accumulation in certain cells.

Several groups of researchers have demonstrated UCNP-mediated PDT *in vitro* and *in vivo* [34–38]. UCNPs were first used for *in vivo* PDT in 2011 in mice with a 4T1 mammary tumor [33]. The chlorin e6 PS was adsorbed onto the surface of the $NaYF_4$:Yb,Er UCNPs via hydrophobic interactions with the oleic acid layer. UCNPs coated with CaF_2 and functionalized with 5-aminolevulinic acid (5-ALA) were studied in [35], where the high efficiency of using such a complex with excitation radiation at 980 nm and an increase in the depth of therapeutic action were shown. Several studies have shown that PDT can activate the immune system. The combination of PS with immune adjuvants, which can be nanoparticles, can additionally enhance the immune response. X. Duan et al. [39] showed that PDT using nanoparticles can activate the immune response, causing immunogenic death of cancer cells.

The key process involved in the upconversion transformation is the energy transfer between the sensitizer ion and the activator ion [40]. In the case of hybrid nanostructures consisting of UCNP and PS, the pair of sensitizer-activator ions, in turn, acts as a sensitizer for PS in the case of IR-mediated PDT. Despite the fact that there are a fairly large number of examples in the literature of using combinations of UCNPs and dye molecules, they are mainly focused on the direct practical application of the obtained structures *in vitro* and *in vivo* [41–47]. At the same time, there have been relatively few studies on the optimization of energy transfer between UCNP and PS molecules in such systems [48 – 51].

The aim of this work is to study the processes of energy transfer between nanoparticles doped with REIs and dye molecules for excitation of PS by IR radiation and PDT of deep-seated neoplasms.

Materials and methods

$NaGdF_4$:Yb:Er UCNPs (Yb:Er = 20:2) coated with an inert $NaYF_4$ shell were synthesized by the anhydrous method in oleic acid. The synthesis procedure is described in detail in [52, 53]. The ligand exchange method was used to transfer hydrophobic nanoparticles into the aqueous phase. Polyvinylpyrrolidone (PVP) (Sigma Aldrich, USA) was used as a surfactant.

For the studies, we selected the clinically approved PS Photosens ("NIOPIK", Russia), Fotoditazin (Belmedpreparaty, Belarus), Temoporfin (Sigma-Aldrich, USA) and PS Phthalosens not yet used in clinical practice ("NIOPIK", Russia).

The absorption of aqueous solutions of PS in the concentration range from 1 mg/mL to 20 mg/L in the spectral wavelength range of 350 – 900 nm was measured on a Hitachi U-3410 double-beam spectrophotometer (Hitachi, Japan). Spectral fluorescence studies were carried out using a LESA-01 "BIOSPEC" spectrometer. A laser with a wavelength of 980 nm (Biospec, Russia) was used as a source of laser radiation for excitation of the UCNP luminescence with 1 W/cm^2 power density. To record the spectrum of upconversion luminescence in the visible range, an optical filter FESH900 (Thorlabs, USA) was used, which suppresses radiation with wavelengths greater than 900 nm. UCNP colloids with the addition of phthalosens PS were additionally examined using a Carl Zeiss LSM 710 NLO laser scanning microscope (Carl Zeiss, Germany). A colloid drop was dried on glass, and then its luminescence image and spectrum were recorded using a 32-channel GaAsP PMT spectral detector in the range 410 – 750 nm under excitation by a pulsed femtosecond laser Chameleon Ultra II (Coherent, USA) at a wavelength of 980 nm.

The kinetic characteristics of the upcconversion luminescence were recorded in the range from 1 ns to 10 ms using a C9300-508 streak camera and a Hamamatsu Photonics streak scope C10627-13 (Hamamatsu, Japan) in the spectral range of 300–900 nm with wavelength resolution of 1.4 nm. As a source of laser radiation, a LSR980H IR laser with a wavelength of 980 nm operating in the modulation mode was used. A Hamamatsu C10647-01 delay generator was used as a source of trigger pulses. We measured the decay time of the upconversion luminescence in the green and red spectral ranges, corresponding to the radiative transitions of Er^{3+} ions $^2H_{11/2}$, $^4S_{3/2}$–$^4I_{15/2}$, and $^4F_{9/2}$–$^4I_{15/2}$, respectively.

The efficiency of singlet oxygen generation for a system consisting of UCNP with a PS was calculated

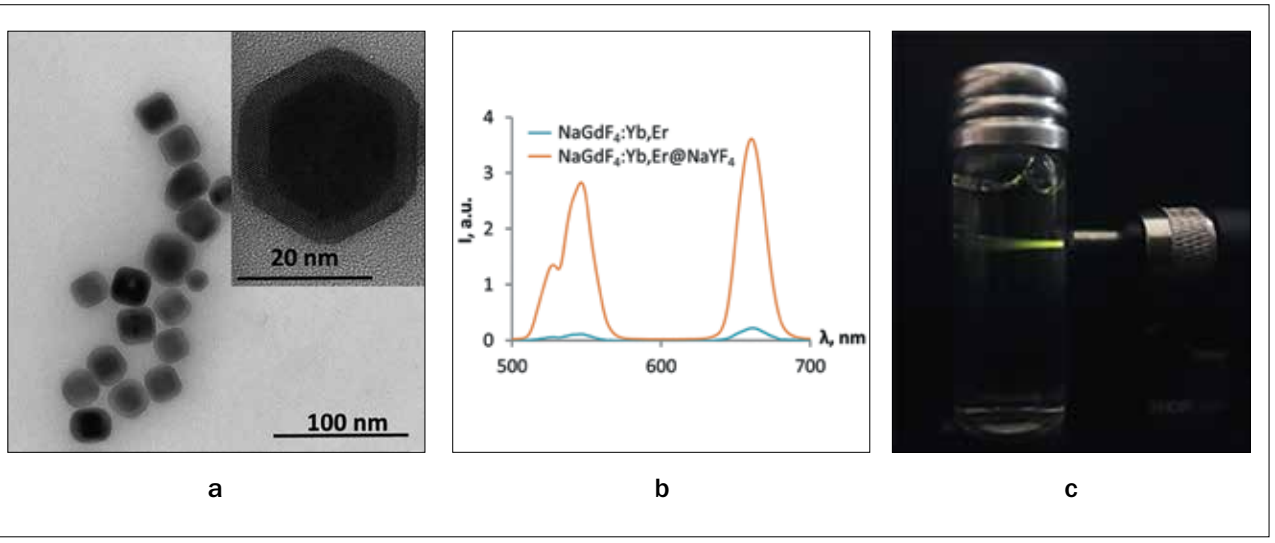

Рис. 1. a – просвечивающая электронная микроскопия полученных наночастиц $NaGdF_4$: Yb, Er (соотношение концентраций легирующих примесей Yb: Er = 20:2); b – спектры ап-конверсионной люминесценции наночастиц $NaGdF_4$: Yb, Er (соотношение концентраций легирующих примесей 20:2) до и после покрытия инертной оболочкой; c – фото люминесценции полученного коллоида при возбуждении длиной волны 980 нм.
Fig. 1. a – TEM of the obtained $NaGdF_4$: Yb, Er nanoparticles (the ratio of the dopant concentrations Yb: Er = 20:2); b – the up-conversion luminescence spectra of the $NaGdF_4$: Yb, Er nanoparticles (the ratio of the dopant concentrations 20:2) before and after coating with an inert shell; c – luminescence of the obtained colloid upon excitation with a 980 nm wavelength.

from a decrease in the optical absorption of a chemical "trap", a molecule of sodium tetra-a, a` (anthracene-9,10-diyl)- bis-methylmalonate (ADMA, produced by "NIOPIK", Russia) [54]. The ADMA molecule absorbs in the range of 350–400 nm, however, interacting with singlet oxygen, ADMA is oxidized. The oxidized form of the molecule is optically transparent. Optical density measurements were carried out on a Hitachi U-3400 double-beam spectrophotometer; a decrease in the ADMA absorption peak was recorded in the wavelength range 350 – 410 nm. The studied colloids were a mixture of UCNPs with a concentration of 0.3 mg/ml with phthalosens at concentrations of 1, 2, and 5 mg/L in cuvettes with an optical path length of 10 mm. A mixture of UCNPs with a concentration of 0.3 mg/mL and a photosens with a concentration of 5 mg/L was used as a sample for comparing the efficiency of singlet oxygen generation. ADMA was added to the investigated colloids immediately before irradiation, the concentration was 0.025 mg/mL. The studied samples were irradiated by a continuous wave diode laser with a wavelength of 980 nm, focused into a spot with an area of 1 cm^2 with 2 W/cm^2 power density. The samples were irradiated for 5 min, for the total light dose of 600 J (5 min, 2 W/cm^2). A mixture of PS with ADMA without the addition of UCNPs was used as a control.

Results and discussion

As a result of the synthesis, aqueous colloids of $NaGdF_4$:Yb, Er@$NaYF_4$ UCNPs stabilized with PVP were obtained, the particle size was about 30 nm (Fig. 1a).

The coating of UCNPs with an inert shell made it possible to significantly increase the intensity of upconversion luminescence (Figs. 1b, 1c).

An analysis was made of the overlap between the upconversion luminescence spectra of the UCNP colloidal solution and the absorption spectra of the studied PS. For this purpose, solutions of photosens, fotoditazin and temoporfin at concentrations of 2, 8, and 4 mg/L, respectively, and phthalosens (concentration 2 mg/L), were prepared, and their absorption spectra were recorded (Fig. 2).

Among the studied PSs, the strongest overlap of the upconversion luminescence in the red part of the spectrum (transition $^4F_{9/2} - {}^4I_{15/2}$, wavelength 665 nm) was observed with the absorption spectrum of photosens and phthalosens in the red region (wavelength 680 nm), so further studies were carried out with them.

The concentration dependence of the upconversion luminescence intensity of UCNP colloids with photosens and phthalosens upon excitation of colloids at a wavelength of 980 nm was studied. To study the possibility of energy transfer from UCNPs to PS molecules, UCNP colloids were prepared with the PS concentration of 1, 2, 5, 10, and 20 mg/L. The spectra exhibited characteristic peaks corresponding to the upconversion luminescence of Er^{3+} ions in green (transitions $^2H_{11/2}$, $^4S_{3/2} - {}^4I_{15/2}$, wavelengths 525, 545 nm) and red (transitions $^4F_{9/2} - {}^4I_{15/2}$, wavelength 665 nm) parts of the spectrum (Fig. 1b).

The dependence of the up-conversion luminescence intensity in the green and red parts

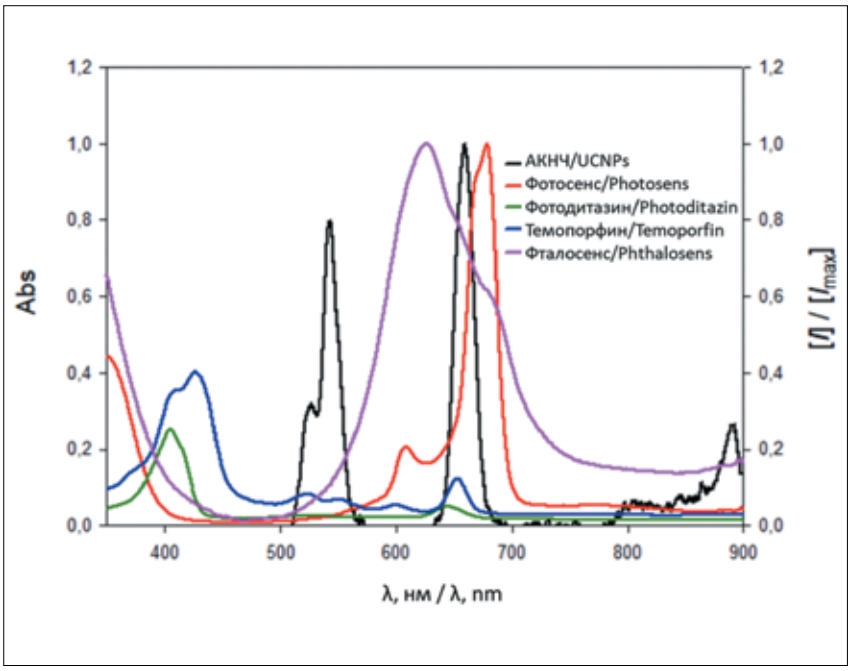

Рис. 2. Спектр люминесценции коллоида АКНЧ и спектры поглощения фотосенса, фотодитазина, темопорфина и фталосенса.
Fig. 2. The luminescence spectrum of the UCNPs colloid and the absorption spectra of photosens, photoditazin, temoporfin and phthalosens.

of the spectrum on PS concentration was analyzed. Graphs of the dependence of the integral area under the green (525, 540 nm) and red (660 nm) peaks on the concentration of photosens and phthalosens are shown in Fig. 3.

The intensity of the green component, both for colloids with photosens and for colloids with phthalosens, first increases and then decreases. It is assumed that the enhancement of green luminescence is caused by the interaction with the PS and with the transfer of energy from the PS triplet state to the REI. The dependences obtained show that the intensity of the red peak decreases with increasing concentrations of photosens and phthalosens. It is assumed that this occurs as a result of the absorption of part of the red luminescence of the PS, as well as a result of energy transfer between the UCNP and the PS molecules. Over time, a precipitate formed in the colloids of UCNP with phthalosens, which was examined using a laser scanning microscope. Images of the precipitate are shown in Fig. 4.

Aggregation of UCNP and phthalosens is observed, the aggregates are colored blue due to the addition of PS. The precipitate was excited at a wavelength of 980 nm (into the absorption band of UCNPs); the obtained upconversion luminescence spectra are shown in Fig. 4b. The spectra show peaks of upconversion luminescence at wavelengths of 525 and 540 nm and a small peak at a wavelength of about 690 nm, which is the luminescence of phthalosens. The study of a sample with a precipitate using laser scanning microscopy allows us to conclude that the PS and UCNPs are unevenly distributed in the solution and bond with each other, as a result of which the distance between the UCNPs and the PS molecule is small, which makes possible nonradiative energy transfer between them.

To study the processes of energy transfer and quantify their efficiency, we investigated the decay characteristics of the upconversion luminescence for UCNPs colloids with the addition of photosens and phthalosens using the method of single photon counting. The measured upconversion luminescence lifetimes in the green (525, 545 nm) and red (660 nm) spectral ranges are given in Table 1.

A significant decrease in the lifetime of upconversion luminescence in the red range is observed for UCNPs acting as a sensitizer, which indicates the presence of nonradiative energy transfer. The calculated efficiency of energy transfer by the Foerster mechanism was 41% for the UCNP + photosens system and 69% for the UCNP + phthalosens system. The increase in the lifetime in the green part of the spectrum confirms the earlier assumption that there is an additional energy transfer between PS and the $^2H_{11/2}$, $^4S_{3/2}$ states, from which the upconversion luminescence occurs in the green part of the spectrum.

To confirm this assumption about the binding of PS molecules to UCNPs by means of surfactants, we studied the lifetime for UCNP colloids prepared without the use of surfactants by dispersing UCNP powders thoroughly washed to remove oleic acid

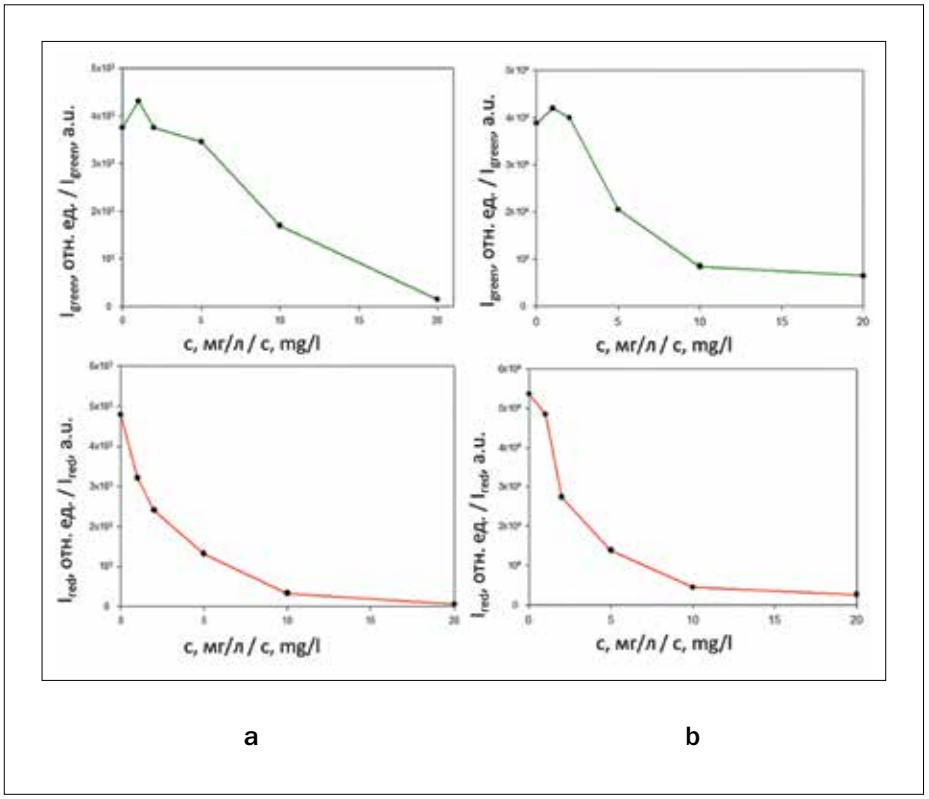

Рис. 3. Графики зависимости площади под зеленым (525, 540 нм) и красным (660 нм) пиком ап-конверсионной люминесценции от концентрации фотосенса (a) и фталосенса (b) при возбуждении длиной волны 980 нм.
Fig. 3. Dependence of the area under the green (525, 540 nm) and red (660 nm) peak of upconversion luminescence on the concentration of photosens (a) and phthalosens (b) under excitation with a 980 nm wavelength.

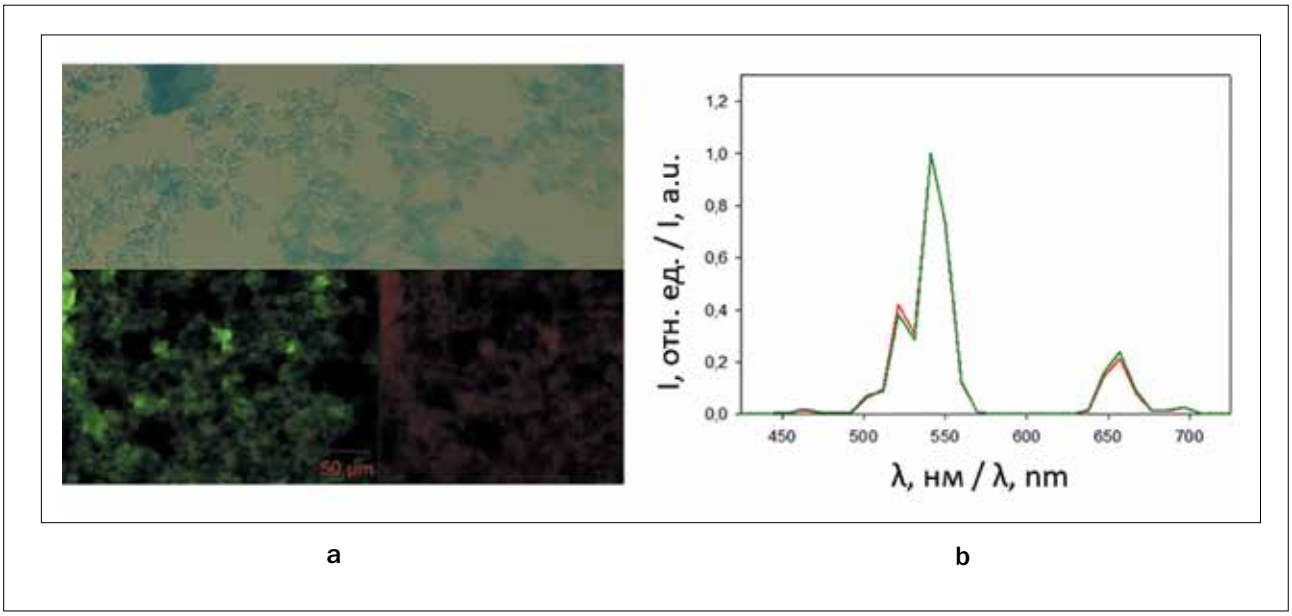

Рис. 4. a – микроскопическое изображение осадка, наблюдаемого в коллоидах АКНЧ с фталосенсом в концентрации 5 мг/л, полученное в проходящем свете в видимом диапазоне и люминесцентные изображения осадка в зеленом (525 нм) и красном диапазонах (660 нм) при возбуждении длиной волны 980 нм; b – спектры ап-конверсионной люминесценции осадка.
Fig. 4. a – microscopic image of the sediment observed in UCNPs colloids with phthalosens at a 5 mg/L concentration, obtained in transmitted light in the visible range and luminescent images of the sediment in the green (525 nm) and red ranges (660 nm) with excitation at a wavelength of 980 nm; b – upconversion luminescence spectra of the precipitate.

Таблица
Времена жизни люминесценции коллоидов АКНЧ в смеси с ФС
Table
UCNPs luminescence lifetimes of colloids mixed with PS

Образец Sample	τ_{green}, мкс τ_{green}, us	τ_{red}, мкс τ_{red}, us	Эффективность Фёрстеровской резонансной передачи энергии между АКНЧ и ФС (в красном диапазоне) FRET efficiency (red),%
$NaGdF_4$: Yb: Er@$NaYF_4$ (ПВП/PVP)	123	320	–
$NaGdF_4$: Yb: Er@$NaYF_4$ (ПВП/PVP) + Фотосенс 20 мг/л / Photosens 20 mg/l	144	189	41
$NaGdF_4$: Yb: Er@$NaYF_4$ (ПВП/PVP) + Фталосенс 20 мг/л / Phtalosens 20 mg/l	150	100	69
$NaGdF_4$: Yb: Er@$NaYF_4$ (вода / water)	215	428	–
$NaGdF_4$: Yb: Er@$NaYF_4$ (вода / water)+ Фотосенс 1 мг/л / Photosens 1 mg/l	221	419	2
$NaGdF_4$: Yb: Er@$NaYF_4$ (вода / water) + Фотосенс 10 мг/л / Photosens 10 mg/l	223	410	4

Примечание: τ_{green} – время жизни ап-конверсионной люминесценции в зеленом диапазоне; τ_{red}, мкс – время жизни ап-конверсионной люминесценции в красном диапазоне.
Note: τ_{green} – green upconversion luminescence lifetime; τ_{red} – red upconversion luminescence lifetime; FRET efficiency (red),% – Forster resonance energy transfer efficiency (in red range)

residues in water. Photosens was added to the obtained colloids at concentrations of 1 and 10 mg/L. As can be seen from the obtained results, the trend towards a decrease in the lifetime in the red part of the spectrum, along with an increase in the lifetime in the green part of the spectrum, remains. However, the relative change in both components is much smaller than in the case of surfactant-coated nanoparticles. This fact confirms the presence of PS binding with UCNP via surfactants, which leads to more efficient nonradiative energy transfer between them due to the decreased distance. The increase in the lifetime of upconversion luminescence for colloids of nanoparticles obtained without the use of surfactants is due to their thorough washing from oleic acid residues, which can act as quenching ligands on the surface of nanoparticles.

To evaluate the efficiency of singlet oxygen generation upon excitation at a 980 nm wavelength (in the UNCP absorption band), the absorption spectra of the ADMA singlet oxygen trap added to the studied colloids of UCNPs with PS at various concentrations were recorded. The ADMA absorption spectra recorded before and after irradiation are shown in Fig. 5a.

It can be seen that with an increase in the concentration of phthalosens in the colloid from 1 mg/L to 5 mg/L, the optical absorption of the trap decreases after irradiation compared to the value before irradiation, which indicates that with an increase in the phthalosens concentration, the amount of energy transferred from the UCNP to the phthalosens increases and, accordingly, the generation of singlet oxygen increases. The percentage change in optical absorption for various concentrations of phthalosens before and after irradiation is shown in Fig. 5b. With an increase in the PS concentration, an increase in the efficiency of singlet oxygen generation is observed, which indicates that UCNPs provide efficient energy transfer and PS excitation in the studied concentration range. The generation efficiency of singlet oxygen by phthalosens is comparable to the generation efficiency for photosens.

Conclusion

In this work, the processes of energy transfer from UCNPs (Er^{3+} ions act as a sensitizer of PS fluorescence) to PS molecules photosens and phthalosens and the possibility of PDT under IR excitation were studied. Using spectroscopic and time-resolved methods, it

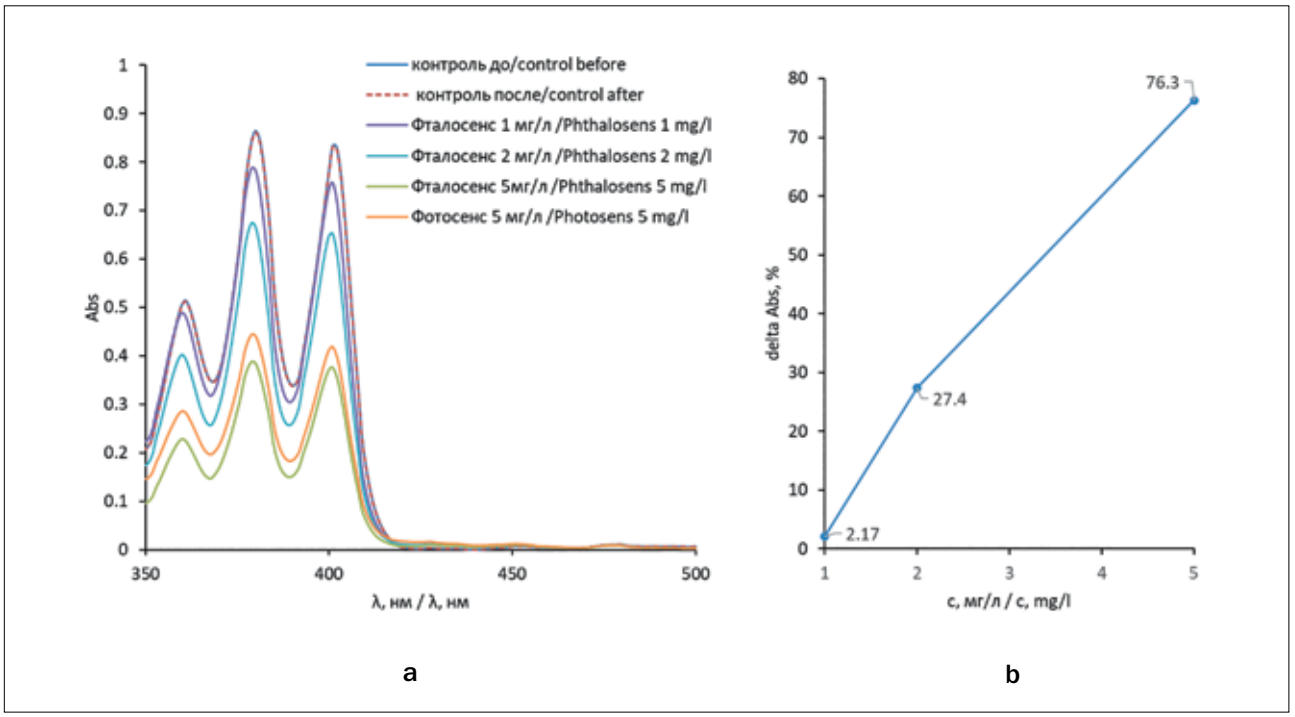

Рис. 5. a – оптическое поглощение ловушки на синглетный кислород ADMA до и после облучения коллоидов АКНЧ с различной концентрацией фталосенса и фотосенса для оценки генерации синглетного кислорода, контроль – смесь фталосенса с ADMA без добавления АКНЧ; b – процентное изменение оптического поглощения ловушки ADMA в зависимости от концентрации фталосенса в коллоиде.
Fig. 5. a – optical absorption of the singlet oxygen trap ADMA before and after irradiation of UCNPs colloids with different concentrations of phthalosens and photosens to assess the singlet oxygen generation, control – mix of phthalosens and ADMA without UCNPs; b – percentage change in the optical absorption of the ADMA depending on the Phthalosens concentration in the colloid.

was demonstrated that for phthalosens and photosens there is a strong overlap of the absorption spectra with the upconversion luminescence spectra, and an efficient energy transfer was also observed. The calculated efficiency of energy transfer by the Foerster mechanism was 41% for the UCNP + photosens system and 69% for the UCNP + phthalosens system. It has been established that the main mechanism of energy transfer is non-radiative. It has been experimentally and theoretically proved that there is a binding of PS molecules with UCNP by means of surfactants, leading to a reduction in the distance between them, due to which effective nonradiative energy transfer is realized. In addition, the generation of singlet oxygen by the phthalosens PS upon excitation by means of energy transfer from UCNP, excited at 980 nm wavelength, has been demonstrated. At the same time, with an increase in the PS concentration, an increase in the efficiency of singlet oxygen generation is observed, which indicates that UCNPs provide efficient energy transfer and PS excitation in the studied concentration range.

The study was carried out as part of the MEPhI State Assignment: "New phenomena in the interaction of laser radiation, plasma, corpuscular and radiative flows with condensed matter as the basis of innovative technologies" mnemonic code 0723-2020-0035, 2020-2022.

REFERENCES

1. Algorri, J.F., Ochoa, M., Roldán-Varona, P., Rodríguez-Cobo, L., López-Higuera, J.M. Photodynamic Therapy: A Compendium of Latest Reviews, *Cancers*, 2021, vol. 13, pp. 4447. https://doi.org/10.3390/cancers13174447
2. Filonenko E.V., Trushina O.I., Novikova E.G., Zarochentseva N.V., Rovinskaya O.V., Ivanova-Radkevich V.I., Kaprin A.D. Photodynamic therapy in the treatment of intraepithelial neoplasia of the cervix, vulva and vagina, *Biomedical Photonics*, 2020, vol. 9, no. 4, pp. 31–39. (in Russian). doi: 10.24931/2413–9432–2020–9–4–31–39
3. Semyonov D.Yu., Vasil'ev Yu.L., Dydykin S.S., Stranadko E.F., Shubin V.K., Bogomazov Yu.K., Morokhotov V.A., Shcherbyuk A.N., Morozov S.V., Zakharov Yu.I. Antimicrobial and antimycotic photodynamic therapy (review of literature), *Biomedical Photonics*, 2021, vol. 10, no. 1, pp. 25–31. (in Russian). doi: 10.24931/2413–9432–2021–10–1–25–31
4. Filonenko E.V., Kaprin A.D., Alekseev B.Ya., Apolikhin O.I., Slovokhodov E.K., Ivanova-Radkevich V.I., Urlova A.N. 5-Aminolevulinic acid in intraoperative photodynamic therapy of bladder cancer (results of multicenter trial), *Photodiagnosis and Photodynamic Therapy*, 2016, vol. 16, pp. 106–109. doi: 10.1016/j.pdpdt.2016.09.009
5. Sokolov V.V., Chissov V.I., Filonenko E.V. et al. Photodynamic therapy of cancer with the photosensitizer PHOTOGEM, *Proceedings of SPIE – The International Society for Optical Engineering*, 1995, vol. 2325, pp. 367–374. doi: 10.1117/12.199169
6. Oleinick N.L., Morris R.L., Belichenko I. The role of apoptosis in response to photodynamic therapy: what, where, why, and how, *Photochemical & Photobiolological Sciences*, 2002, Vol. 1, pp. 1–21.
7. Krammer B. Vascular effects of photodynamic therapy, *Anticancer Research*, 2001, vol. 21, no. 6, pp. 4271–4277.
8. Sanarova E.V., Lantsova A.V., Dmitrieva M.V., et al. Photodynamic therapy – a way to increase the selectivity and effectiveness of tumor treatment, *Russian Biotherapeutic journal*, 2014, vol. 13, no. 3, pp. 109–118.
9. Sokolov V.V., Chissov V.I., Yakubovskya R.I. et al. Photodynamic therapy (PDT) of malignant tumors by photosensitzer photosens: results of 45 clinical cases. *Proceedings of SPIE – The International Society for Optical Engineering,* 1996, vol. 2625, pp. 281–287.
10. Sokolov V.V., Filonenko E.V., Telegina L.V. et al. Combination of fluorescence imaging and local spectrophotometry in fluorescence diagnostics of early cancer of larynx and bronchi, *Quantum Electronics*, 2002, vol. 32, no. 11, pp. 963–969. doi: 10.1070/QE2002v032n11ABEH002329
11. Pikin O., Filonenko E., Mironenko D., Vursol D., Amiraliev A. Fluorescence thoracoscopy in the detection of pleural malignancy, *European Journal of Cardio-Thoracic Surgery,* 2012, vol. 41, no. 3, pp. 649–652. doi: 10.1093/ejcts/ezr086
12. Panaseykin Y.A., Filonenko E.V., Sevrukov F.E., Kapinus V.N., Polkin V.V., Isaev P.A., Kaprin A.D., Ivanov S.A. Possibilities of photodynamic therapy in the treatment of malignant tumors of the oral cavity, *Biomedical Photonics*, 2021, vol. 10, no. 3, pp. 32–38 (in Russian). doi: 10.24931/2413–9432–2021–10–3–32–38
13. Kaprin A.D., Mardinskiy Yu.S., Smirnov V.P., Ivanov S.A., Kostin A.A., Polikhov S.A., Reshetov I.V., Fatianova A.S., Denisenko M.V., Epatova T.V., Korenev S.V., Tereshchenko A.V., Filonenko E.V., Gafarov M.M., Romanko Yu.S. The history of radiation therapy (part I), *Biomedical Photonics*, 2019, vol. 8, no. 1, pp. 52–62 (in Russian). doi: 10.24931/2413–9432–2019–8–1–52–62
14. Castano A.P., Mroz P., Hamblin M. R Photodynamic therapy and anti-tumour immunity, *Nature Reviews Cancer*, 2006, vol. 6, no. 7, pp. 535–545 (In Russ.).
15. Clement M., Daniel G., Trelles M. Optimising the design of a broad band light source for the treatment of skin, *Journal of Cosmetic and Laser Therapy*, 2005, vol. 7, no. 3, pp. 177–189.

ЛИТЕРАТУРА

1. Algorri, J.F., Ochoa, M., Roldán-Varona, P., Rodríguez-Cobo, L., López-Higuera, J.M. Photodynamic Therapy: A Compendium of Latest Reviews//Cancers. – 2021. – Vol. 13. – P. 4447. https://doi.org/10.3390/cancers13174447
2. Филоненко Е.В., Трушина О.И., Новикова Е.Г., Зароченцева Н.В., Ровинская О.В., Иванова-Радкевич В.И., Каприн А.Д. Фотодинамическая терапия в лечении интраэпителиальных неоплазий шейки матки, вульвы и влагалища//Biomedical Photonics. – 2020. Vol. 9 (4). – P. 31–39. https://doi.org/10.24931/2413–9432–2020–9–4–31–39
3. Семенов Д.Ю., Васильев Ю.Л., Дыдыкин С.С., Странадко Е.Ф., Шубин В.К., Богомазов Ю.К., Морохотов В.А., Щербюк А.Н., Морозов С.В., Захаров Ю.И. Антимикробная и антимикотическая фотодинамическая терапия (обзор литературы)//Biomedical Photonics. – 2021. – Vol. 10 (1). – P. 25–31. https://doi.org/10.24931/2413–9432–2021–10–1-25–31
4. Filonenko E.V., Kaprin A.D., Alekseev B.Ya., Apolikhin O.I., Slovokhodov E.K., Ivanova-Radkevich V.I., Urlova A.N. 5-Aminolevulinic acid in intraoperative photodynamic therapy of bladder cancer (results of multicenter trial)//Photodiagnosis and Photodynamic Therapy. – 2016. – Т. 16. – С. 106–109. doi: 10.1016/j.pdpdt.2016.09.009
5. Sokolov V.V., Chissov V.I., Filonenko E.V., Kozlov D.N., Smirnov V.V. Photodynamic therapy of cancer with the photosensitizer PHOTOGEM//Proceedings of SPIE – The International Society for Optical Engineering. – 1995. – Vol. 2325. – P. 367–374. doi: 10.1117/12.199169
6. Oleinick N.L., Morris R.L., Belichenko I. The role of apoptosis in response to photodynamic therapy: what, where, why, and how//Photochemical & Photobiolological Sciences. – 2002. – Vol. 1. – P. 1–21.
7. Krammer B. Vascular effects of photodynamic therapy//Anticancer Research. – 2001. – Vol. 21 (6). – P. 4271–4277.
8. Санарова Е.В., Ланцова А.В., Дмитриева М.В., и др Фотодинамическая терапия – способ повышения селективности и эффективности лечения опухолей//Российский биотерапевтический журнал. – 2014. – Т. 13, № 3. – С. 109–118.
9. Sokolov V.V., Chissov V.I., Yakubovskya R.I., Smirnov V.V., Zhitkova M.B. Photodynamic therapy (PDT) of malignant tumors by photosensitzer photosens: results of 45 clinical cases//Proceedings of SPIE – The International Society for Optical Engineering. – 1996. – Vol. 2625. – P. 281–287.
10. Sokolov V.V., Filonenko E.V., Telegina L.V., Boulgakova N.N., Smirnov V.V. Combination of fluorescence imaging and local spectrophotometry in fluorescence diagnostics of early cancer of larynx and bronchi//Quantum Electronics. – 2002. – Vol. 32 (11). – P. 963–969. doi: 10.1070/QE2002v032n11ABEH002329
11. Pikin O., Filonenko E., Mironenko D., Vursol D., Amiraliev A. Fluorescence thoracoscopy in the detection of pleural malignancy//European Journal of Cardio-Thoracic Surgery. – 2012. – Т. 41, № 3. – С. 649–652. doi: 10.1093/ejcts/ezr086
12. Панасейкин Ю.А., Филоненко Е.В., Севрюков Ф.Е., Капинус В.Н., Полькин В.В., Исаев П.А., Каприн А.Д., Иванов С.А. Возможности фотодинамической терапии при лечении злокачественных опухолей полости рта//Biomedical Photonics. – 2021. – Vol. 10 (3). – P.32–38. https://doi.org/10.24931/2413–9432–2021–10–3-32–38
13. Каприн А.Д., Мардынский Ю.С., Смирнов В.П., Иванов С.А., Костин А.А., Полихов С.А., Решетов И.В., Фатьянова А.С., Денисенко М.В., Эпатова Т.В., Коренев С.В., Терещенко А.В., Филоненко Е.В., Гафаров М.М., Романко Ю.С. К истории развития лучевой терапии (часть I)//Biomedical Photonics. – 2019. – Т. 8, № 1. – С. 52–62. doi: 10.24931/2413–9432–2019–8–1–52–62.
14. Castano A.P., Mroz P., Hamblin M. R Photodynamic therapy and anti-tumour immunity//Nature Reviews Cancer. – 2006. Vol. 6 (7). – P. 535–45.

16. Pierroz V., Folcher M. From Photobiolumination to Optogenerapy, Recent Advances in NIR Light Photomedicine Applications, *Journal of molecular and genetic medicine*, 2018, vol. 2, no. 2, pp. 1–7.
17. Wang F., Banerjee D., Liu Y., et al. Upconversion nanoparticles in biological labeling, imaging, and therapy, *Analyst*, 2010, vol. 135, no. 8, pp. 1839–1854.
18. Ismael F. S., Amasha H. M., Bachir W. H. A diffusion equation based algorithm for determination of the optimal number of fibers used for breast cancer treatment planning in photodynamic therapy, *Biomedical Photonics*, 2019, vol. 8, no. 4, pp. 17–27. doi: 10.24931/2413–9432– 2019–8–4–17–27
19. Can T. X., Svensson N., Axelsson J., et al. Autofluorescence insensitive imaging using upconverting nanocrystals in scattering media, *Applied Physics Letters*, 2008, vol. 93, no. 17, pp. 171103.
20. Nyk M., Kumar R., Ohulchanskyy T. Y., et al. High contrast in vitro and in vivo photoluminescence bioimaging using near infrared to near infrared up-conversion in Tm3+ and Yb3+ doped fluoride nanophosphors, *Nano Letters*, 2008, vol. 8, no. 11, pp. 3834–3838.
21. Jacques S. L. Optical properties of biological tissues: a review, *Physics in Medicine and Biology*, 2013, vol. 58, no. 14, pp. 5007–5008.
22. Gallavardin T., Maurin M., Marotte S., et al Photodynamic therapy and two-photon bio-imaging applications of hydrophobic chromophores through amphiphilic polymer delivery, *Photochemical and Photobiological Sciences*, 2011, vol. 10, no. 7, pp.1216–1225.
23. Velusamy M., Shen J. Y., Lin J. T., et al. A New Series of Quadrupolar Type Two-Photon Absorption Chromophores Bearing 11,12-Dibutoxydibenzo [a, c]-phenazine Bridged Amines; Their Applications in Two-Photon Fluorescence Imaging and Two-Photon Photodynamic Therapy, *Advanced Functional Materials*, 2009, vol. 19, no. 15, pp. 2388–2397.
24. Chen G., Shen J., Ohulchanskyy T.Y, et al. (alpha-NaYbF4: Tm3+)/CaF2 Core/Shell Nanoparticles with Efficient Near-Infrared to Near-Infrared Upconversion for High-Contrast Deep Tissue Bioimaging, *ACS Nano*, 2012 vol. 6, no. 9, pp. 8280–8287.
25. Wang C., Cheng L., Liu Z. Upconversion nanoparticles for potential cancer theranostics, *Ther. Deliv*, 2011, vol. 2, no. 10, pp. 1235–1239. doi: 10.4155/tde.11.93. PMID: 22826879.
26. Liu W., Chen R., He S. Ultra-stable near-infrared Tm3+-doped upconversion nanoparticles for in vivo wide-field two-photon angiography with a low excitation intensity, *Journal of innovative optical health sciences*, 2019, vol. 12, no. 3, pp. 1950013.
27. Tse W. H., Chen L., McCurdy C. M., et al. Development of biocompatible NaGdF4: Er3+, Yb3+ upconversion nanoparticles used as contrast agents for bio-imaging, *The Canadian Journal of Chemical Engineering*, 2019, vol. 97, no. 10, pp. 2678–2684.
28. Xu J., Gulzar A., Yang P., et al. Recent advances in near-infrared emitting lanthanide-doped nanoconstructs: Mechanism, design and application for bioimaging, *Coordination Chemistry Reviews*, 2019, vol. 381, pp.104–134.
29. Xue X. J., Wang F., Liu X. G. Emerging functional nanomaterials for therapeutics, *Journal of Materials Chemistry*, 2011, vol. 21, no. 35, pp. 13107–13127.
30. Mader H. S., Kele P., Saleh S. M., et al. Upconverting luminescent nanoparticles for use in bioconjugation and bioimaging, *Current Opinion in Chemical Biology*, 2010, vol. 14, no. 5, pp. 582–596.
31. Shen, J., Zhao L., Han G. Lanthanide-doped upconverting luminescent nanoparticle platforms for optical imaging-guided drug delivery and therapy, *Advanced drug delivery reviews*, 2012, vol. 65, no. 5, pp. 744–755.
32. Liu Y., Meng X., Bu W. Upconversion-based photodynamic cancer therapy, *Coordination chemistry reviews*, 2019, vol. 379, pp. 82–98.
33. Obaid G., Russell D. A. Nanoparticles for PDT: Handbook of Pho-

15. Clement M., Daniel G., Trelles M. Optimising the design of a broad band light source for the treatment of skin//Journal of Cosmetic and Laser Therapy. – 2005. – Vol. 7 (3). – P. 177–189.
16. Pierroz V., Folcher M. From Photobiolumination to Optogenerapy, Recent Advances in NIR Light Photomedicine Applications//Journal of molecular and genetic medicine. – 2018. – Vol. 2 (2). – P. 1–7.
17. Wang F., Banerjee D., Liu Y., et al. Upconversion nanoparticles in biological labeling, imaging, and therapy//Analyst. – 2010. – Vol. 135 (8). – P. 1839–1854.
18. Ismael F. S., Amasha H. M., Bachir W. H. Алгоритм определения оптимального числа волокон используемых при внутритканевой фотодинамической терапии рака молочной железы на основании диффузионного уравнения//Biomedical Photonics. – 2019. Vol. 8 (4). – P. 17–27.
19. Can T. X., Svensson N., Axelsson J., et al. Autofluorescence insensitive imaging using upconverting nanocrystals in scattering media//Applied Physics Letters. – 2008. – Vol. 93 (17). – P. 171103.
20. Nyk M., Kumar R., Ohulchanskyy T. Y., et al. High contrast in vitro and in vivo photoluminescence bioimaging using near infrared to near infrared up-conversion in Tm^{3+} and Yb^{3+} doped fluoride nanophosphors//Nano Letters. – 2008. – Vol. 8 (11). – P. 3834–3838.
21. Jacques S. L. Optical properties of biological tissues: a review//Physics in Medicine and Biology. – 2013. – Vol. 58 (14). – P. 5007–5008.
22. Gallavardin T., Maurin M., Marotte S., et al Photodynamic therapy and two-photon bio-imaging applications of hydrophobic chromophores through amphiphilic polymer delivery//Photochemical and Photobiological Sciences. – 2011.– Vol. 10 (7).– P.1216–1225.
23. Velusamy M., Shen J. Y., Lin J. T., et al. A New Series of Quadrupolar Type Two-Photon Absorption Chromophores Bearing 11,12-Dibutoxydibenzo [a, c]-phenazine Bridged Amines; Their Applications in Two-Photon Fluorescence Imaging and Two-Photon Photodynamic Therapy//Advanced Functional Materials. – 2009. – Vol. 19 (15). – P. 2388–2397.
24. Chen G., Shen J., Ohulchanskyy T.Y, et al. (alpha-$NaYbF_4$: Tm^{3+})/CaF_2 Core/Shell Nanoparticles with Efficient Near-Infrared to Near-Infrared Upconversion for High-Contrast Deep Tissue Bioimaging//ACS Nano. – 2012. – Vol. 6 (9). – P. 8280–8287.
25. Wang C., Cheng L., Liu Z. Upconversion nanoparticles for potential cancer theranostics//Ther. Deliv. – 2011. – Vol. 2 (10). – P. 1235–1239. doi: 10.4155/tde.11.93. PMID: 22826879.
26. Liu W., Chen R., He S. Ultra-stable near-infrared Tm3+-doped upconversion nanoparticles for in vivo wide-field two-photon angiography with a low excitation intensity//Journal of innovative optical health sciences. – 2019. – Vol. 12 (3). – P. 1950013.
27. Tse W. H., Chen L., McCurdy C. M., et al. Development of biocompatible $NaGdF_4$: Er^{3+}, Yb^{3+} upconversion nanoparticles used as contrast agents for bio-imaging//The Canadian Journal of Chemical Engineering. – 2019. – Vol. 97 (10). – P. 2678–2684.
28. Xu J., Gulzar A., Yang P., et al. Recent advances in near-infrared emitting lanthanide-doped nanoconstructs: Mechanism, design and application for bioimaging//Coordination Chemistry Reviews. – 2019. – Vol. 381. – P.104–134.
29. Xue X. J., Wang F., Liu X. G. Emerging functional nanomaterials for therapeutics//Journal of Materials Chemistry. – 2011. – Vol. 21 (35).– P. 13107–13127.
30. Mader H. S., Kele P., Saleh S. M., et al. Upconverting luminescent nanoparticles for use in bioconjugation and bioimaging//Current Opinion in Chemical Biology. – 2010 – Vol. 14 (5). – P. 582–596.
31. Shen, J., Zhao L., Han G. Lanthanide-doped upconverting luminescent nanoparticle platforms for optical imaging-guided drug delivery and therapy//Advanced drug delivery reviews. – 2012. – Vol. 65 (5). – P. 744–755.

tomedicine/eds. M. R. Hamblin, Y.-Y. Huang. Boca Raton. *FL: Taylor & Francis, CRC Press*, 2013, pp. 367–378.
34. Shan G., Weissleder R., Hilderbrand S. A. Upconverting organic dye doped core-shell nano-composites for dual-modality NIR imaging and photo-thermal therapy, *Theranostics*, 2013, vol. 3, no. 4, pp. 267–274. doi: 10.7150/thno.5226
35. Wang C., Cheng L., Liu Z. Imaging-Guided pH-Sensitive Photodynamic Therapy Using Charge Reversible Upconversion Nanoparticles under Near-Infrared Light, *Advanced Functional Materials*, 2013, vol. 23, no. 24, pp. 3077–3086. doi: 10.1002/adfm.201202992
36. Zhang L., Zeng L., Pan Y. et al. Inorganic photosensitizer coupled Gd-based upconversion luminescent nanocomposites for in vivo magnetic resonance imaging and near infrared-responsive photodynamic therapy in cancers, *Biomaterials*, 2015, Vol. 44, pp. 82–90. doi: 10.1016/j.biomaterials.2014.12.040
37. Shan G., Weissleder R., Hilderbrand S. A. Upconverting organic dye doped core-shell nano-composites for dual-modality NIR imaging and photo-thermal therapy, *Theranostics*, 2013, vol. 3, no. 4, pp. 267–274.
38. C. Wang, L. Cheng, Z. Liu Imaging-Guided pH-Sensitive Photodynamic Therapy Using Charge Reversible Upconversion Nanoparticles under Near-Infrared Light, *Advanced Functional Materials*, 2013, vol. 23, no. 24, pp. 3077–3086.
39. Duan X., Chan C., Lin W. Nanoparticle-mediated Immunogenic Cell Death Enables and Potentiates Cancer Immunotherapy, *Angewandte Chemie International Edition*, 2019, vol. 58, no. 3, pp. 670–680.
40. Auzel F. Upconversion and anti-Stokes processes with f and d ions in solids, *Chemical Reviews*, 2004, vol. 104, no. 1, pp. 139–173.
41. Terenin A. N. Photochemical processes in aromatic compounds, *Acta physicochim. UESS*, 1943, vol. 18, no. 4, pp. 210–241.
42. Wang L., Yan R., Huo Z., et al. Fluorescence resonant energy transfer biosensor based on upconversion-luminescent nanoparticles, *Angewandte Chemie International Edition*, 2005, vol. 44, no. 37, pp. 6054–6057.
43. Rantanen T., Jarvenpaa M.-L., Vuojola J., et al. Upconverting phosphors in a dual-parameter LRET-based hybridization assay, *Analyst*, 2009, vol. 134, pp. 1713–1716.
44. Jo E. J., Mun H., Kim M. G. Homogeneous immunosensor based on luminescence resonance energy transfer for glycated hemoglobin detection using upconversion nanoparticles, *Analytical Chemistry*, 2016, vol. 88, no. 5, pp. 2742–2746.
45. Rantanen T.; Päkkilä H.; Jämsen L., et al. Tandem dye acceptor used to enhance upconversion fluorescence resonance energy transfer in. homogeneous assays, *Analytical Chemistry*, 2007, vol. 79, pp. 6312–6318.
46. Vetrone F., Naccache R., Morgan C. G., et al. Luminescence resonance energy transfer from an upconverting nanoparticle to a fluorescent phycobiliprotein, *Nanoscale*, 2010, vol. 2, no. 7, pp. 1185–1189.
47. Cheng L., Yang K., Shao M., et al. Multicolor in vivo imaging of upconversion nanoparticles with emissions tuned by luminescence resonance energy transfer. *The Journal of Physical Chemistry C*, 2011, Vol. 115 (6), pp. 2686–2692.
48. Ding Y., Wu F., Zhang Y., et al. Interplay between Static and Dynamic Energy Transfer in Biofunctional Upconversion Nanoplatforms, *Journal of Physical Chemistry Letters*, 2015, vol. 6, pp. 2518–2523.
49. Muhr V., Würth C., Kraft M., et al. Particle-Size-Dependent Förster Resonance Energy Transfer from Upconversion Nanoparticles to Organic Dyes, *Analytical Chemistry*, 2017, vol. 89, no. 9, pp. 4868–4874.
50. Shao W., Chen G., Kuzmin A., et al. Tunable narrow band emissions from dye-sensitized core/shell/shell nanocrys-
32. Liu Y., Meng X., Bu W. Upconversion-based photodynamic cancer therapy//Coordination chemistry reviews. – 2019. – Vol. 379. – P. 82–98.
33. Obaid G., Russell D. A. Nanoparticles for PDT: Handbook of Photomedicine/eds. M. R. Hamblin, Y.-Y. Huang. Boca Raton. – FL: Taylor & Francis, CRC Press. – 2013. – P. 367–378.
34. Shan G., Weissleder R., Hilderbrand S. A. Upconverting organic dye doped core-shell nano-composites for dual-modality NIR imaging and photo-thermal therapy//Theranostics. – 2013. – Vol. 3 (4). – P. 267–274. doi: 10.7150/thno.5226
35. Wang C., Cheng L., Liu Z. Imaging-Guided pH-Sensitive Photodynamic Therapy Using Charge Reversible Upconversion Nanoparticles under Near-Infrared Light//Advanced Functional Materials. – 2013. – Vol. 23 (24). P. 3077–3086. doi: 10.1002/adfm.201202992
36. Zhang L., Zeng L., Pan Y. et al. Inorganic photosensitizer coupled Gd-based upconversion luminescent nanocomposites for in vivo magnetic resonance imaging and near infrared-responsive photodynamic therapy in cancers//Biomaterials. – 2015. – Vol. 44, P. 82–90. doi: 10.1016/j.biomaterials.2014.12.040
37. Shan G., Weissleder R., Hilderbrand S. A. Upconverting organic dye doped core-shell nano-composites for dual-modality NIR imaging and photo-thermal therapy//Theranostics. – 2013. – Vol. 3 (4). – P. 267–274.
38. Wang C., Cheng L., Liu Z. Imaging-Guided pH-Sensitive Photodynamic Therapy Using Charge Reversible Upconversion Nanoparticles under Near-Infrared Light//Advanced Functional Materials. – 2013. – Vol. 23 (24). – P. 3077–3086.
39. Duan X., Chan C., Lin W. Nanoparticle-mediated Immunogenic Cell Death Enables and Potentiates Cancer Immunotherapy//Angewandte Chemie International Edition. – 2019. – Vol. 58 (3). – P. 670–680.
40. Auzel F. Upconversion and anti-Stokes processes with f and d ions in solids//Chemical Reviews. – 2004. – Vol. 104 (1). – P. 139–173.
41. Terenin A. N. Photochemical processes in aromatic compounds//Acta physicochim. UESS. – 1943. – Vol. 18 (4). – P. 210–241.
42. Wang L., Yan R., Huo Z., et al. Fluorescence resonant energy transfer biosensor based on upconversion-luminescent nanoparticles//Angewandte Chemie International Edition. – 2005. – Vol. 44 (37). – P. 6054–6057.
43. Rantanen T., Jarvenpaa M.-L., Vuojola J., et al. Upconverting phosphors in a dual-parameter LRET-based hybridization assay//Analyst. – 2009. – Vol. 134. – P. 1713–1716.
44. Jo E. J., Mun H., Kim M. G. Homogeneous immunosensor based on luminescence resonance energy transfer for glycated hemoglobin detection using upconversion nanoparticles//Analytical Chemistry. – 2016. – Vol. 88 (5). – P. 2742–2746.
45. Rantanen T.; Päkkilä H.; Jämsen L., et al. Tandem dye acceptor used to enhance upconversion fluorescence resonance energy transfer in. homogeneous assays//Analytical Chemistry. – 2007. – Vol. 79. – P. 6312–6318.
46. Vetrone F., Naccache R., Morgan C. G., et al. Luminescence resonance energy transfer from an upconverting nanoparticle to a fluorescent phycobiliprotein//Nanoscale. – 2010. – Vol. 2 (7). – P. 1185–1189.
47. Cheng L., Yang K., Shao M., et al. Multicolor in vivo imaging of upconversion nanoparticles with emissions tuned by luminescence resonance energy transfer//The Journal of Physical Chemistry C. – 2011. – Vol. 115 (6).– P. 2686–2692.
48. Ding Y., Wu F., Zhang Y., et al. Interplay between Static and Dynamic Energy Transfer in Biofunctional Upconversion Nanoplatforms//Journal of Physical Chemistry Letters. – 2015. – Vol. 6. – P. 2518–2523.
49. Muhr V., Würth C., Kraft M., et al. Particle-Size-Dependent Förster Resonance Energy Transfer from Upconversion Nanoparticles

tals in the second near-infrared biological window, *Journal of the American Chemical Society*, 2016, vol. 138, no. 50, pp. 16192–16195.

51. Drees C., Raj A.N., Kurre R., et al. Engineered Upconversion Nanoparticles for Resolving Protein Interactions inside Living Cells, *Angewandte Chemie International Edition*, 2016, vol. 55, no. 38, pp. 11668–11672.
52. Pominova D., Proydakova V., Romanishkin I., et al. Temperature sensing in the short-wave infrared spectral region using core-shell NaGdF4: Yb3+, Ho3+, Er3+@NaYF4 nanothermometers, *Nanomaterials*, 2020, vol. 10, no. 10, pp. 1992.
53. Pominova, D., Romanishkin, I., Proydakova, V., et al Optimization of upconversion luminescence excitation mode for deeper in vivo bioimaging without contrast loss or overheating, *Methods and Applications in Fluorescence*, 2020, vol. 8, pp. 025006.
54. Kuznetsova, N.A., Gretsova N.S., Yuzhakova O.A., et al. New reagents for determination of the quantum efficiency of singlet oxygen generation in aqueous media, *Russian Journal of General Chemistry*, 2001, vol. 71, no. 1, pp. 36–41.

to Organic Dyes//Analytical Chemistry. – 2017. – Vol. 89 (9). – P. 4868–4874.

50. Shao W., Chen G., Kuzmin A., et al. Tunable narrow band emissions from dye-sensitized core/shell/shell nanocrystals in the second near-infrared biological window//Journal of the American Chemical Society. – 2016. – Vol. 138 (50). – P. 16192–16195.
51. Drees C., Raj A.N., Kurre R., et al. Engineered Upconversion Nanoparticles for Resolving Protein Interactions inside Living Cells//Angewandte Chemie International Edition. – 2016. – Vol. 55 (38). – P. 11668–11672.
52. Pominova D., Proydakova V., Romanishkin I., et al. Temperature sensing in the short-wave infrared spectral region using core-shell NaGdF4: Yb3+, Ho3+, Er3+@NaYF4 nanothermometers//Nanomaterials. – 2020. – 10 (10). – P. 1992
53. Pominova, D., Romanishkin, I., Proydakova, V., et al Optimization of upconversion luminescence excitation mode for deeper in vivo bioimaging without contrast loss or overheating.//Methods and Applications in Fluorescence. – 2020. – Vol. 8. – P. 025006
54. Kuznetsova, N.A., Gretsova N.S., Yuzhakova O.A., et al. New reagents for determination of the quantum efficiency of singlet oxygen generation in aqueous media//Russian Journal of General Chemistry. – 2001. – Vol.71 (1). – P. 36–41

FLUORESCENT DIAGNOSTICS WITH CHLORIN e6 IN SURGERY OF LOW-GRADE GLIOMA

Rynda A.Yu., Olyushin V.E., Rostovtsev D.M., Zabrodskaya Y.M., Papayan G.V.
Polenov Neurosurgical Institute – a branch of Almazov National Medical Research Center, Saint-Petersburg, Russia

Abstract

Intraoperative fluorescence diagnostics of high-grade gliomas is widely used in neurosurgical practice. This work analyzes the possibilities of fluorescence diagnostics for low-grade gliomas (LGG) using chlorin e6 photosensitizer. The study included patients with newly diagnosed LGG, for whom chlorin e6 was used for intraoperative fluorescence control at a dose of 1 mg/kg. During the operation, the fluorescence intensity of various areas of the putative tumor tissue was analyzed using the RSS Cam – Endo 1.4.313 software. Tissue samples with various degrees of fluorescence intensity were compared with the results of their histopathological analysis (WHO tumor diagnosis, Ki-67 index, P53, VEGF). Fluorescence was detected in more than half of the cases, but in most cases had a focal character and low fluorescence intensity. The fluorescence intensity directly correlated with the data of histopathological examination of tumor tissues (Ki-67 index (p=0.002), expression of P53 (p=0.0015) and VEGF (p=0.001)). The sensitivity of the method for LGG surgery was 72%, the specificity was 56,7%. Intraoperative fluorescence diagnostics with chlorin e6 can be used in LGG surgery, especially to visualize intratumoral areas with a higher degree of anaplasia.

Key words: low-grade gliomas, chlorin e6, intraoperative fluorescence diagnostics, neurooncology.

For citations: Rynda A.Yu., Olyushin V.E., Rostovtsev D.M., Zabrodskaya Yu.M., Papayan G.V. Fluorescent diagnostics with chlorin e6 in surgery of low-grade glioma, *Biomedical Photonics*, 2021, vol. 10, no. 4, pp. 35-43. doi: 10.24931/2413–9432–2021–10-4-35-43

Contacts: Rynda A.Yu., e-mail: artemii.rynda@mail.ru.

ФЛУОРЕСЦЕНТНАЯ ДИАГНОСТИКА С ХЛОРИНОМ e6 В ХИРУРГИИ ГЛИОМ НИЗКОЙ СТЕПЕНИ ЗЛОКАЧЕСТВЕННОСТИ

А.Ю. Рында, В.Е. Олюшин, Д.М. Ростовцев, Ю.М. Забродская, Г.В. Папаян
Российский нейрохирургический институт имени профессора А.Л. Поленова – филиал ФГБУ «Национальный медицинский исследовательский центр имени В.А. Алмазова», Санкт-Петербург, Россия

Резюме

Применение интраоперационной флуоресцентной диагностики для глиом высокой степени злокачественности широко используется в нейрохирургической практике. В работе проанализированы возможности флуоресцентной диагностики для глиом низкой степени злокачественности с использованием хлорина e6. В исследование были включены пациенты с впервые диагностированной глиомой низкой степени злокачественности (low-grade glioma, LGG), у которых с целью интраоперационного флуоресцентного контроля применен препарат хлорин e6 в дозе 1 мг/кг массы тела. В процессе операции анализировали интенсивность флуоресценции различных участков предполагаемой опухолевой ткани с использованием программного обеспечения RSS Cam – Endo 1.4.313. Образцы тканей различной степени интенсивности флуоресценции сопоставляли с результатами их гистопатологического анализа (диагностика опухоли ВОЗ, индекс Ki-67, P53, VEGF). Флуоресценция выявлена в более чем половине случаев, но в большинстве случаев имела очаговый характер и низкую интенсивность флуоресценции. Интенсивность флуоресценции напрямую коррелировала с данными гистопатологического исследования тканей опухоли: индекс Ki-67 (p=0,002), экспрессия P53 (p=0,0015), VEGF (p=0,001). Чувствительность метода для хирургии LGG составила 72%, специфичность 56,7%. Проведенное исследование подтвердило, что технология интраоперационной флуоресцентной диагностики с применением хлорина e6 может применяться в хирургии LGG, особенно для визуализации внутриопухолевых участков с более высокой степенью анаплазии.

Ключевые слова: глиомы низкой степени злокачественности, хлорин e6, интраоперационная флуоресцентная диагностика, нейроонкология.

Для цитирования: Рында А.Ю., Олюшин В.Е., Ростовцев Д.М., Забродская Ю.М., Папаян Г.В. Флуоресцентная диагностика с хлорином e6 в хирургии глиом низкой степени злокачественности // Biomedical Photonics. – 2021. – Т. 10, № 4. – С. 35–43. doi: 10.24931/2413–9432–2021–10-4-35-43

Контакты: Рында А.Ю., e-mail: artemii.rynda@mail.ru.

Introduction

Low-grade gliomas (LGGs) are a heterogeneous group of astrocytic and oligodendroglial tumors and account for about 20% of all newly diagnosed brain tumors, with an incidence of 5.2 cases per 100,000 people per year. The mean survival of patients with LGG ranges from 5 to 13 years. This wide range of LGG survival rates is most likely due to differences in clinical, histopathological, and molecular genetic factors. Age and clinical status, histopathological, molecular genetic (1p19q co-deletion, isocitrate dehydrogenase (IDH) mutation status, O^6-methylguanine methyltransferase promoter methylation status (MGMT)) and other factors play an important role in predicting the course of the disease in patients [1– four].

LGGs present a particular challenge for the neurosurgeon during surgery due to the histopathological heterogeneity of the tumor and the lack of a clear tumor margin. The goal of surgical intervention in LGG is to perform resection of the neoplasm to the maximum extent, but allowing to preserve neurological functions and create conditions for an optimal prognosis of the course of the disease. Therefore, new methods are needed to overcome this surgical problem [1, 3, 4]. Intraoperative imaging of brain tumors using fluorescence is one of the major advances in neurosurgery over the past decades. Initially, this method was used exclusively for surgery of high-grade gliomas (HGG) [5–8]. In recent years, the use of fluorescence has been extended to other cases, such as neuroimaging suspicion of LGG on MRI (CT) or PET [3, 7, 9, 10].

Commonly used modern neuronavigation systems (MRI spectroscopy, diffusion-weighted MRI, perfused-weighted MRI, PET using amino acids) lack accuracy when performing glioma resection due to the so-called "brain shift", leading to significant inaccuracies in image management, since neuronavigation is based on preoperative image data. The occurrence of brain shift during surgery with suspected LGG may preclude accurate detection of the tumor margin and anaplastic lesion. Insufficient intraoperative identification of LGG tissue, as well as insufficient differentiation of intratumoral HGG focal tissue, which is an anaplastic lesion in LGG tissue, are a serious problem for the neurosurgeon. As a result, incomplete resection is observed in 88% of cases with surgical intervention for LGG, and histopathological inaccuracy in postoperative diagnosis is not uncommon in routine neurosurgical practice [4, 6, 7, 9, 11].

Intraoperative imaging of brain tumor tissue using fluorescence is one of the most effective methods for visualizing tumor tissue during surgery [5, 6, 8, 13]. An analysis of modern literature sources has shown that there are very few works that have published the results of using fluorescence in LGG surgery [6, 7, 11, 14, 15].

In this study, we present our experience of using fluorescent navigation in LGG surgery using a medicinal product from the e6 chlorin group as a photosensitizer.

Materials and methods

The study involved 7 patients with LGG operated at the Russian Research Neurosurgical Institute named after prof. A.L. Polenova. All patients underwent fluorescent navigation with chlorin e6 during tumor resection in case of suspected newly diagnosed LGG. According to the postoperative pathohistological examination, two pilocytic astrocytomas (PA), two fibrillar protoplasmatic astrocytoma (FPA), two oligoastrocytomas (OA), and one oligodendroglioma (ODG) were diagnosed. There were 4 men in the study, 3 women (see table).

Preoperative neuroimaging assessment in all patients was performed according to MRI of the brain with gadolinium contrast enhancement using a Siemens apparatus (1.5 T) and PET with methionine. A mandatory criterion for inclusion of a patient in the study was the possibility of removing more than 90% of the tumor tissue according to the expected MRI data with contrast. To calculate the tumor volume from MRI data, the diameters at right angles were measured in the axial, frontal, and sagittal planes. The calculation was carried out according to the modified ellipsoidal volume according to the formula MER=A+B+C/2, where A, B, and C are the orthogonal values of the tumor.

Before surgery, all patients gave informed written consent to the administration of chlorin e6. No side effects associated with the use of 2nd generation chlorin e6 (photoditazine, produced by VETA-GRAND LLC, Russia) were noted in the study.

2 hours before the proposed durotomy, the patient was intravenously injected with the medicinal product chlorin e6 at the rate of 1 mg/kg of body weight, dissolved in 200 ml of isotonic solution. The vial with 0.9% sodium chloride solution was previously closed from the outside with an opaque material. During the operation, a modified neurosurgical microscope (Leica OHS-1) Karl Storz (Germany) with a built-in fluorescent module manufactured by LOMO (Saint-Petersburg, Russia) was used. During the operation, to visualize fluorescent tissue areas, the microscope was constantly switched to the fluorescent mode.

The fluorescence intensity was assessed using special software RSS Cam – Endo 1.4.313, which makes it possible to measure the fluorescence intensity in a given place in real time in numerical terms (Fig. 1A). The fluorescence intensity was distributed on a scale from 0 to 9 points depending on the numerical indicator in the software, where 0 is the complete absence of

Таблица
Клиническая характеристика пациентов
Table
Clinical characteristics of the patients

№п\п Sequential number	Пол Sex	Возраст Age	Доля мозга Lobe of the brain	Предоперационный индекс Карновского Preoperative Karnofsky index	Размеры опухоли (по данным МРТ), см^3 Tumor size (according to MRI data), cm^3	ПЭТ с метионином (индекс накопления РФП) PET with methionine (RP accumulation index)	Гистология Histology	Стадия Grade
1	М M	41	левая височная left temporal	80	5,5	0,15	пилоцитарная астроцитома pilocytic astrocytoma	I
2	Ж F	55	правая лобная right frontal	80	4,3	0,11	пилоцитарная астроцитома pilocytic astrocytoma	I
3	М M	45	левая височная и теменная left temporal and parietal	90	6,1	0,7	фибриллярно-протоплазматическая астроцитома fibrillar-protoplasmic astrocytoma	II
4	Ж F	60	правая лобная right frontal	70	3,7	0,91	фибриллярно-протоплазматическая астроцитома fibrillar-protoplasmic astrocytoma	II
5	М M	33	правая височная right temporal	80	6,3	0,78	олигоастроцитома oligoastrocytoma	II
6	Ж F	29	левая височная left temporal	80	4,9	0,93	олигоастроцитома oligoastrocytoma	II
7	М M	47	правая лобная и височная right frontal and temporal	90	6,7	0,55	олигодендроглиома oligodendroglioma	II

fluorescence, 9 is a bright red intense glow. During the operation, a biopsy was performed from fluorescent and non-fluorescent areas of the tumor. A total of 80 biopsy samples with different fluorescence intensities were examined.

The biopsy material obtained during the operation was fixed in 10% buffered formalin, dehydrated and embedded in paraffin. Next, sections 3 μm thick were stained with hematoxylin-eosin.

Immunohistochemical (IHC) markers were also detected, in particular, Ki-67 (MIB-1), p53 (TP53), and VEGF (vascular endothelial growth factor) (Fig. 1Д). The paraffin blocks were sectioned 3-5 μm thick, deparaffinized using xylene, and rehydrated with various concentrations of ethanol. Sections were dried in a thermostat at 45°C. The standard IHC protocol was used with antigen demasking in a water bath (GFL, 1002), using primary antibodies from Dako (Ki-67, Clone Mib-1, cat. no. M7240; P53, Clone DO-7, cat. no. M7001; VEGF, Clone VC1, cat. no. M7273) and imaging systems from Diagnostic BioSystems (UMR1000PD-BMS).

The Ki-67 proliferation index was determined by the percentage of cells with immunoreactive nuclei to the total number of cells. According to WHO (2016),

these parameters are as follows: G I – 1-3%, G II – 4-5%, G III – 5-10%, G IV – an average of 15-20% and above.

For the IHC study of P53, monoclonal antibodies DO-7 were used, which detect both wtP53 and mtP53. It is believed that the IHC response depends mainly on the presence of mtP53 in the tissue, since wtP53 is a short-lived protein with a half-life of no more than 20 min, and its content may be below the sensitivity of the IHC study. The half-life of mtP53 lasts up to 24 hours, so the level of its accumulation in the tissue is sufficient for visualization. To quantify the proliferative activity, as well as the expression of the P53 protein, the ratio of stained nuclei per 300 cells was calculated at a magnification of 400 times. Conditionally, the following gradation was adopted: no expression (0 points); weak expression (1 point) – less than 10% of cell nuclei are stained; moderate expression (2 points) – more than 10% of the nuclei are stained, but less than 33%; strong expression (3 points) – more than 33% of cell nuclei in the tissue are positive. The color of more than 5% of cell nuclei was considered as the control level.

The expression level of VEGF was estimated as % of the control level (0.4 ng/ml), the measurement was carried out in ng/mg.

Subsequently, intraoperative fluorescence data were compared with the data obtained from the results of histopathological examination.

Statistical analysis was performed using the STATISTICA 13.0 software package (StatSoft, USA). When correlating non-binary variables such as Ki-67 (MIB-1), p53 (TP53), VEGF, histological subtype with fluorescence intensity categorical variables, the Mann-Whitney U-test was used. Statistical analysis of other data was performed using non-parametric methods using Spearman's rank correlation coefficient. Differences were considered statistically significant at $p<0.05$.

Results

Visual fluorescence was obtained in 4 out of 7 patients. In 2 observations, fluorescence had a focal character, in 2 cases it was homogeneous. Fluorescence was further studied using the RSS Cam–Endo 1.4.313 software (Fig. 1A). Out of 50 biopsies with varying fluorescence intensity, about 26% were false positives according to the software, which was confirmed by histopathological examination. But, despite this, the sensitivity of the technique in detecting tumor sites was high (Fig. 1Б) (p=0.002).

When studying the distribution of fluorescence intensity in areas of tumor tissue depending on the WHO histological classification of tumors of the central nervous system (2016), it was found that ODG (Grade II) was characterized by a greater number of intense fluorescence regions and a more developed vascular network. The smallest number of fluorescence sites was characteristic of PA (Grade I), in addition, they were characterized by the largest number of false positive fluorescence sites in the analysis of biopsy material (Fig. 1B). Pronounced development of the vascular network was characteristic of FPA.

In the study of the relationship between the fluorescence intensity of LGG tumor tissue areas and the data of their histopathological examination (Ki-67, P53, VEGF), a direct correlation was obtained. The higher the fluorescence intensity, the higher the Ki-67 nuclear expression index (p=0.002), the higher the level of transcription factor of the cell cycle protein P53 (p=0.002), the higher the level of VEGF expression (p=0.001) (Fig. 2). A stronger correlation was between fluorescence intensity and VEGF expression (p=0.001) (Fig. 2C).

A study of the sensitivity and specificity of the fluorescent navigation method for LGG surgery, based on the evaluation of histopathological data from fluorescent and non-fluorescent biopsy specimens, showed that the sensitivity of the method was 72% (36/50), the specificity was 56.7% (13/30) (p= 0.003).

Clinical example

A 45-year-old patient was admitted with a diagnosis of a mass lesion in the left temporal and parietal lobes of the brain. From the anamnesis it is known that he has been ill for a year, when he began to notice the following symptoms: headache, difficulty in pronouncing words, convulsions. The neurologist sent for an MRI of the brain with contrast enhancement. A volumetric formation of the left temporal and parietal lobes was revealed, evenly accumulating a contrast agent with a moderate change in the architectonics of the gyri. According to PET-CT of the brain with methionine, the accumulation index of the radiopharmaceutical agent (RPC) is 0.7.

During the operation, the method of fluorescent diagnostics with a preparation of the chlorin e6 group (photoditazine) was used. A microscope Leica-OHS1 with a fluorescent module developed by LOMO (St. Petersburg) was used. During the removal of the tumor in the fluorescent mode, a red glow (5–6 points) was noted, homogeneous in all areas of the altered tissue. Histopathological examination revealed fibrillar-protoplasmatic astrocytoma (Grade II) (Fig. 3).

Discussion

In the study of Goryainov S.A. et al. [3], which included 27 patients with morphologically confirmed LGG, of which 14 were diagnosed with diffuse astrocytoma, 6 with ODG, 4 with PA, 2 with gemistocytic astrocytoma, 1 with desmoplastic ganglioglioma, visible fluorescence of 5-aminolevulinic acid (5 -ALK) was detected in 14 (52%) patients. According to the homo-

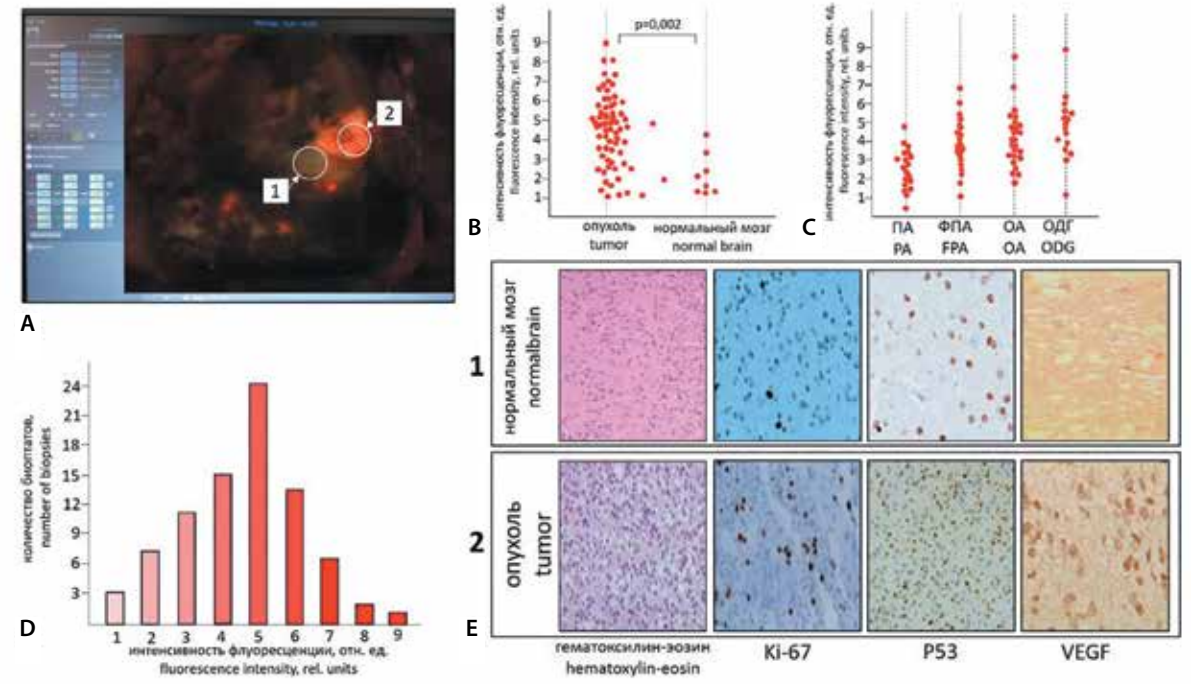

Рис. 1. Анализ интенсивности флуоресценции участков опухолевой ткани. А – анализ флуоресценции участков ткани с использованием программного обеспечения RSS Cam – Endo 1.4.313; В – зависимость между интенсивностью флуоресценции биоптата и результата гистологического исследования (опухоль – неизмененная мозговая ткань) (p=0,002); С – распределение интенсивности флуоресценции в участках опухолевой ткани в зависимости от гистологической классификации опухоли по данным ВОЗ (ПА – пилоцитарная астроцитома, ФПА – фибриллярно-протоплазматическая астроцитома, ОА – олигоастроцитома, ОДГ – олигодендроглиома); D – график распределения интенсивности флуоресценции в отобранных биоптатах; Е – гистопатологическое исследование участков опухоли в зависимости от интенсивности флуоресценции.

Fig. 1. Analysis of the intensity of fluorescence of areas of tumor tissue. A – analysis of the fluorescence of tissue sites using the RSS Cam Endo 1.4.313 software; B – the relationship between the fluorescence intensity of the biopsy specimen and the result of histological examination (tumor – unchanged brain tissue (normal brain)) (p=0,002); C – distribution of fluorescence intensity in areas of tumor tissue depending on the histological classification of the tumor according to WHO data (PA – pilocytic astrocytoma, FPA – fibrillar-protoplasmic astrocytoma, OA – oligoastrocytoma, ODG – oligodendroglioma); D – graph of the distribution of fluorescence intensity in the selected biopsy specimens; E – histopathological examination of tumor sites depending on the intensity of fluorescence.

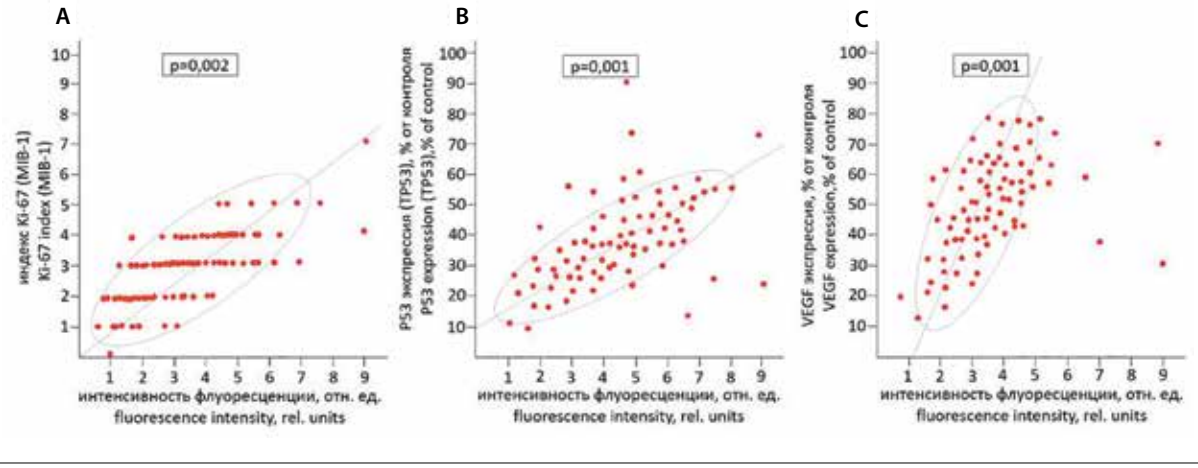

Рис. 2. Зависимость между интенсивностью флуоресценции участков опухолевой ткани и индексом ядерной экспрессии Ki-67 (MIB-1) (А); экспрессией транскрипционного фактора клеточного цикла P53 (TP53) (В) и VEGF (С).

Fig. 2. Dependence between the intensity of fluorescence of tumor tissue sites and the index of Ki-67 nuclear expression (MIB-1) (A); cell cycle transcription factor P53 (TP53) expression (B) and VEGF expression (C).

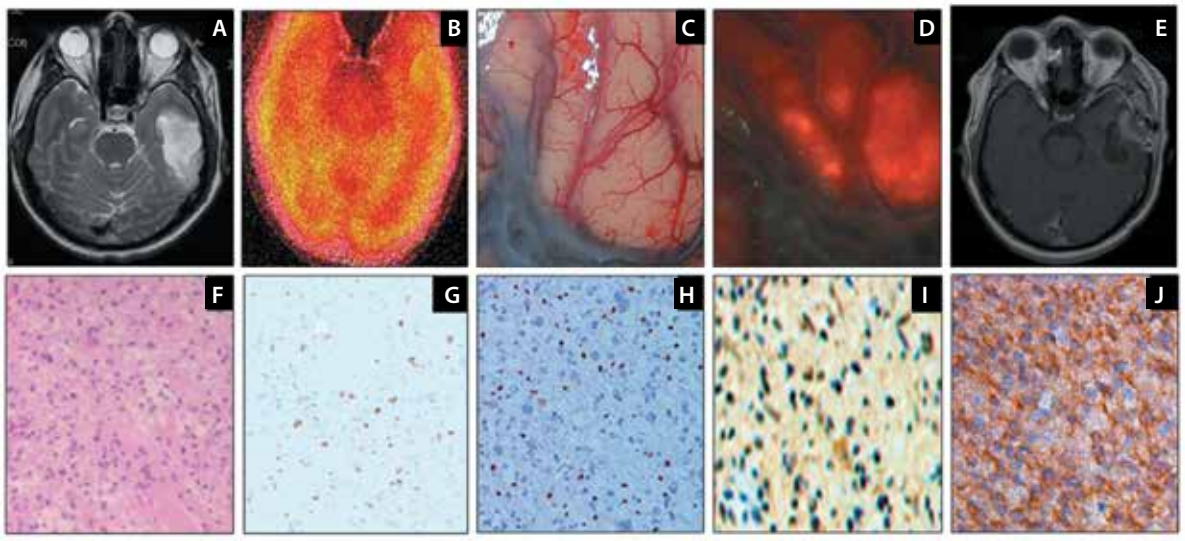

Рис. 3. Фибриллярно-протоплазматическая астроцитома левой теменной и височной долей головного мозга.
A – предоперационное МРТ головного мозга с контрастом (Т2-режим);
B – ПЭТ с метионином (индекс накопления РФП – 0,7);
C – интраоперационная картина без флуоресцентного режима;
D – интраоперационная картина, полученная во флуоресцентном режиме с хлорином е6;
E – послеоперационное МРТ,
F – фибриллярно-протоплазматическая астроцитома. Окрашивание гематоксилин-эозином. Иммуногистохимия. Ув. 200;
G – экспрессия белка пролиферативной активности Ki-67= 9. Иммуногистохимия. Ув. 200;
H – экспрессия транскрипционного фактора клеточного цикла P53 (+). Иммуногистохимия. Ув. 200;
I – экспрессия транскрипционного фактора Olig 2. Иммуногистохимия. Ув. 200;
J – экспрессия VEGF (+). Иммуногистохимия. Ув. 400.

Fig. 3. Fibrillar-protoplasmic astrocytoma of the left parietal and temporal lobes.
A – preoperative MRI of the brain with contrast (T2-mode);
B – PET with methionine (index of RP accumulation – 0.7);
C – intraoperative picture without fluorescence mode;
D – intraoperative picture in fluorescent mode with chlorin e6;
E – postoperative MRI;
F – hematoxylin-eosin (magnification 200);
G – Ki-67 protein expression (index of proliferative activity – 9). Immunohistochemistry. (magnification 200);
H – cell cycle transcription factor P53 (+) expression. Immunohistochemistry. (magnification 200);
I – transcription factor Olig 2 expression. Immunohistochemistry. (magnification 200);
J – VEGF (+) expression. Immunohistochemistry. (magnification 400).

geneity of fluorescence, 7 tumors showed diffuse fluorescence, 7 gliomas showed focal fluorescence. Cell density and proliferation rate were significantly higher in positive fluorescent samples than in negative fluorescent samples.

Jaber M. et al. [9] found fluorescence in 16 (21.6%) LGG patients out of 74. Fluorescence was partly associated with weak enhancement on MRI and increased radiopharmaceutical uptake on PET-CT, and was not related to Karnofsky score, tumor size, or patients' age. With regard to molecular markers, only increased EGFR expression differed slightly (in 19% in fluorescent tumors, versus 5% in non-fluorescent ones (p=0.057). The median of the relapse-free period was shorter in fluorescent tumors and amounted to 46.4 months (95% CI 41.8-51.1 months). At the same time, IDH status and the presence of fluorescence were directly dependent on the duration of the period before malignant transformation of the tumor and overall survival.

When working with 5-ALA Ji S.Y. et al. [4] also recorded fluorescence in Grade I–II gliomas. Fluorescence was detected in 5 out of 9 patients with PA, in 3 cases of strong intensity, in 2 – weak. All PA could be completely removed regardless of the positive fluorescence. Out of 87 patients with Grade II gliomas, ODG predominated (57.5%, n=50). The majority of ODG showed no fluorescence (82.0%). However, there were

9 cases of fluorescence with a positive result (18.0%), including 2 cases with high intensity (4.0%). Out of 20 patients with diffuse astrocytic gliomas and OA, fluorescence was absent in 18 cases, and focal fluorescence was observed in 2 cases. Total resection was achieved in 15 patients, including those with positive fluorescence.

In an additional study published in 2017, Saito K. et al. [16] evaluated the relationship between 5-ALA fluorescence and proliferation rate, as well as molecular markers, including IDH1 mutation status and 1p19q co-deletion in a series of anaplasia grade II gliomas. Univariate analysis showed that 5-ALA fluorescence was significantly associated with proliferation rate, as well as IDH1 mutation status and 1p19q co-deletion. According to multivariative analysis, only IDH1 status remained a statistically significant factor. Gliomas with visible 5-ALA fluorescence showed a significantly higher incidence of wild-type IDH1 tumors.

T. Tsurubuchi et al. [17] used chlorin e6 (talaporfin sodium) in LGG surgery. The scientists observed strong fluorescence in a patient with PA, although only 1 case was studied. In patients with ODG with a large volume of the vascular bed of the tumor, they also managed to reliably fix fluorescence during a morphological study.

In the work of J. Akimoto et al. [18], studying intraoperative fluorescence using the photosensitizer chlorin e6 (talaporfin sodium), a weak fluorescence intensity in all patients with Grade II gliomas was revealed. The average concentration of chlorin e6 in tissues was 1.62 μg/g in areas with strong fluorescence, 0.67 μg/g with weak fluorescence and 0.19 μg/g without fluorescence.

In general, fluorescent diagnostics is of limited use in Grade I–II glioma surgery and can be used to a greater extent for visualization of anaplastic areas of the tumor. The sensitivity of the method, according to different authors, varies from 20 to 58% [3, 5, 14, 15, 19, 20]. Fluorescence can serve as a marker for the onset of malignant transformation and is an independent marker in contrast to known prognostic factors. LGG fluorescence can be taken into account when choosing adjuvant therapy [3, 19].

In our study, we obtained a high sensitivity of the fluorescent navigation technique in LGG surgery (72%), which is most likely due to a small sample of patients, and creates the need for further study of this issue. However, the specificity of the technique (56.7%) is comparable with the data obtained by a number of other authors [3, 9, 12, 17, 18].

Conclusion

The use of intraoperative fluorescent navigation with chlorin e6 in the treatment of patients with low-grade gliomas provides the doctor with additional information about the structure of the tumor in a particular patient, which allows the neurosurgeon to individualize the approach to surgical tactics during surgery. Further research in this direction seems promising in terms of determining the volume of resected tissues, which allows maintaining the ablasticity of the intervention and does not adversely affect the patient's quality of life.

REFERENCES

1. Diwanji T.P., Engelman A., Snider J.W., Mohindra P. Epidemiology, Diagnosis, and Optimal Management of Glioma in Adolescents and Young Adults, *Adolescent Health, Medicine and Therapeutics*, 2017, no. 8, pp. 99–113. https://doi.org/10.2147/AHMT.S53391
2. Lombardi G., Barresi V., Castellano A. et al. Clinical Management of Diffuse Low-Grade Gliomas, *Cancers*, 2020, vol. 12, no. 10, pp. 3008. https://doi.org/10.3390/cancers12103008
3. Goryaynov S.A., Widhalm G., Goldberg M.F. et al. The Role of 5-ALA in Low-Grade Gliomas and the Influence of Antiepileptic Drugs on Intraoperative Fluorescence, *Frontiers in Oncology*, 2019, no. 9, pp.423. https://doi.org/10.3389/fonc.2019.00423
4. Ji S.Y., Kim J.W., Park C.K. Experience Profiling of Fluorescence-Guided Surgery I: Gliomas, *Brain Tumor Research and Treatment*, 2019, vol. 7, no. 2, pp. 98–104. https://doi.org/10.14791/btrt.2019.7.e38
5. Rynda A.Yu., Rostovtsev D.M., Olyushin V.E. Fluorescence-Guided Resection of Glioma – literature review, *Rossijskij nejroxirurgicheskij zhurnal imeni professora A.L. Polenova*, 2018, vol. 10, no. 1, pp. 97–110. (In Russ.)
6. Goryaynov S.A., Potapov A.A., Pitskhelauri D.I. et al. Intraoperative Fluorescence Diagnosis and Laser Spectroscopy in

ЛИТЕРАТУРА

1. Diwanji T.P., Engelman A., Snider J.W., Mohindra P. Epidemiology, Diagnosis, and Optimal Management of Glioma in Adolescents and Young Adults//Adolescent Health, Medicine and Therapeutics.– 2017.– Vol.8.– P.99–113. https://doi.org/10.2147/AHMT.S53391
2. Lombardi G., Barresi V., Castellano A., Tabouret E., Pasqualetti F., Salvalaggio A., Cerretti G., Caccese M., Padovan M., Zagonel V., Ius T. Clinical Management of Diffuse Low-Grade Gliomas//Cancers.– 2020.– Vol.12 (10).– P.3008. https://doi.org/10.3390/cancers12103008
3. Goryaynov S.A., Widhalm G., Goldberg M.F., Chelushkin D., Spallone A., Chernyshov K.A., Ryzhova M., Pavlova G., Revischin A., Shishkina L., Jukov V., Savelieva T., Loschenov V., Potapov A. The Role of 5-ALA in Low-Grade Gliomas and the Influence of Antiepileptic Drugs on Intraoperative Fluorescence//Frontiers in Oncology.– 2019.– Vol.9.– P.423. https://doi.org/10.3389/fonc.2019.00423
4. Ji S.Y., Kim J.W., Park C.K. Experience Profiling of Fluorescence-Guided Surgery I: Gliomas//Brain Tumor Research and Treatment.– 2019. –Vol.7 (2).– P.98–104. https://doi.org/10.14791/btrt.2019.7.e38

Repeated Operations for Brain Gliomas, *Zhurnal Voprosy Neyrokhirurgii imeni N. N. Burdenko*, 2014, vol. 78, no. 2, pp. 22–31. (In Russ.). https://doi.org/zhurnal-voprosy-nejrokhirurgii-imeni-n-n-burdenko/2014/2/030042–8817201423

7. Opoku-Darko M., Lang S.T., Artindale J., Cairncross J.G., Sevick R.J, Kelly J.J.P. Surgical management of incidentally discovered diffusely infiltrating low-grade glioma, *Journal of Neurosurgery*, 2018, no. 129, pp.19–26. https://doi.org/10.3171/2017.3.JNS17159
8. Rynda A.Yu., Olyushin V.E., Rostovtsev D.M. et al. Intraoperative fluorescence control with chlorin E6 in resection of glial brain tumors, *Zhurnal Voprosy Neirokhirurgii Imeni N. N. Burdenko*, 2021, vol. 85, no. 4, pp. 20–28. (In Russ.). https://doi.org/10.17116/neiro20218504120
9. Jaber M., Wölfer J., Ewelt C. et al. The value of 5-aminolevulinic acid in low-grade gliomas and high-grade gliomas lacking glioblastoma imaging features: an analysis based on fluorescence, magnetic resonance imaging, 18F-fluoroethyl tyrosine positron emission tomography, and tumor molecular factors, *Neurosurgery*, 2016, no. 78, pp.401–411. https://doi.org/10.1227/NEU.0000000000001020.
10. Shaver M.M., Kohanteb P.A., Chiou C. et al. Optimizing Neuro-Oncology Imaging: A Review of Deep Learning Approaches for Glioma Imaging, *Cancers*, 2019, vol. 11, no. 6, pp. 829. https://doi.org/10.3390/cancers11060829
11. Mert A., Kiesel B., Wohrer A. et al. Introduction of a Standardized Multimodality Image Protocol for Navigation-Guided Surgery of Suspected Low-Grade Gliomas, *Neurosurgical Focus*, 2015, vol. 38, no. 1, pp. E4. https://doi.org/10.3171/2014.10.FOCUS14597
12. Hendricks B.K., Sanai N., Stummer W. Fluorescence-guided surgery with aminolevulinic acid for low-grade gliomas, *Journal of Neuro-Oncology*, 2019, no. 141, pp. 13–18. https://doi.org/10.1007/s11060–018–03026–6
13. Rynda A.Yu., Zabrodskaya Yu.M. et al. Morphological evaluation of the effectiveness of fluorescence navigation with chlorin e6 in surgery for malignant gliomas, *Arkhiv Patologii*, 2021, vol. 83, no. 5, pp. 13–20. (In Russ.). https://doi.org/10.17116/patol20218305113
14. Widhalm G., Olson J., Weller J., Bravo J. et al. The value of visible 5-ALA fluorescence and quantitative protoporphyrin IX analysis for improved surgery of suspected low-grade gliomas, *Journal of Neurosurgery*, 2019, no. 10, pp. 1–10. https://doi.org/10.3171/2019.1.JNS182614
15. Sanai N., Snyder L.A., Honea N.J. et al. Intraoperative confocal microscopy in the visualization of 5-aminolevulinic acid fluorescence in low-grade gliomas, *Journal of Neurosurgery*, 2011, no. 115, pp. 740–748. https://doi.org/10.3171/2011.6.JNS11252
16. Saito K., Hirai T., Takeshima H. et al. Genetic Factors Affecting Intraoperative 5-Aminolevulinic Acid-Induced Fluorescence of Diffuse Gliomas, *Radiology and Oncology*, 2017, vol. 51, no. 2, pp. 142–150. https://doi.org/10.1515/raon-2017–0019
17. Tsurubuchi T., Zaboronok A., Yamamoto T. et al. The optimization of fluorescence imaging of brain tumor tissue differentiated from brain edema – in vivo kinetic study of 5-aminolevulinic acid and talaporfin sodium, *Photodiagnosis and Photodynamic Therapy*, 2009, vol. 6, no. 1, pp.19–27. https://doi.org/10.1016/j.pdpdt.2009.03.005
18. Akimoto J., Fukami S., Ichikawa M., Mohamed A., Kohno M. Intraoperative Photodiagnosis for Malignant Glioma Using Photosensitizer Talaporfin Sodium, *Frontiers in Surgery*, 2019, vol. 21, no. 6, pp. 12. https://doi.org/10.3389/fsurg.2019.00012

5. Рында А.Ю., Ростовцев Д.М., Олюшин В.Е. Флуоресцентно-контролируемая резекция астроцитарных опухолей головного мозга – обзор литературы//Российский нейрохирургический журнал имени профессора А.Л. Поленова. – 2018. – Т. 10, № 1. – С. 97–110.
6. Горяйнов С.А., Потапов А.А., Пицхелаури Д.И., Кобяков Г.Л., Охлопков В.А., Гаврилов А.Г., Шурхай В.А., Жуков В.Ю., Шишкина Л.В., Лощенов В.Б., Савельева Т.А., Кузьмин С.Г., Чумакова А.П., Spallone A. Интраоперационная флуоресцентная диагностика и лазерная спектроскопия при повторных операциях по поводу глиом головного мозга//Журнал «Вопросы нейрохирургии» имени Н.Н. Бурденко. – 2014. – Т. 78, № 2. – С. 22–31. https://doi.org/zhurnal-voprosy-nejrokhirurgii-imeni-n-n-burdenko/2014/2/030042–8817201423
7. Opoku-Darko M., Lang S.T., Artindale J., Cairncross J.G., Sevick R.J., Kelly J.J.P. Surgical management of incidentally discovered diffusely infiltrating low-grade glioma//Journal of Neurosurgery. – 2018. – Vol.129. – P.19–26. https://doi.org/10.3171/2017.3.JNS17159
8. Рында А.Ю., Олюшин В.Е., Ростовцев Д.М., Забродская Ю.М., Тастанбеков М.М., Папаян Г.В. Результаты использования интраоперационного флюоресцентного контроля с хлорином Е6 при резекции глиальных опухолей головного мозга//Журнал «Вопросы нейрохирургии» имени Н.Н. Бурденко. – 2021. – Т. 85, № 4. – С. 20–28. https://doi.org/10.17116/neiro20218504120
9. Jaber M., Wölfer J., Ewelt C., Holling M., Hasselblatt M.., Niederstadt T., Zoubi T., Weckesser M., Stummer W. The value of 5-aminolevulinic acid in low-grade gliomas and high-grade gliomas lacking glioblastoma imaging features: an analysis based on fluorescence, magnetic resonance imaging, 18F-fluoroethyl tyrosine positron emission tomography, and tumor molecular factors//Neurosurgery. – 2016. – Vol.78. – P.401–411. https://doi.org/10.1227/NEU.0000000000001020.
10. Shaver M.M., Kohanteb P.A., Chiou C., Bardis M.D., Chantadu ly C., Bota D., Filippi C.G., Weinberg B., Grinband J., Chow D.S., Chang P.D. Optimizing Neuro-Oncology Imaging: A Review of Deep Learning Approaches for Glioma Imaging//Cancers. – 2019. – Vol.11 (6). – P.829. https://doi.org/10.3390/cancers11060829
11. Mert A., Kiesel B., Wohrer A., Martinez-Moreno M., Minchev G., Furtner J., Knosp E., Wolfsberger S., Widhalm G. Introduction of a Standardized Multimodality Image Protocol for Navigation-Guided Surgery of Suspected Low-Grade Gliomas//Neurosurgical Focus. – 2015. – Vol.38 (1). – P.E4. https://doi.org/10.3171/2014.10.FOCUS14597
12. Hendricks B.K., Sanai N., Stummer W. Fluorescence-guided surgery with aminolevulinic acid for low-grade gliomas//Journal of Neuro-Oncology. – 2019. – Vol.141. – P.13–18. https://doi.org/10.1007/s11060–018–03026–6
13. Рында А.Ю., Забродская Ю.М., Олюшин В.Е., Ростовцев Д.М., Соколова Т.В., Папаян Г.В. Морфологическая оценка эффективности флуоресцентной навигации с хлорином е6 в хирургии злокачественных глиом//Архив патологии. – 2021. – Vol. 83 (5). – С.13–20. https://doi.org/10.17116/patol20218305113
14. Widhalm G., Olson J., Weller J., Bravo J., Han S.J., Phillips J., Hervey-Jumper S.L., Chang S.M., Roberts D.W., Berger M.S. The value of visible 5-ALA fluorescence and quantitative protoporphyrin IX analysis for improved surgery of suspected low-grade gliomas//Journal of Neurosurgery. – 2019. – Vol. 10. – P. 1–10. https://doi.org/10.3171/2019.1.JNS182614
15. Sanai N., Snyder L.A., Honea N.J., Coons S.W., Eschbacher J.M., Smith K.A., Robert F., Spetzler M.D. Intraoperative confocal mi-

19. Jaber M., Ewelt C., Wölfer J., Brokinkel B., Thomas C., Hasselblatt M., Grauer O., Stummer W. Is Visible Aminolevulinic Acid-Induced Fluorescence an Independent Biomarker for Prognosis in Histologically Confirmed (World Health Organization 2016) Low-Grade Gliomas? *Neurosurgery*, 2019, vol. 81, no. 6, pp.1214–1224. https://doi.org/10.1093/neuros/nyy365.
20. Kiesel B., Freund J., Reichert D., Wadiura L., Erkkilae M.T., Woehrer A., Hervey-Jumper S., Berger M.S., Widhalm G. 5-ALA in Suspected Low-Grade Gliomas: Current Role, Limitations, and New Approaches, *Frontiers Oncology*, 2021, vol. 11, pp. 699301. https://doi.org/10.3389/fonc.2021.699301

croscopy in the visualization of 5-aminolevulinic acid fluorescence in low-grade gliomas//Journal of Neurosurgery. – 2011. – Vol.115. – P.740–748. https://doi.org/10.3171/2011.6.JNS11252
16. Saito K., Hirai T., Takeshima H., Kadota Y., Yamashita S., Ivanova A., Yokogami K. Genetic Factors Affecting Intraoperative 5-Aminolevulinic Acid-Induced Fluorescence of Diffuse Gliomas//Radiology and Oncology. – 2017. – Vol. 51 (2). – P. 142–150. https://doi.org/10.1515/raon-2017–0019
17. Tsurubuchi T., Zaboronok A., Yamamoto T., Nakai K., Yoshida F., Shirakawa M., Matsuda M., Matsumura A. The optimization of fluorescence imaging of brain tumor tissue differentiated from brain edema – in vivo kinetic study of 5-aminolevulinic acid and talaporfin sodium//Photodiagnosis and Photodynamic Therapy. – 2009. – Vol. 6 (1). – P.19–27. https://doi.org/10.1016/j.pdpdt.2009.03.005
18. Akimoto J., Fukami S., Ichikawa M., Mohamed A., Kohno M. Intraoperative Photodiagnosis for Malignant Glioma Using Photosensitizer Talaporfin Sodium//Frontiers in Surgery. – 2019. – Vol.21 (6). – P. 12. https://doi.org/10.3389/fsurg.2019.00012
19. Jaber M., Ewelt C., Wölfer J., Brokinkel B., Thomas C., Hasselblatt M., Grauer O., Stummer W. Is Visible Aminolevulinic Acid-Induced Fluorescence an Independent Biomarker for Prognosis in Histologically Confirmed (World Health Organization 2016) Low-Grade Gliomas?//Neurosurgery. – 2019. – Vol. 84 (6). – P. 1214–1224. https://doi.org/10.1093/neuros/nyy365.
20. Kiesel B., Freund J., Reichert D., Wadiura L., Erkkilae M.T., Woehrer A., Hervey-Jumper S., Berger M.S., Widhalm G. 5-ALA in Suspected Low-Grade Gliomas: Current Role, Limitations, and New Approaches//Frontiers Oncology. – 2021. – Vol.11. – P. 699301. https://doi.org/10.3389/fonc.2021.699301

ORIGINAL ARTICLES

PHOTO-INDUCED PROCESSES OF IRON OXIDE NANOPARTICLES TO ENHANCE LASER THERAPY

Pominova D.V.[1,2], Romanishkin I.D.[1], Plotnikova E.A.[3], Morozova N.B.[3], Loschenov V.B.[1,2], Wittig R.[4], Linden M.[5], Steiner R.W.[2], Ryabova A.V.[1,2]
[1]Prokhorov General Physics Institute of the Russian Academy of Sciences, Moscow, Russia
[2]National Research Nuclear University «MEPhI», Moscow, Russia
[3]P.A. Herzen Moscow Oncology Research Center – branch of FSBI NMRRC of the Ministry of Health of the Russian Federation, Moscow, Russia
[4]Institute for Laser Technologies in Medicine & Metrology, Ulm, Germany
[5]Institute for Inorganic Chemistry II at Ulm University, Ulm, Germany

Abstract

Nanoparticles are used as drug carriers to increase the selectivity and effectiveness of therapy, as well as for combined therapy that utilizes different effects. Iron oxide nanoparticles are promising in this aspect. Due to magnetic properties, they can be used as a contrast agent for magnetic resonance imaging. Also, iron oxide nanoparticles could be coated with a photosensitizer for photodynamic therapy and their laser or magnetic heating can be used for phototherapy. Local enhancement of the electromagnetic field near iron oxide nanoparticles can increase the fluorescence intensity of photosensitizers and the efficiency of singlet oxygen generation.

This paper presents the results of a study of iron oxide nanoparticles focused on the photophysical aspects of the formation of "hot spots" under laser irradiation. The photoinduced effects of iron oxide nanoparticles observed in *in vitro* experiments lead to the rupture of lysosomes. Theoretical modeling showed that the heating of iron oxide nanoparticles with a radius of 35 nm under the action of laser radiation is about 89°C and 19°C for wavelengths of 458 and 561 nm, respectively. Local field enhancement occurs in pairs of nanoparticles of various sizes and strongly depends on the distance between them. The maximum gain is achieved at small distances between nanoparticles. For a dimer of nanoparticles with radii of 10 and 35 nm at a distance of 1 nm, an enhancement factor of two orders of magnitude was obtained. The investigated phenomenon of «hot spots» is in demand for precision therapy, because the photo-induced processes occur at small distances between nanoparticles, in areas of their high accumulation.

Keywords: Iron oxide nanoparticles, plasmon polaritons, «hot spots», modeling, laser hyperthermia, electromagnetic field amplification.

For citations: Pominova D.V., Romanishkin I.D., Plotnikova E.A., Morozova N.B., Loschenov V.B., Wittig R., Linden M., Steiner R.W., Ryabova A.V. Photo-induced processes of iron oxide nanoparticles to enhance laser therapy, *Biomedical Photonics*, 2021, vol. 10, no. 4, pp. 44–58. doi: 10.24931/2413–9432–2021–10-4-44-58

Contacts: Ryabova A.V., e-mail: nastya.ryabova@gmail.com

ФОТОИНДУЦИРОВАННЫЕ ПРОЦЕССЫ НАНОЧАСТИЦ ОКСИДА ЖЕЛЕЗА ДЛЯ УСИЛЕНИЯ ЛАЗЕРНОЙ ТЕРАПИИ

Д.В. Поминова[1,2], И.Д. Романишкин[1], Е.А. Плотникова[3], Н.Б. Морозова[3], В.Б. Лощенов[1,2], R. Wittig[4], M. Linden[5], R.W. Steiner[2], А.В. Рябова[1,2]
[1]Институт общей физики им. А.М. Прохорова Российской академии наук, Москва, Россия
[2]Национальный исследовательский ядерный университет «МИФИ», Москва, Россия
[3]Московский научно-исследовательский онкологический институт им. П.А. Герцена – филиал ФГБУ «Национальный медицинский исследовательский центр радиологии» Министерства здравоохранения Российской Федерации, Москва, Россия
[4]Институт лазерных технологий в медицине и метрологии, Ульм, Германия
[5]Институт неорганической химии II Университета г. Ульм, Ульм, Германия

Резюме

Наночастицы используются в качестве носителей лекарственных средств для повышения селективности и эффективности терапии, а также для сочетанной терапии, объединяющей разные виды воздействия. Перспективными в этом аспекте являются наночастицы оксида железа. Благодаря магнитным свойствам, они могут быть применяться в качестве контраста для магнитно-резонансной томографии. Также наночастицы оксида железа могут быть покрыты фотосенсибилизатором для фотодинамической терапии, а их лазерный или магнитный нагрев этих частиц может используется для проведения фототерапии. При этом локальное усиление электромагнитного поля вблизи наночастиц оксида железа может повысить интенсивность флуоресценции фотосенсибилизаторов и эффективность генерации синглетного кислорода.

В работе представлены результаты исследования наночастиц оксида железа, сфокусированного на фотофизических аспектах образования «горячих точек» при лазерном облучении. Фотоиндуцированные эффекты наночастиц оксида железа, наблюдаемые в экспериментах *in vitro*, приводят к разрыву лизосом. Теоретическое моделирование показало, что нагрев наночастиц оксида железа радиусом 35 нм под действием лазерного излучения составляет порядка 89°C и 19°C для длин волн 458 и 561 нм, соответственно. Локальное усиление поля возникает в парах из наночастиц различного размера и сильно зависит от расстояния между ними. Максимальное усиление достигается при малых расстояниях между наночастицами. Для димера наночастиц с радиусами 10 нм и 35 нм на расстоянии 1 нм получен фактор усиления на два порядка. Рассмотренное явление «горячих точек» востребовано для прецизионной терапии, так как фотоиндуцированные процессы возникают на малых расстояниях между наночастицами, в областях с их высоким накоплением.

Ключевые слова: наночастицы оксида железа, плазмон-поляритоны, «горячие точки», моделирование, лазерная гипертермия, усиление электромагнитного поля.

Для цитирования: Поминова Д.В., Романишкин И.Д., Плотникова Е.А., Морозова Н.Б., Лощенов В.Б., Wittig R., Linden M., Steiner R.W., Рябова А.В. Фотоиндуцированные процессы наночастиц оксида железа для усиления лазерной терапии // Biomedical Photonics. – 2021. – Т. 10, № 4. – С. 44–58. doi: 10.24931/2413–9432–2021–10-4-44-58

Контакты: Рябова А.В., e-mail: nastya.ryabova@gmail.com

Introduction

Nanoparticles (NPs) are attracting great attention due to the recent progress in their synthesis and surface functionalization, along with their ability of photothermal conversion [1] and fluorescence in the near infrared region [2]. The photothermal conversion produces heating and leads to the formation of reactive oxygen species, which destroy cancer cells [3]. NPs can become an ideal drug carrier when modified for vector delivery and controlled release [4].

Hyperthermia is an attractive physical approach for cancer treatment [5-8]. When the tissue temperature rises, usually to 40–45 °C, blood flow and tissue oxidation increase [9], collagen fibers weaken [10], and tumors become more sensitive to chemotherapy drugs [11, 12] or radiation [13-14]. Currently, there are various clinical approaches that use special probes and needles to generate heat using microwaves, radiofrequencies or ultrasound [15, 16], but they do not allow local heating of the targeted pathological areas.

Iron oxide exhibits amazing physical properties, especially in the nanometer range. Iron oxide NPs (IONPs) can be used for magnetic resonance imaging (MRI) / optical multimodal imaging, as well as a therapeutic mediator in the treatment of cancer [17]. IONPs themselves show promising preclinical results in cancer therapy by modulating tumor-associated macrophages [18]. Recently, data were published on the therapeutic effect of Ferumoxytol — suppression of cancer cells and activation of the immune response to tumor [19]. IONPs have low cytotoxicity [20], and their coating with silicon dioxide further reduces both histo- and cytotoxicity [21, 22].

To localize the process of laser hyperthermia, thermal sensitizers like magnetic or plasmon resonance NPs are increasingly used [23]. Ultra small (about 30 nm in size) superparamagnetic IONPs (SPIO) can effectively inhibit tumor progression as photothermal agents [24]. The SPIO heat dissipation mechanism is closely related to dipole-dipole interactions in an alternating magnetic field. For a mixture of IONPs colloids with different sizes, the possibility of simultaneously creating several types of "hot spots" by varying the parameters of the magnetic field has been demonstrated [25]. Thus, the local temperature rise, measured by fluorescent proteins on the surface of IONPs, reached 85 °C. Superparamagnetic particles dissipate heat due to the Néel-Brown relaxation [26, 27]. In magnetic hyperthermia, intracellular aggregation of IONPs inside endosomes is recognized as an important problem, because both physical mechanisms are suppressed: Brownian relaxation of nanoparticles —rotation of whole magnetic nanoparticles in their environment, and Néel relaxation, or rotation of the magnetic moment inside magnetic circuits [28]. Additional disadvantage of the clinical use of magnetic hyperthermia is the need for high concentrations of IONPs, [Fe]=1–2 M, several orders of magnitude higher than the concentrations used for MRI [29]. Efforts are being made to optimize the heating efficiency of the IONPs [30, 31].

More recently, IONPs have been tested for *in vitro* and *in vivo* photothermal therapy. The use of iron oxide nanocubes as sensors for both magnetic and laser hyperthermia has shown high efficiency of hyperthermia in mouse tumor models [32]. The effect of laser hyperthermia has also been demonstrated on magnetic IONPs coated with infrared (IR) dyes Cyanine7 [33] and IR-780 [34]. It was noted that intracellular aggregation of IONPs leads to some increase in the photothermal heating of nanoparticles [35]. There are also reports about the successful use of IONPs in combination with photosensitizers for photodynamic therapy [36,37].

When laser radiation interacts with nanoparticles, light is absorbed and heat is scattered. The study of these processes forms the currently actively developing area of called thermoplasmonics [38]. The interaction of an incident wave with a NP can be characterized using the scattering and absorption cross sections of NPs. The scattering cross section characterizes the part of the radiation that, after interacting with the NP, is scattered in different direction. The absorption cross section describes the energy absorbed by the NP. However, the absorption and scattering cross sections do not in any way characterize the processes occurring in NPs in the plasmon resonance region [39]. It was shown that in the region of plasmon resonance, the energy flux lines form vortex structures around the nanoparticle, which explains the increase in the absorption cross section of nanoparticles compared to the geometric cross section: due to the formation of vortex structures, the energy flux lines pass through the particle several times, which enhances the interaction between light and the material.

The heating that occurs when light interacts with nanomaterials can have different physical mechanisms, which depend on the nature of the nanomaterial. The absorption of photons usually leads to the excitation of photocarriers into excited states determined by quantum mechanics, and their return to the ground state is regulated by radiative (i.e. emission of photons) or nonradiative processes. The latter are associated with photonic, charge, or spin excitations or processes of photocarrier tunneling between defect / impurity electronic states, when the transition energy is very low. At the nanoscale, nonradiative processes lead to highly efficient photothermal conversion processes in which absorbed optical energy is dissipated into heat.

In semiconducting materials such as iron oxides, the energy of optical radiation allows for a temporary transition of electrons from the valence band to the conduction band, which leads to the release of heat with the electrons relaxation back to the valence band [40]. Photothermal conversion of non-metallic inorganic nanoparticles demonstrates moderate efficiency and broader optical absorption than of their metallic counterparts. Interestingly, diffuse and direct optical transmission and reflection components play an important role in the absorption / scattering of photons by colloids, especially when IONPs are aggregated [41].

In plasmon-resonant NPs, a localized surface exciton creates a high-intensity localized electromagnetic (EM) field near the surface, which has a significant effect on the probability of optical processes, such as absorption and radiative transitions (Purcell effect) [42]. An increase in the electric field strength between two gold nanoparticles of different sizes by two to three orders of magnitude is well described in the literature. However, similar phenomena for dielectric nanoparticles, such as iron oxide nanoparticles, are poorly studied. Large resonant field increases were predicted in the gap (from 1 to 30 nm) between two dielectric silicon microdiscs [43].

According to our experimental data, when studying the accumulation of iron oxide nanoparticles in cells using laser scanning microscopy, bright sparks or "hot spots" were observed in the images. As shown in *in vitro* experiments, the emergence of "hot spots" between IONPs during laser irradiation leads to cell death. Presumably, the emergence of "hot spots" and the enhancement of the therapeutic effect may be associated with an increase in the EM field between several IONPs, by analogy with metal NPs [44], or their heating. In this work, we performed theoretical modeling of the EM field enhancement for individual IONPs and their dimers.

Materials and methods

We used commercially available NPs of iron oxide Fe_2O_3 (IONPs) obtained by gas-phase condensation (NanoArc® by AlfaAesar®, USA), particle size 20–70 nm, surface area 30–60 m^2/g, γ-phase.

Sizing and Spectral Characterization of IONPs

The size and morphology of IONPs were analyzed by transmission electron microscopy (TEM) using a LEO 912 AB Omega microscope (Carl Zeiss Group, Germany). The hydrodynamic sizes of NPs and the ζ-potential were determined using a Zetasizer Nano ZS (Malvern Instruments, UK) in dH_2O at 25 °C. All measurements were triplicated. The absorption of colloids IONPs in the 0.4–0.8 μm spectral range was studied using a Hitachi U-3400 spectrophotometer (Hitachi Ltd., Japan). The absorbance was measured in cuvettes with an optical path length of 1 cm; the mass concentration of IONPs was 0.02 mg/mL.

"Hot spot" detection

To detect "hot spots" under laser irradiation, a laser scanning confocal microscope LSM-710 (Carl Zeiss,

Germany) was used. For measurements, the samples were placed between two cover glasses with a fixed distance determined by the thickness of the silicone spacer between them. Scanning was performed with lasers with 488 and 561 nm wavelengths. The laser power at the exit from the objective was determined using a LabMax-TO laser power meter (Coherent, USA).

The intensity distribution of the scanning laser spot was calculated from considerations of the size of the area bounded by the first-order diffraction ring for the PSF_{ill} point (or Airy disk) distribution function, with radius r:

$$r = \frac{0.61\lambda_{\mathbf{exc}}}{NA}, (1)$$

where *NA* is the numerical aperture of the microscope objective, λ_{exc} is the excitation wavelength.

For a 458 nm laser and a 63× oil objective with NA = 1.4, r = 200 nm, spot area S = 0.13 μm^2, measured power density at the lens exit = 1 mW, scanning power density ρ = 0.839 * P/S = 0.668 MW/cm^2, at a scanning speed of 0.53 μs/pixel (for temperature measurements) and 1.62 μs/pixel (for cells), the radiation dose for a single scan A = ρ×t was 0.35 J/cm^2 (for temperature measurements) and 1.08 J/cm^2 (for cells).

For a 561 nm laser, 63× oil objective with NA = 1.4, r = 244 nm, spot area S = 0.19 μm^2, measured power density at the objective exit = 1 mW, scanning power density ρ = 0.445 MW/cm^2, at a scanning speed of 0.53 μs/pixel (for temperature measurements) and 1.62 μs/pixel (for cells), the radiation dose in a single scan was 0.24 J/cm^2 (for temperature measurements) and 0.72 J/cm^2 (for cells).

The dependence of the "hot spots" number on the concentration of IONPs, as well as on the ambient temperature, was studied. For this, two colloids were prepared with IONPs concentrations of 0.1 and 0.01 mg/L. To study the effect of heating on the "hot spots" number, the studied samples were heated on the microscope thermostat (PeCon GmbH, Erbach, Germany) in the 20–60 °C temperature range.

The "hot spots" spectra were also studied using the laser scanning microscope. The emission spectra of "hot spots" were recorded with a 32-channel GaAsP detector in the 400–750 nm spectral range. Each "hot spot" was visualized by a microscope as a group of several pixels with different brightness. At the initial moment of time, which corresponds to the first pixel, the brightness is low. Then there is a flare-up to maximum brightness, after which the brightness decreases again. To obtain the resulting spectrum, averaging was carried out for several "hot spots" over pixels with the same step after the occurrence, i.e. with approximately the same brightness.

Registration of "hot spots" in cells in vitro

The intracellular distribution of IONPs and laser-induced "hot spots" were studied in HeLa cell culture. HeLa cells were cultured in RPMI-1640 medium containing 10% fetal calf serum at 37°C in 5% CO_2. The cells were subcultured every third day. For confocal microscopy, cells were plated onto a Petri dish with a glass bottom POC-R2 (PeCon GmbH, Erbach, Germany) at a density of 100 × 10^3 /cm^2 one day before the experiment. The next day, IONPs were added to the cells 4 hours before the start of microscopic examination. Before microscopic examination, cells were washed twice with pre-warmed phosphate buffered saline.

Theoretical modeling of the spectroscopic properties of IONPs

We simulated the scattering and absorption cross sections of individual IONPs in water, as well as local field enhancement near individual IONPs and between two nanoparticles of different sizes, forming a dimer. Water was used as the surrounding dielectric medium in the model.

The optical properties of individual spherical IONPs with a radius of 10 and 35 nm in the near and far fields were simulated using the T-matrix method [45, 46]. The scattering was calculated for the 400-800 nm optical wavelength range. The complex refractive indices of gold and iron oxide were taken from https://refractiveindex.info/, where data from [47] and [48] are presented.

The field enhancement near the surface of a NP can be described by the formula:

$$u = \gamma_E u(v_{if}), (2)$$

where u and u (v_{if}) are the energy of the external field in a unit spectral range with and without a nanoparticle, γ_E is the field enhancement factor equal to the ratio of the field generated by the particle to the initial one:

$$\gamma_E = \left|\frac{E}{E_0}\right|^2, (3)$$

where E is the field created by the particle, E_0 is the incident field.

The calculation made it possible to obtain the dependences of the absorption and scattering cross sections, as well as to calculate the field enhancement factor depending on the wavelength of the incident radiation in the medium containing the simulated NPs. Scattering by dimers consisting of two NPs with a radius of 10 and 30 nm located at a distance of 1, 5, 10, and 50 nm from each other was calculated using the finite difference time domain (FDTD) method [49, 50]. The finite difference method was used to numerically solve partial differential equations for three-dimensional

objects. In the calculation, it was assumed that the dimer is illuminated by a plane wave propagating along the z-axis and polarized along x-axis. The calculation takes into account the geometric parameters of the NPs and the dielectric constants of the medium and NPs. The calculation of the spatial distribution of the field and the local field enhancement between the particles was carried out for 458 and 561 nm wavelengths, which were used in the experiment.

Simulation of NP heating under the laser irradiation

Heating was calculated using the formula derived in [50]:

$$\Delta T_{NP} = \frac{\sigma_{abs} I}{4\pi R \kappa_{water}} = \frac{P}{4\pi R \kappa_{water}}, (4)$$

where σ_{abs} is the absorption cross section of the nanoparticle, I is the intensity of the incident laser radiation (W/m^2), P is the absorbed power (W), R is the nanoparticle radius, κ_{water} is the thermal conductivity of water, 0.56 W/(m·K). The heating was calculated using the absorption and scattering cross-sections calculated with the T-matrix method for the corresponding wavelengths.

Equation (4) makes it possible to calculate the heating of nanoparticles located in water irradiated with continuous laser radiation. The source of heat is optical absorption, which is locally proportional to the electric field strength and the imaginary part of the dielectric constant. We considered that water does not absorb the incident laser radiation. Thus, laser radiation is absorbed only by IONPs and creates a heating source located completely inside the nanoparticle. Due to the large difference in the thermal conductivity of water and Fe_2O_3 (0.56 and 7 W/(m·K) for water and iron oxide Fe_2O_3, respectively) we can assume that heat is distributed inside a particle so quickly, compared to the external environment, that its temperature is almost uniform for medium-sized particles, and thermal energy accumulates at the particle boundary before diffusing into the water. It should be noted that this approach was proposed by the authors of [51] for gold NPs in water, the difference in the thermal conductivity of gold and water is significantly higher (318 W/(m·K) for gold). However, in addition to the ratio of thermal conductivities, one should also take into account the time required to reach the steady state τ, which can be calculated as:

$$\tau \sim R^2 \frac{\rho c_p}{\kappa} = \frac{R^2}{9D}, (5)$$

where R is the radius of the nanoparticle, D is the thermal diffusivity (m^2/s). For water, the thermal diffusivity is 1.43×10^{-8} m^2/s.

The authors considered gold NPs 100 nm in size. The largest size of the NPs considered in this work is 70 nm. Due to the quadratic dependence of τ on the NP radius, the time to reach the steady state for our NPs is significantly shorter.

Since the temperature distribution corresponds to the Poisson equation, which is scale-invariant, it depends on the particle size only indirectly, through the absorbed power P. For a small sphere, the distribution $P(r)$ is uniform, and the temperature rise inside the NP can be described by the equation:

$$\Delta T(r) = \frac{p(R^2 - r^2)}{6\kappa_{NP}} + \Delta T_{NP}, (6)$$

where ΔT_{NP} is the temperature calculated using (4).

The temperature is the highest at the center of the particle, and tends to T_{NP} at the surface of the particle. Thermal heterogeneity can be calculated using the formula:

$$\frac{\Delta T_{max}}{\Delta T_{min}} = 1 + \frac{\kappa_{water}}{2\kappa_{NP}}, (7)$$

For Fe_2O_3 NPs, the ratio $\Delta T_{max}/\Delta T_{min}$ is 1.04. It can be said that the heat inside the NPs propagates rather quickly compared to the external environment, and the temperature is almost uniform inside the particles of the considered sizes. Thus, the approach proposed for gold nanoparticles is applicable to the IONPs considered in this work.

Results

The TEM results show that the IONPs of hexagonal shape and have diameters ranging from 20 to 70 nm (Fig. 1). The hydrodynamic size of particles in the colloid is 130±65 nm, which indicates some aggregation, the ζ-potential measured in distilled water (pH = 7.0) was 35±4 mV.

The intracellular distribution of IONPs in HeLa cell culture obtained using laser scanning microscopy is shown in Fig. 2.

In cells, "hot spots" are localized within endolysosomes, which is confirmed by the rapid discoloration of the lysosomal dye LysoTracker™ Green DND-26 (Invitrogen, USA), data not shown. A similar intracellular localization of IONPs is observed in many works, for example [32]. The emission spectra of "hot spots" are shown in Fig. 3.

The shape of the recorded spectra of "hot spots" is characteristic for thermal radiation, which indicates a high local temperature. To analyze and interpret the observed effect, we performed theoretical modeling of the local field enhancement between IONPs with a radius of 10 and 35 nm (the largest and smallest NP size

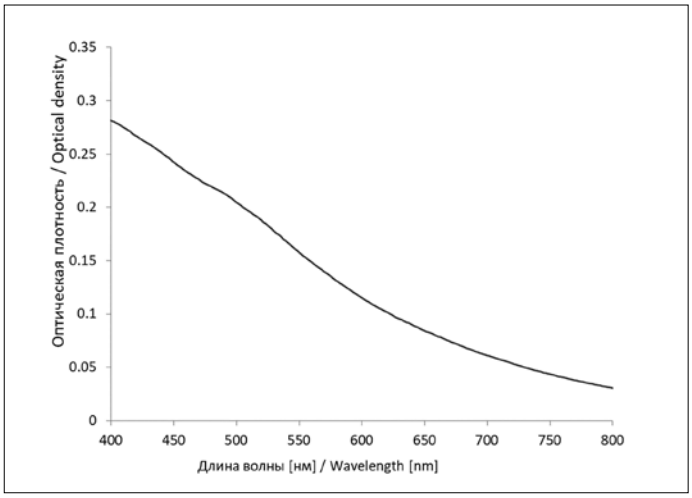

a

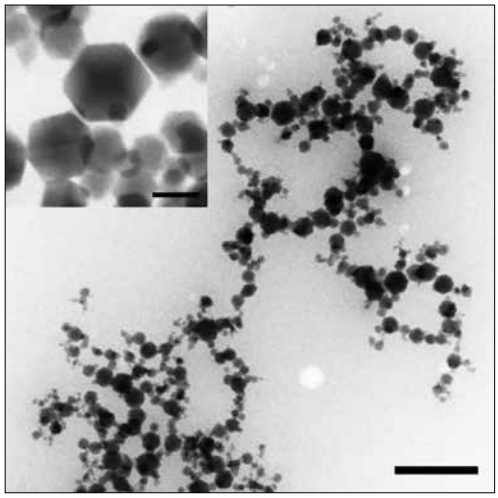

b

Рис. 1. a – спектры поглощения водного коллоида IONPs; b – ПЭМ IONPs, шкала 200 нм, на вставке – 30 нм.
Fig. 1. a – absorption spectra of IONPs water colloid; b – TEM of IONPs, scale 200 nm, scale on the inset – 30 nm.

in the studied colloids) and the heating of IONPs under the laser irradiation. The scattering and absorption cross-sections for single IONPs with a radius of 10 and 35 nm, calculated using the T-matrix method, are shown in Fig. 4.

The dependence of the field enhancement for single IONPs with a radius of 10 and 35 nm from the wavelength, calculated using the T-matrix method, is shown in Fig. 5.

It can be seen that the observed field enhancement for individual IONPs is rather low. For a pair of two particles, the field enhancement is much higher, Fig. 6.

The maximum enhancement is achieved at a small distance between nanoparticles and is 112 and 96 at a distance between nanoparticles of 1 nm for 458 and 561 nm wavelengths, respectively. These field enhancement values are comparable to the enhancement obtained with gold NPs. The field enhancement factor exponentially depends on the distance between particles, Fig. 5, and tends to the value for a large particle at large distances between particles. The calculated

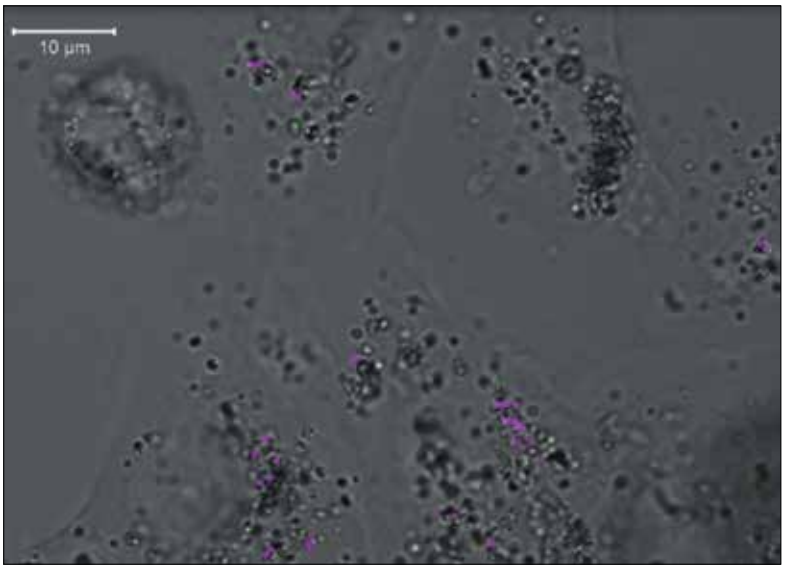

Рис. 2. Микроскопические изображения культуры клеток HeLa, полученные при лазерном сканировании с длиной волны 561 нм. Фиолетовым цветом показаны индуцируемые при лазерном сканировании «горячие точки».
Fig. 2. Microscopic images of a HeLa cell culture obtained by laser scanning at a wavelength of 561 nm. The «hot spots» induced by laser scanning are shown in purple.

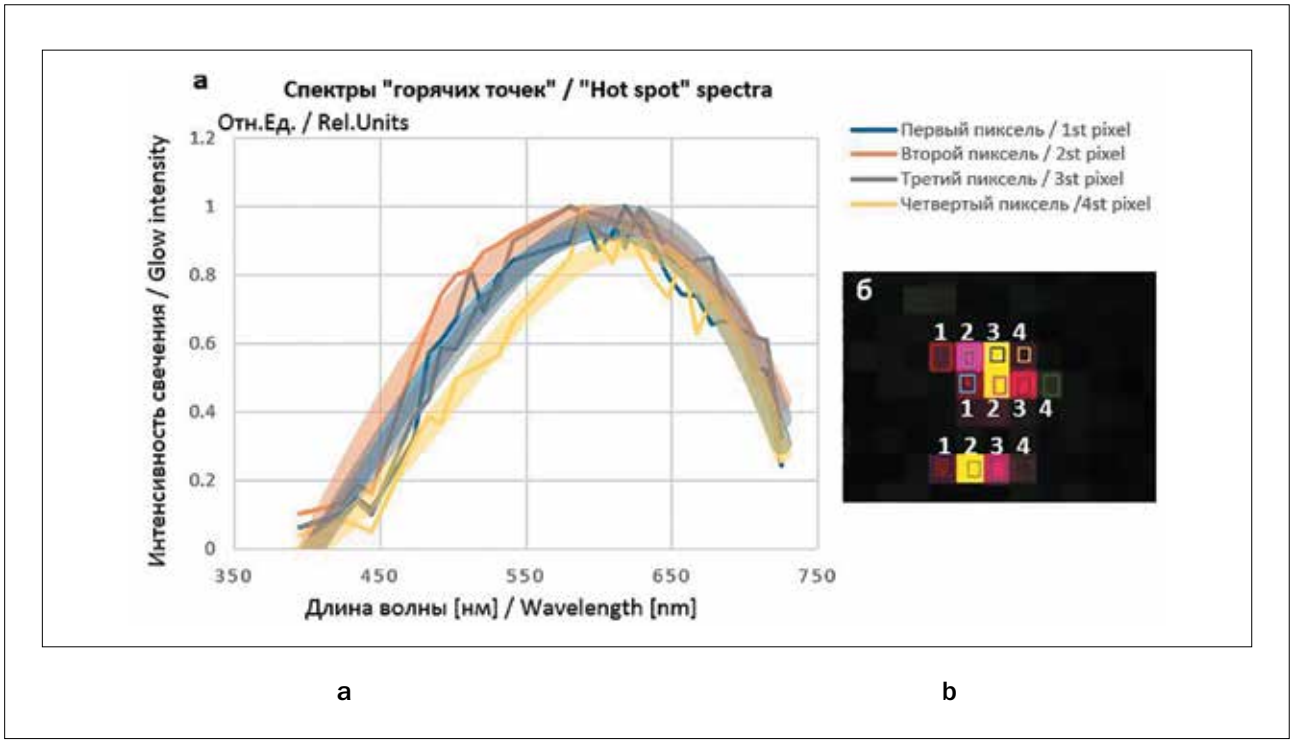

Рис. 3. a – спектры индуцируемых при лазерном сканировании «горячих точек», b – иллюстрация используемого метода усреднения. Показаны три «горячие точки», представляющие собой группу пикселей с различной яркостью. Для получения результирующих спектров проводили усреднение по пикселям с одинаковой яркостью (пиксель 1, пиксель 2 и т. д.) для четырех «горячих точек».
Fig. 3. a – spectra of laser-scanned «hot spots», b – illustration of the averaging method used. Three «hot spots» are shown, which are a group of pixels with different brightness. To obtain the resulting spectra, averaging was performed over pixels with the same brightness (pixel 1, pixel 2, etc.) for four «hot spots».

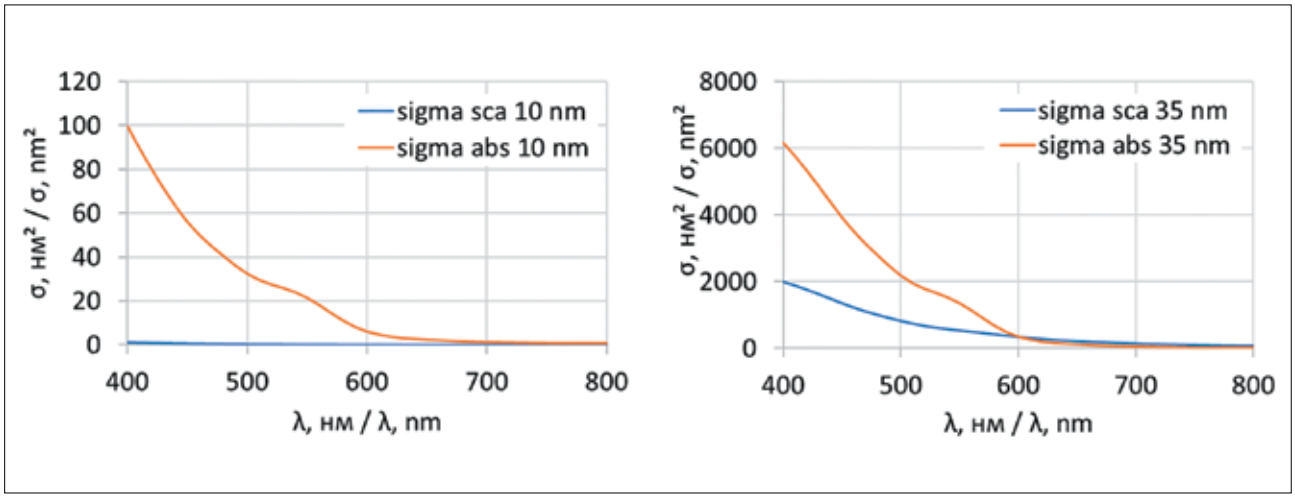

Рис. 4. Сечения рассеяния и поглощения для одиночных IONPs радиусом 10 нм и 35 нм, рассчитанные при помощи метода Т-матриц.
Fig. 4. Scattering and absorption cross sections for single IONPs with a radius of 10 nm and 35 nm, calculated using the T-matrix method.

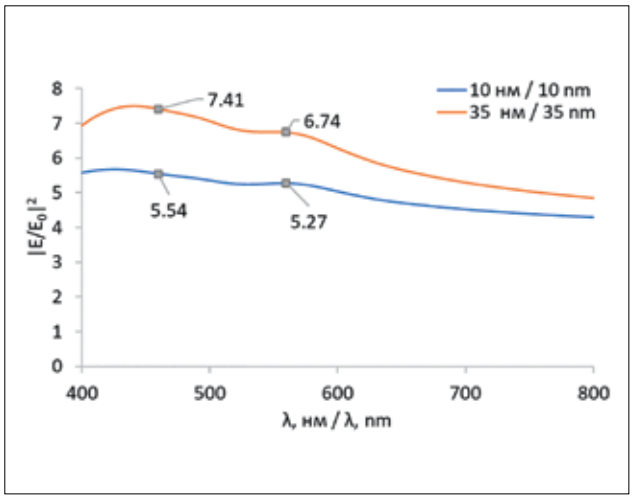

Рис. 5. Фактор усиления поля для одиночных IONPs радиусом 10 нм и 35 нм, рассчитанный при помощи метода Т-матриц. Сносками показаны значения фактора усиления поля для длин волн 458 нм и 561 нм.
Fig. 5. Field enhancement factor for single IONPs with a radius of 10 nmand 35 nm, calculated using the T-matrix method. Data labels show the values of the field amplification factor for the wavelengths of 458 nm and 561 nm.

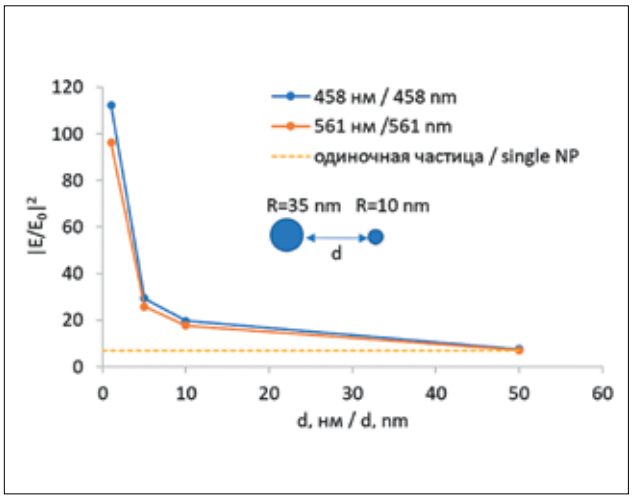

Рис. 6. Фактор усиления поля для димеров из двух IONPs радиусами 10 нм и 35 нм, рассчитанный при помощи метода конечных разностей во временной области для длин волн 458 нм и 561 нм в зависимости от расстояния между наночастицами *d*.
Fig. 6. Field enhancement factor for dimers from IONPs with a radius of 10 nm and 35 nm, calculated using the finite difference method in the time domain for wavelengths of 458 nm and 561 nm depending on the distance between nanoparticles *d*.

enhancement values for single IONPs and dimers are shown in Table 1.

When analyzing the results obtained for the spatial distribution of the field, several characteristic zones can be distinguished in the EM interaction of two particles, Fig. 7.

At distances of more than 10 nm, the particles practically do not interact with each other. The enhancement is almost the same as for individual IONPs (Table 1). As the distance decreases to less than 10 nm, the field enhancement zones around the nanoparticles begin to overlap and local "hot spots" appear, the enhancement in which significantly exceeds the field enhancement for individual NPs. With a change in the distance from 10 to 1 nm, an exponential increase in the field enhancement factor is observed, as well as localization of the resulting enhancement in a small region of the space between NPs.

The values of the heating temperature under the laser irradiation, calculated for IONPs with a radius of 10 and 35 nm (the smallest and largest particle size in a colloid), under the laser irradiation with wavelengths of 458 and 561 nm, are shown in Table 2.

It is shown that the heating temperature of large NPs (70 nm in size) approximately corresponds to the heating temperature of 100 nm gold NPs by laser radiation at the absorption maximum. The total heating of a 100 nm NP by two wavelengths is 107.9 °C. Despite the rather high heating temperature, the occurrence of thermal emission of nanoparticles at

Таблица 1
Фактор усиления поля, рассчитанный для одиночных IONP и их димеров
Table 1
Field enhancement factor calculated for single IONPs and their dimers

Димеры IONPs IONPs dimers		
Параметр Parameter	$\|E/E_0\|^2$	$\|E/E_0\|^2$
d, нм d, nm	λ = 458 нм λ = 458 nm	λ = 561 нм λ = 561 nm
1	112	96
5	29	26
10	20	18
50	8	7
Одиночные IONPs Single IONPs		
	$\|E/E_0\|^2$	$\|E/E_0\|^2$
λ, нм λ, nm	R = 10 нм R = 10 nm	R = 35 нм R = 35 nm
460	6	8
560	5	7

Примечание: *d* – расстояние между наночастицами, λ – длина волны, R – радиус наночастиц.
Note: d – distance between nanoparticles, λ – wavelength, R – radius of nanoparticles.

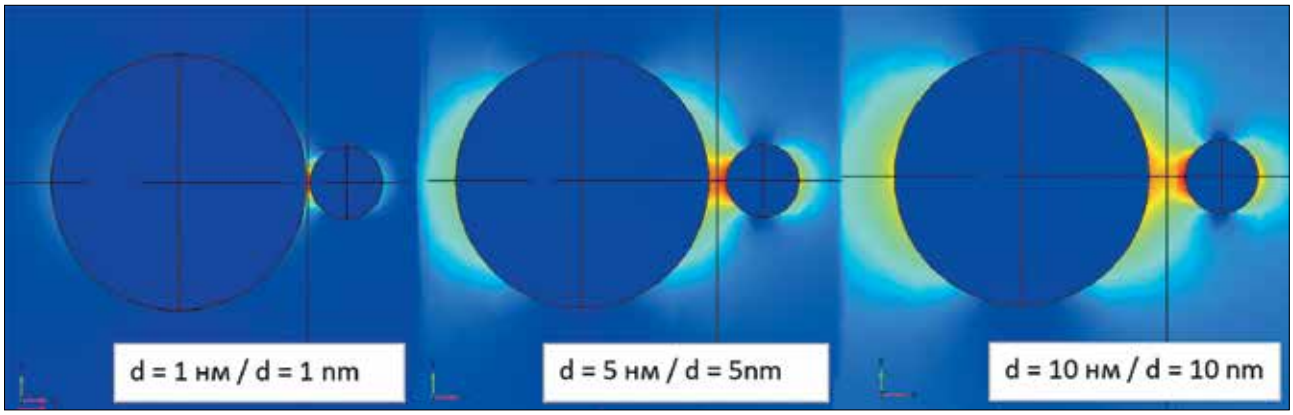

Рис. 7. Пространственное распределение поля и локального усиления поля между IONPs с радиусами 10 нм и 35 нм в зависимости от расстояния между наночастицами *d*.
Fig. 7. Spatial field distribution and local field enhancement between IONPs with 10 nm and 35 nm radii depending on distance between NPs *d*.

Таблица 2
Время достижения установившегося режима τ и относительное изменение температуры ΔT под действием лазерного излучения для исследованных IONPs
Table 2
Time to reach steady state conditions τ and relative temperature change ΔT under the laser irradiation for the studied IONPs

НЧ / NPs	Среда / Medium	R, нм / R, nm	τ, мкс / τ, μs	σ_{abs}, нм^2 / σ_{abs}, nm^2	ΔT, °C	Источник / Reference
Fe_2O_3	вода	10	0.001	50 (458 нм) 18 (560 нм)	4.4 1.1	эта работа / this work
Fe_2O_3		35	0.003	3522 (458 нм) 1157 (560 нм)	88.9 19.0	эта работа / this work
Au		50	0.019	(в работе не указано) / NA	100	[50]

Примечание: R – радиус наночастиц, τ – время достижения установившегося режима, σ_{abs} – сечение поглощения наночастицы, ΔT – относительное изменение температуры под действием лазерного излучения.
Note: R – radius of nanoparticles, τ – time to reach steady state conditions, σ_{abs} – absorption cross section of nanoparticle, ΔT – relative temperature change under the laser irradiation.

such temperatures is unlikely. In this regard, we assume that the observed "hot spots" arise mainly due to the local field enhancement.

Since the field enhancement is highly dependent on the distance between particles, we investigated the effect of temperature on the number of observed "hot spots". Presumably, as the temperature rises, the particles more often find themselves at a close distance from each other and the number of observed "hot spots" should increase.

The IONPs colloid image obtained by laser scanning at wavelengths of 488 and 561 nm is shown in Fig. 8a. The dependence of the number of "hot spots" on temperature and particle concentration is shown in Fig. 8b.

With an increase in temperature by 30°C, the number of "hot spots" increased by about 7000 on average. This is

due to the fact that with an increase in temperature, the diffusion coefficient increases, which is proportional to the temperature, and the particles more often approach each other. Thus, due to more frequent approaches of nanoparticles, enhancement occurs more often, which confirms the assumption made about the appearance of the observed "hot spots" due to the local enhancement of the electromagnetic field between NPs.

Discussion and conclusion

Over the past 20 years, there has been a significant increase in the number of reports on hyperthermia. Many focused on the local heating effect, a special temperature profile near NPs with little or no macroscopic heating. This approach has many benefits. First, the effect becomes less dependent on the number of NPs usually required to significantly increase the macroscopic temperature in the target area. Consequently, biological tissues are not exposed to serious stress, and the toxic effects are highly localized. Second, the thermal profile around the NP can cause drug release without thermal damage to the treatment area.

The temperature profile of heating near a nanoparticle is difficult to study due to its nanoscopic size and short event time. Measurements can be an indirect (for example, using thermosensitive reactions) or a direct estimate of the thermal gradient in the region of interest. Direct estimation of the local temperature profile around nanoparticles is less studied [52]. Using nanotherometers, such as up-conversion NPs [53], sensors based on DNA hybridization [54], thermosensitive polymers [55], a strong temperature gradient was recorded from the surface of nanoparticles to the environment.

Another interesting effect is the local enhancement of the electromagnetic field near nanoparticles, which can lead to an increase in the luminescence intensity of nanoparticles and dyes [56], an increase in the Raman scattering signal [57], and an increase in the efficiency of singlet oxygen generation by photosensitizers [58]. It was shown in [59] that the field enhancement for non-spherical gold nanoparticles E/E_0 is 25 to 35 times. The use of dimers made of non-spherical gold nanoparticles and careful optimization of their parameters made it possible to obtain a field enhancement of 270 for two gold nanoparticles, elliptical and spherical, differing 1000 times in volume, located at a distance of 17 nm from each other. The field enhancement between two spherical silver nanoparticles with a radius of 0.5 and 5 nm exceeds the field enhancement of one NP by a factor of 75 and is about 400 at the resonance wavelength.

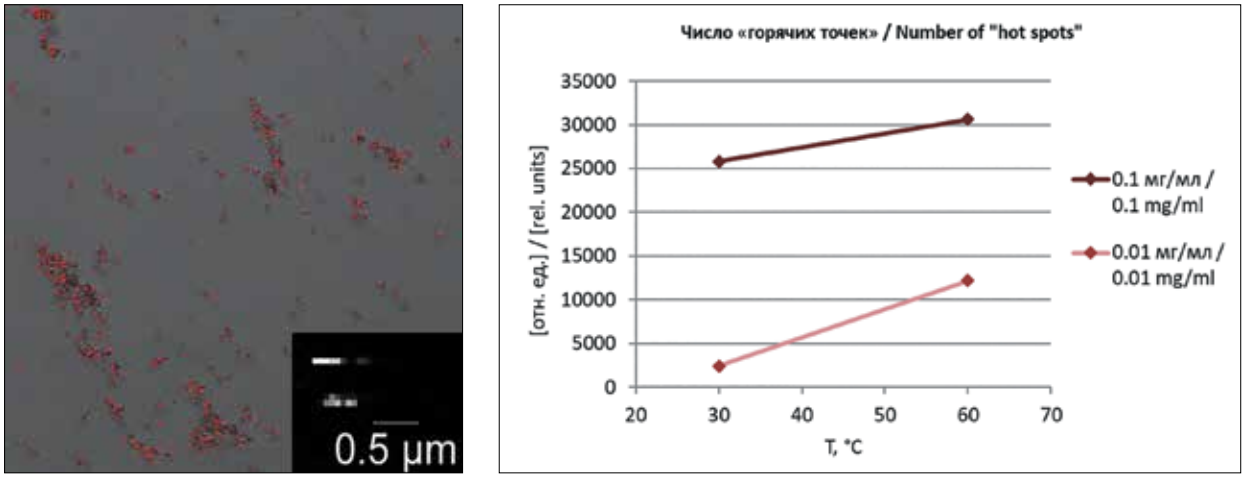

a b

Рис. 8. a – красным цветом представлены «горячие точки» для водного коллоида IONPs с концентрацией 0,1 мг/мл при облучении одновременно лазерами с длинами волн 488 нм и 561 нм при 100% мощности; b – зависимости количества наблюдаемых вспышек от концентрации IONPs и температуры.

Fig. 8. a – red color represents «hot spots» for an aqueous colloid of IONPs with a concentration of 0.1 mg/ml under simultaneous irradiation with 488 nm and 561 nm lasers at 100% power; b – dependences of the number of observed «hot spots» on the concentration of IONPs and temperature.

In our work, we have demonstrated that, upon laser excitation of the investigated IONPs, individual regions with a bright glow, the so-called "hot spots", are observed in the obtained images. In the case of *in vitro* studies, these points were localized in areas of accumulation of nanoparticles inside cells, presumably in lysosomes. Exposure of cell cultures to high power density laser radiation leads to cell death. It was assumed that the cause of the observed effect may be laser-induced heating and / or local enhancement of the electromagnetic field near the surface of nanoparticles.

Based on our recorded luminescence spectra of "hot spots" in an aqueous colloid of polydisperse IONPs at a sufficiently high laser scanning power density (MW/cm^2) characteristic of thermal radiation, conclusions can be drawn about a very high local temperature.

However, using theoretical modeling, it was shown that the heating temperature of large NPs (70 nm in size) approximately corresponds to the heating temperature of 100 nm gold NPs by continuous laser radiation to the absorption maximum. The total heating of a 100 nm NP by two wavelengths is 107.9 °C. Despite the rather high heating temperature, the occurrence of thermal emission of nanoparticles at such temperatures is unlikely. However, upon reaching 100 °C, water begins to boil, the NP will end up in a vapor bubble, this will reduce the rate of heat dissipation and lead to even greater overheating. It should be noted that, according to the literature data, in the case of pulsed laser excitation, heating can be significantly higher and reach 1000 K at the end of the laser pulse [60].

Theoretical modeling of the local field enhancement for IONPs with a radius of 10 and 35 nm showed that the dependence of the enhancement for single NPs is rather low. For a pair of particles with a radius of 10 and 35 nm, the field enhancement is much higher. The maximum enhancement is achieved at a small distance between nanoparticles and is two orders of magnitude at a distance between nanoparticles of 1 nm. Such values of the field enhancement are comparable to the enhancement obtained for plasmonic NPs made of noble metals.

At distances more than 10 nm, the particles practically do not interact with each other. When the distance changes from 10 to 1 nm, an exponential increase in the field enhancement factor is observed, as well as localization of the resulting enhancement in a small region of the space between nanoparticles, and local "hot spots" appear. It was also shown in [60] that, in contrast to single spherical nanoparticles, for which a uniform temperature distribution is observed in the bulk of the nanoparticle, in the case of dimers and trimers from gold nanoparticles, hot and cold zones arise in the bulk of the particles with plasmon resonance. The location of the maximum density of the plasma of free electrons surrounding the nanoparticles coincides with the location of the "hot spots" of the hot zones with high temperature and with the location of the maximum enhancement of the electric field inside the particles. Thus, the observed thermal emission may be due to the local enhancement of the electric field in IONPs dimers.

Funding
This work was funded by the RFBR, grant 21-52-12030.

REFERENCES

1. X. Xu, W. Ho, X. Zhang, N. Bertrand, and O. Farokhzad, Cancer nanomedicine: from targeted delivery to combination therapy, *Trends in Molecular Medicine*, 2015, vol. 21, no. 4, pp. 223–232.
2. R. Borlan, M. Focsan, D. Maniu, and S. Astilean, Interventional NIR Fluorescence Imaging of Cancer: Review on Next Generation of Dye-Loaded Protein-Based Nanoparticles for Real-Time Feedback During Cancer Surgery, *IJN 16*, 2021, pp. 2147–2171.
3. B. S. Dash, S. Das, and J.-P. Chen, Photosensitizer-Functionalized Nanocomposites for Light-Activated Cancer Theranostics, *IJMS*, 2021, vol. 22, no. 13, pp. 6658.
4. G. Liu, L. Yang, G. Chen et al., A Review on Drug Delivery System for Tumor Therapy, *Front. Pharmacol*, 2021, vol. 12, pp. 735446
5. P. Wust, B. Hildebrandt, G. Sreenivasa, B. Rau, et al., Hyperthermia in combined treatment of cancer, *The Lancet Oncology*, 2002, vol. 3, no. 8, pp. 487–497.
6. J. Kolosnjaj-Tabi and C. Wilhelm, Magnetic nanoparticles in cancer therapy: how can thermal approaches help? *Nanomedicine*, 2017, vol. 12, no. 6, pp. 573–575.
7. Sidorov D.V., Grishin N.A., Lozhkin M.V., Troitsky A.A., Moshurov R.I., Bykasov S.A., Urlova A.N., Filonenko E.V. Intraoperative photodynamic therapy and hyperthermic intraperitoneal chemotherapy in cytoreductive treatment of patients with disseminated mucinous carcinoma of appendix, *Biomedical Photonics*, 2020, vol. 9, no. 4, pp. 23–30 (in Russian) doi: 10.24931/2413–9432–2020–9–4-23–30
8. Kaprin A.D., Mardinskiy Yu.S., Smirnov V.P., Ivanov S.A., Kostin A.A., Polikhov S.A., Reshetov I.V., Fatianova A.S., Denisenko M.V., Epatova T.V., Korenev S.V., Tereshchenko A.V., Filonenko E.V., Gafarov M.M., Romanko Yu.S. The history of radiation therapy (part I), *Biomedical Photonics*, 2019, vol. 8, no. 1, pp. 52–62 (in Russian). doi: 10.24931/2413–9432–2019–8–1–52–62
9. M.R. Horsman, Tissue physiology and the response to heat, *International Journal of Hyperthermia*, 2006, vol. 22, no. 3, pp. 197–203.
10. J. Kolosnjaj-Tabi, R. Di Corato, L. Lartigue, et al., Heat-Generating Iron Oxide Nanocubes: Subtle "Destructurators" of the Tumoral Microenvironment, *ACS Nano*, 2014, vol. 8, no. 5, pp. 4268–4283.
11. F. Mohamed, P. Marchettini, O.A. Stuart et al., Thermal Enhancement of New Chemotherapeutic Agents at Moderate Hyperthermia, *Ann Surg Oncol*, 2003, vol. 10, no. 4, pp. 463–468.
12. R. Issels, Hyperthermia Combined with Chemotherapy – Biological Rationale, Clinical Application, and Treatment Results, *Oncol Res Treat*, 1999, vol. 22, no. 5, pp. 374–381.
13. H.D. Suit and L.E. Gerweck, Potential for hyperthermia and radiation therapy, *Cancer Res*, 1979, vol. 39 (6 Pt 2), pp. 2290–2298.
14. S. Spirou, M. Basini, A. Lascialfari et al., Magnetic Hyperthermia and Radiation Therapy: Radiobiological Principles and Current Practice, *Nanomaterials*, 2018, vol. 8, no. 6, pp. 401.
15. O. Dahl, Status of Clinical Hyperthermia, *Acta Oncologica*, 1999, vol. 38, no. 7, pp. 863–873.
16. K. Hynynen, D. Shimm, D. Anhalt et al., Temperature distributions during clinical scanned, focused ultrasound hyperthermia treatments, *International Journal of Hyperthermia*, 1990, vol. 5, no. 5, pp. 891–908.
17. Gorshkova A.S., Shilov I.P., Ivanov A.V., Rumyantseva V.D. Synthesis and research of nanoparticles for magnetic-luminescent tumor theranostics based on the Yb-complex of DME protoporphyrin IX and iron oxide. Proceedings of the IX International Congress "Photodynamic therapy and photodiagnostics" Moscow October 23–24, 2020, *Biomedical Photonics*. 2020, vol. 8, no. 4s, pp. 5–6.
18. V. Mulens-Arias, J.M. Rojas, and D.F. Barber, The Use of Iron Oxide Nanoparticles to Reprogram Macrophage Responses and the Immunological Tumor Microenvironment. *Front. Immunol*, 2021, vol. 12, pp. 693709.

ЛИТЕРАТУРА

1. Xu X., Ho W., Zhang X., Bertrand N. and Farokhzad O. Cancer nanomedicine: from targeted delivery to combination therapy//Trends in Molecular Medicine. – 2015. –Vol. 21 (4). – P. 223–232.
2. Borlan R., Focsan M., Maniu D. and Astilean S. Interventional NIR Fluorescence Imaging of Cancer: Review on Next Generation of Dye-Loaded Protein-Based Nanoparticles for Real-Time Feedback During Cancer Surgery//IJN 16. – 2021. – P. 2147–2171.
3. Dash B.S., Das S., Chen J.-P. Photosensitizer-Functionalized Nanocomposites for Light-Activated Cancer Theranostics//IJMS. 2021. – 22 (13). – P. 6658.
4. Liu G., Yang L., Chen G. et al. A Review on Drug Delivery System for Tumor Therapy//Front. Pharmacol. – 2021. – Vol.12. – P. 735446
5. Wust P., Hildebrandt B., Sreenivasa G., Rau B. et al. Hyperthermia in combined treatment of cancer//The Lancet Oncology. – 2002. – Vol. 3 (8). – P. 487–497.
6. Kolosnjaj-Tabi J., Wilhelm C. Magnetic nanoparticles in cancer therapy: how can thermal approaches help?//Nanomedicine. – 2017. – Vol. 12 (6). – P. 573–575.
7. Сидоров Д.В., Гришин Н.А., Ложкин М.В., Троицкий А.А., Мошуров Р.И., Быкасов С.А., Урлова А.Н., Филоненко Е.В. Интраоперационная фотодинамическая терапия и гипертермическая внутрибрюшная химиотерапия при циторедуктивном хирургическом лечении больных диссеминированной муцинозной карциномой аппендикса//Biomedical Photonics. 20. – Т. 9, № 4. – P. 23–30. https://doi.org/10.24931/2413–9432–2020–9-4–23–30
8. Каприн А.Д., Мардынский Ю.С., Смирнов В.П., Иванов С.А., Костин А.А., Полихов С.А., Решетов И.В., Фатьянова А.С., Денисенко М.В., Эпатова Т.В., Коренев С.В., Терещенко А.В., Филоненко Е.В., Гафаров М.М., Романко Ю.С. К истории развития лучевой терапии (часть I)//Biomedical Photonics. – 2019. – Т. 8, № 1. – С. 52–62. doi: 10.24931/2413–9432–2019–8–1–52–62.
9. Horsman M.R. Tissue physiology and the response to heat//International Journal of Hyperthermia. – 2006. – Vol. 22 (3). – P. 197–203.
10. Kolosnjaj-Tabi J., Di Corato R., Lartigue L. et al. Heat-Generating Iron Oxide Nanocubes: Subtle "Destructurators" of the Tumoral Microenvironment//ACS Nano. –2014. – Vol. 8 (5). – P. 4268–4283.
11. Mohamed F., Marchettini P., Stuart O.A. et al. Thermal Enhancement of New Chemotherapeutic Agents at Moderate Hyperthermia//Ann Surg Oncol. – 2003. – Vol. 10 (4). – P. 463–468.
12. Issels R. Hyperthermia Combined with Chemotherapy – Biological Rationale, Clinical Application, and Treatment Results//Oncol Res Treat. – 1999. – Vol. 22 (5). – P. 374–381.
13. Suit H.D. and Gerweck L.E., Potential for hyperthermia and radiation therapy//Cancer Res. – 1979. – Vol. 39 (6 Pt 2). – P. 2290–2298.
14. Spirou S., Basini M., Lascialfari A. et al. Magnetic Hyperthermia and Radiation Therapy: Radiobiological Principles and Current Practice//Nanomaterials. – 2018. –Vol. 8 (6). – P. 401.
15. Dahl O. Status of Clinical Hyperthermia//Acta Oncologica. – 1999. – Vol. 38 (7). – P. 863–873.
16. Hynynen K., Shimm D., Anhalt D. et al. Temperature distributions during clinical scanned, focused ultrasound hyperthermia treatments//International Journal of Hyperthermia. – 1990. – Vol. 6 (5). – P. 891–908.
17. Горшкова А.С., Шилов И.П., Иванов А.В., Румянцева В.Д. Синтез и исследование наночастиц для магнитно-люминесцентеной тераностики опухолей на основе Yb-комплекса ДМЭ протопорфирина IX и оксида железа//Материалы IX Международного конгресса «Фотодинамическая терапия и фотодиагностика» Москва 23–24 октября 2020 г. Biomedical Photonics. 20. – Т. 9, № 4s. – P. 5–6.

19. S. Zanganeh, G. Hutter, R. Spitler et al., Iron oxide nanoparticles inhibit tumour growth by inducing pro-inflammatory macrophage polarization in tumour tissues. *Nature Nanotech*, 2016, vol. 11, no. 11, pp. 986–994.
20. U. S. Gaharwar, R. Meena, and P. Rajamani, Iron oxide nanoparticles induced cytotoxicity, oxidative stress and DNA damage in lymphocytes: Iron oxide nanoparticles toxicity in lymphocytes, *J. Appl. Toxicol*, 2017, vol. 37, no. 10, pp. 1232–1244.
21. M. A. Malvindi, V. De Matteis, A. Galeone et al., Toxicity Assessment of Silica Coated Iron Oxide Nanoparticles and Biocompatibility Improvement by Surface Engineering, *PLoS ONE*, 2014, Vol. 9 (1), pp. e85835.
22. L. Arias, J. Pessan, A. Vieira et al., Iron Oxide Nanoparticles for Biomedical Applications: A Perspective on Synthesis, Drugs, Antimicrobial Activity, and Toxicity, *Antibiotics*, 2018, vol. 7, no. 2, pp. 46.
23. R. Sun, H. Chen, L. Sutrisno, N. Kawazoe, and G. Chen, Nanomaterials and their composite scaffolds for photothermal therapy and tissue engineering applications, Science and *Technology of Advanced Materials*, 2021, vol. 22, no. 1, pp. 404–428.
24. Q. Liu, L. Liu, C. Mo, X. Zhou et al., Polyethylene glycol-coated ultrasmall superparamagnetic iron oxide nanoparticles-coupled sialyl Lewis X nanotheranostic platform for nasopharyngeal carcinoma imaging and photothermal therapy, J Nanobiotechnol, 2021, vol. 19, no. 1, pp. 171.
25. J. G. Ovejero, I. Armenia, D. Serantes et al., Selective Magnetic Nanoheating: Combining Iron Oxide Nanoparticles for Multi-Hot-Spot Induction and Sequential Regulation, *Nano Lett*, 2021, vol. 21, no. 17, pp. 7213–7220.
26. D. Shi, M. E. Sadat, A. W. Dunn, and D. B. Mast, Photo-fluorescent and magnetic properties of iron oxide nanoparticles for biomedical applications, *Nanoscale*, 2015, vol. 7, no. 18, pp. 8209–8232.
27. G. Vallejo-Fernandez, O. Whear, A. G. Roca et al., Mechanisms of hyperthermia in magnetic nanoparticles, *J. Phys. D: Appl. Phys*, 2013, vol. 46, no. 31, pp. 312001.
28. A. Espinosa, J. Kolosnjaj-Tabi, A. Abou-Hassan et al., Magnetic (Hyper)Thermia or Photothermia? Progressive Comparison of Iron Oxide and Gold Nanoparticles Heating in Water, in Cells, and In Vivo, *Adv. Funct. Mater*, 2018, vol. 28, no. 37, pp. 1803660.
29. M. Johannsen, U. Gneveckow, B. Thiesen et al., Thermotherapy of Prostate Cancer Using Magnetic Nanoparticles: Feasibility, Imaging, and Three-Dimensional Temperature Distribution, *European Urology*, 2007, vol. 52, no. 6, pp. 1653–1662.
30. P. Guardia, R. Di Corato, L. Lartigue et al., Water-Soluble Iron Oxide Nanocubes with High Values of Specific Absorption Rate for Cancer Cell Hyperthermia Treatment, *ACS Nano*, 2012, vol. 6, no. 4, pp. 3080–3091.
31. C. Martinez-Boubeta, K. Simeonidis, A. Makridis et al., Learning from Nature to Improve the Heat Generation of Iron-Oxide Nanoparticles for Magnetic Hyperthermia Applications, *Sci Rep*, 2013, vol. 3, no. 1, pp. 1652.
32. A. Espinosa, R. Di Corato, J. Kolosnjaj-Tabi et al., Duality of Iron Oxide Nanoparticles in Cancer Therapy: Amplification of Heating Efficiency by Magnetic Hyperthermia and Photothermal Bimodal Treatment, *ACS Nano*, 2016, vol. 10, no. 2, pp. 2436–2446.
33. H. Yan, W. Shang, X. Sun, L. Zhao et al., "All-in-One" Nanoparticles for Trimodality Imaging-Guided Intracellular Photo-magnetic Hyperthermia Therapy under Intravenous Administration, *Adv. Funct. Mater*, 2018, vol. 28, no. 9 pp. 1705710.
34. S.-Y. Lin, R.-Y. Huang, W.-C. Liao et al., Multifunctional PEGylated Albumin/IR780/Iron Oxide Nanocomplexes for Cancer Photothermal Therapy and MR Imaging, *Nanotheranostics*, 2018, vol. 2, no. 2, pp. 106–116.
35. S. Cabana, A. Curcio, A. Michel, C. Wilhelm, and A. Abou-Hassan, Iron Oxide Mediated Photothermal Therapy in the Second Biological Window: A Comparative Study between Magnetite/Maghemite Nanospheres and Nanoflowers, *Nanomaterials*, 2020, vol. 10, no. 8, pp.1548.

18. Mulens-Arias V., Rojas J. M. and Barber D. F. The Use of Iron Oxide Nanoparticles to Reprogram Macrophage Responses and the Immunological Tumor Microenvironment//Front. Immunol. – 2021. – Vol. 12. – P. 693709.
19. Zanganeh S., Hutter G., Spitler R. et al. Iron oxide nanoparticles inhibit tumour growth by inducing pro-inflammatory macrophage polarization in tumour tissues//Nature Nanotech. – 2016. – Vol. 11 (11). – P. 986–994.
20. Gaharwar U. S. Meena R., and Rajamani P., Iron oxide nanoparticles induced cytotoxicity, oxidative stress and DNA damage in lymphocytes: Iron oxide nanoparticles toxicity in lymphocytes//J. Appl. Toxicol. – 2017. – Vol. 37 (10). – P. 1232–1244.
21. Malvindi M. A., Matteis V. De, A Galeone. et al. Toxicity Assessment of Silica Coated Iron Oxide Nanoparticles and Biocompatibility Improvement by Surface Engineering//PLoS ONE. – 2014. – Vol. **9** (1). – P. e85835.
22. Arias L., Pessan J., Vieira A. et al. Iron Oxide Nanoparticles for Biomedical Applications: A Perspective on Synthesis, Drugs, Antimicrobial Activity, and Toxicity//Antibiotics. – 2018. – Vol. 7 (2). – P. 46.
23. Sun R., Chen H., Sutrisno L., Kawazoe N., and Chen G., Nanomaterials and their composite scaffolds for photothermal therapy and tissue engineering applications//Science and Technology of Advanced Materials. – 2021. – Vol. 22 (1). – P. 404–428.
24. Liu Q., Liu L., Mo C., Zhou X. et al. Polyethylene glycol-coated ultrasmall superparamagnetic iron oxide nanoparticles-coupled sialyl Lewis X nanotheranostic platform for nasopharyngeal carcinoma imaging and photothermal therapy//J Nanobiotechnol. – 2021. – Vol. 19 (1). – P. 171.
25. Ovejero J. G., Armenia I., Serantes D. et al. Selective Magnetic Nanoheating: Combining Iron Oxide Nanoparticles for Multi-Hot-Spot Induction and Sequential Regulation//Nano Lett. – 2021. – Vol. 21 (17). – P. 7213–7220.
26. Shi D., Sadat M. E., Dunn A. W., and Mast D. B., Photo-fluorescent and magnetic properties of iron oxide nanoparticles for biomedical applications//Nanoscale. – 2015. – Vol. **7** (18). – P. 8209–8232.
27. Vallejo-Fernandez G., Whear O., Roca A. G. et al. Mechanisms of hyperthermia in magnetic nanoparticles//J. Phys. D: Appl. Phys. – 2013. – Vol. 46 (31). – P. 312001.
28. Espinosa A., Kolosnjaj-Tabi J., Abou-Hassan A. et al. Magnetic (Hyper)Thermia or Photothermia? Progressive Comparison of Iron Oxide and Gold Nanoparticles Heating in Water, in Cells, and In Vivo//Adv. Funct. Mater. – 2018. – Vol. 28 (37). – P. 1803660.
29. Johannsen M., Gneveckow U., Thiesen B. et al. Thermotherapy of Prostate Cancer Using Magnetic Nanoparticles: Feasibility, Imaging, and Three-Dimensional Temperature Distribution//European Urology. – 2007. – Vol. 52 (6). – P. 1653–1662.
30. Guardia P., R. Corato Di, Lartigue L. et al., Water-Soluble Iron Oxide Nanocubes with High Values of Specific Absorption Rate for Cancer Cell Hyperthermia Treatment//ACS Nano. – 2012. – Vol. 6 (4). – P. 3080–3091.
31. Martinez-Boubeta C., Simeonidis K., Makridis A. et al., Learning from Nature to Improve the Heat Generation of Iron-Oxide Nanoparticles for Magnetic Hyperthermia Applications//Sci Rep. – 2013. – Vol. 3 (1). – P. 1652.
32. Espinosa A., R. Corato Di, Kolosnjaj-Tabi J. et al., Duality of Iron Oxide Nanoparticles in Cancer Therapy: Amplification of Heating Efficiency by Magnetic Hyperthermia and Photothermal Bimodal Treatment//ACS Nano. –2016. – Vol. 10 (2). – P. 2436–2446.
33. Yan H., Shang W., X. Sun, L. Zhao et al., "All-in-One" Nanoparticles for Trimodality Imaging-Guided Intracellular Photo-magnetic Hyperthermia Therapy under Intravenous Administration//Adv. Funct. Mater. – 2018. – Vol. 28 (9). – P. 1705710.
34. Lin S.-Y., Huang R.-Y., Liao W.-C. et al. Multifunctional PEGylated Albumin/IR780/Iron Oxide Nanocomplexes for Cancer

36. J. Shi, X. Yu, L. Wang, Y. Liu et al., PEGylated fullerene/iron oxide nanocomposites for photodynamic therapy, targeted drug delivery and MR imaging, *Biomaterials*, 2013, vol. 34, no. 37, pp. 9666–9677.
37. O. Penon, M. J. Marín, D. B. Amabilino, D. A. Russell, and L. Pérez-García, Iron oxide nanoparticles functionalized with novel hydrophobic and hydrophilic porphyrins as potential agents for photodynamic therapy, *Journal of Colloid and Interface Science*, 2016, vol. 462, pp. 154–165.
38. V. V. Klimov, Nanoplasmonics. *2nd ed. Fizmatlit*, 2010.
39. M. V. Bashevoy, V. A. Fedotov, and N. I. Zheludev, Optical whirlpool on an absorbing metallic nanoparticle, *Opt. Express*, 2005, vol. 13, no. 21, pp. 8372.
40. S. K. Sharma, N. Shrivastava, F. Rossi et al., Nanoparticles-based magnetic and photo induced hyperthermia for cancer treatment, *Nano Today*, 2019, vol. 29, pp. 100795.
41. C. Lozano-Pedraza, E. Plaza-Mayoral, A. Espinosa, B. Sot, et al., Assessing the parameters modulating optical losses of iron oxide nanoparticles under near infrared irradiation, *Nanoscale Adv*, 2021, vol. 3, no. 22, pp. 6490–6502.
42. Y. Jeong, Y.-M. Kook, K. Lee, and W.-G. Koh, Metal enhanced fluorescence (MEF) for biosensors: General approaches and a review of recent developments, *Biosensors and Bioelectronics*, 2018, vol. 111, pp. 102–116.
43. M. M. Sigalas, D. A. Fattal, R. S. Williams, et al., Electric field enhancement between two Si microdisks, *Opt. Express*, 2007, vol. 15, no. 22, pp. 14711.
44. S. Toroghi and P. G. Kik, Photothermal response enhancement in heterogeneous plasmon-resonant nanoparticle trimmers, *Phys. Rev. B.*, 2014, vol. 90, no. 20, pp. 205414.
45. N. G. Khlebtsov, T-matrix method in plasmonics: An overview, *Journal of Quantitative Spectroscopy and Radiative Transfer*, 2013, vol. 123, pp. 184–217.
46. D. W. Mackowski and M. I. Mishchenko, A multiple sphere T-matrix Fortran code for use on parallel computer clusters, *Journal of Quantitative Spectroscopy and Radiative Transfer*, 2011, vol. 112, no. 13, pp. 2182–2192.
47. A. D. Rakić, A. B. Djurišić, J. M. Elazar, and M. L. Majewski, "Optical properties of metallic films for vertical-cavity optoelectronic devices, *Appl. Opt*, 1998, vol. 37, no. 22, pp. 5271.
48. M. R. Querry, Optical Constants. *MISSOURI UNIV-KANSAS CITY*, 1985.
49. S. Farooq and R. E. de Araujo, Engineering a Localized Surface Plasmon Resonance Platform for Molecular Biosensing, *OJAppS*, 2018, vol. 8, no. 3, pp. 126–139.
50. M. N. Kholodtsova, P. V. Grachev, W. C. Blondel, et al., Application of devices for space-resolved spectroscopy on the example of two-layer phantoms containing metallic nanoparticles, *Biomedical Photonics*, 2018, vol. 7, no. 2, pp. 4–12.
51. G. Baffou, R. Quidant, and F. J. García de Abajo, Nanoscale Control of Optical Heating in Complex Plasmonic Systems, *ACS Nano*, 2010, vol. 4, no. 2, pp. 709–716.
52. E. Cazares-Cortes, S. Cabana, C. Boitard, et al., Recent insights in magnetic hyperthermia: From the "hot-spot" effect for local delivery to combined magneto-photo-thermia using magneto-plasmonic hybrids, *Advanced Drug Delivery Reviews*, 2019, vol. 138, pp. 233–246.
53. J. Dong and J. I. Zink, Taking the Temperature of the Interiors of Magnetically Heated Nanoparticles, *ACS Nano*, 2014, vol. 8, no. 5, pp. 5199–5207.
54. D. Gareau, A. Desrosiers, and A. Vallée-Bélisle, Programmable Quantitative DNA Nanothermometers, *Nano Lett*, 2016, vol. 16, no. 7, pp. 3976–3981.
55. A. Riedinger, P. Guardia, A. Curcio, et al., Subnanometer Local Temperature Probing and Remotely Controlled Drug Release Based on Azo-Functionalized Iron Oxide Nanoparticles, *Nano Lett*, 2013, vol. 13, no. 6, pp. 2399–2406.

Photothermal Therapy and MR Imaging//Nanotheranostics. – 2018. – Vol. 2 (2). – P. 106–116.

35. Cabana S., Curcio A., Michel A., Wilhelm C., and Abou-Hassan A. Iron Oxide Mediated Photothermal Therapy in the Second Biological Window: A Comparative Study between Magnetite/Maghemite Nanospheres and Nanoflowers//Nanomaterials. – 2020. – Vol.10 (8). – P.1548.
36. Shi J., Yu X., Wang L., Liu Y. et al. PEGylated fullerene/iron oxide nanocomposites for photodynamic therapy, targeted drug delivery and MR imaging//Biomaterials. – 2013. – Vol. 34 (37). – P. 9666–9677.
37. Penon O., Marín M. J., Amabilino D. B., Russell D. A. and Pérez-García L. Iron oxide nanoparticles functionalized with novel hydrophobic and hydrophilic porphyrins as potential agents for photodynamic therapy//Journal of Colloid and Interface Science. – 2016. – Vol. 462. – P. 154–165.
38. Климов В. В., Наноплазмоника//2nd ed. Физматлит. – 2010.
39. Bashevoy M. V., Fedotov V. A., and Zheludev N. I. Optical whirlpool on an absorbing metallic nanoparticle//Opt. Express. – 2005. – Vol. 13 (21). – P. 8372.
40. Sharma S. K., Shrivastava N., Rossi F. et al. Nanoparticles-based magnetic and photo induced hyperthermia for cancer treatment//Nano Today. – 2019. – Vol. 29. – P. 100795.
41. Lozano-Pedraza C., Plaza-Mayoral E., Espinosa A., Sot B., et al. Assessing the parameters modulating optical losses of iron oxide nanoparticles under near infrared irradiation//Nanoscale Adv. – 2021. – Vol. 3 (22). – P. 6490–6502.
42. Jeong Y., Kook Y.-M., Lee K., and Koh W.-G. Metal enhanced fluorescence (MEF) for biosensors: General approaches and a review of recent developments//Biosensors and Bioelectronics. – 2018. – Vol. 111. – P. 102–116.
43. M. M. Sigalas, D. A. Fattal, R. S. Williams, et al., Electric field enhancement between two Si microdisks//Opt. Express. – 2007. – Vol. 15 (22). – P. 14711.
44. S. Toroghi and P. G. Kik, Photothermal response enhancement in heterogeneous plasmon-resonant nanoparticle trimmers//Phys. Rev. B. – 2014. – Vol. 90 (20). – P. 205414.
45. N. G. Khlebtsov, T-matrix method in plasmonics: An overview//Journal of Quantitative Spectroscopy and Radiative Transfer. – 2013. – Vol. 123. – P. 184–217.
46. D. W. Mackowski and M. I. Mishchenko, A multiple sphere T-matrix Fortran code for use on parallel computer clusters//Journal of Quantitative Spectroscopy and Radiative Transfer. – 2011. – Vol. 112 (13). – P. 2182–2192.
47. A. D. Rakić, A. B. Djurišić, J. M. Elazar, and M. L. Majewski, "Optical properties of metallic films for vertical-cavity optoelectronic devices//Appl. Opt. – 1998. – Vol. 37 (22). – P. 5271.
48. M. R. Querry, Optical Constants//MISSOURI UNIV-KANSAS CITY. – 1985.
49. S. Farooq and R. E. de Araujo, Engineering a Localized Surface Plasmon Resonance Platform for Molecular Biosensing//OJAppS. – 2018. – Vol. 08 (03). – P. 126–139.
50. Kholodtsova M. N., Grachev P. V., W. Blondel C. et al., Application of devices for space-resolved spectroscopy on the example of two-layer phantoms containing metallic nanoparticles//Biomedical Photonics. – 2018. – Vol. 7 (2). – P. 4–12.
51. Baffou G., Quidant R., and García de Abajo F. J. Nanoscale Control of Optical Heating in Complex Plasmonic Systems//ACS Nano. – 2010. – Vol. 4 (2). – P. 709–716.
52. Cazares-Cortes E., Cabana S., Boitard C. et al., Recent insights in magnetic hyperthermia: From the "hot-spot" effect for local delivery to combined magneto-photo-thermia using magneto-plasmonic hybrids//Advanced Drug Delivery Reviews. – 2019. – Vol. 138. – P. 233–246.
53. Dong J. and Zink J. I. Taking the Temperature of the Interiors of Magnetically Heated Nanoparticles//ACS Nano. – 2014. – Vol. 8 (5). – P. 5199–5207.

56. C. Joyce, S. M. Fothergill, F. Xie, Recent advances in gold-based metal enhanced fluorescence platforms for diagnosis and imaging in the near-infrared, *Materials Today Advances*, 2020, vol. 7, pp. 100073.
57. Ángela I. López-Lorente, Recent developments on gold nanostructures for surface enhanced Raman spectroscopy: Particle shape, substrates and analytical applications, *A review, Analytica Chimica Acta*, 2021, vol. 1168, pp. 338474.
58. Sajid Farooq, Renato E. de Araujo, dentifying high performance gold nanoshells for singlet oxygen generation enhancement, *Photodiagnosis and Photodynamic Therapy*, 2021, vol. 35, pp. 102466.
59. Seyfollah Toroghi and Pieter G. Kik Cascaded plasmon resonant field enhancement in nanoparticle dimers in the point dipole limit Appl, *Phys. Lett*, 2013, vol. 100, pp. 183105.
60. Davletshin Y. R., Kumaradas J. C., *J. Beilstein Nanotechnol*, 2016, vol. 7, pp. 869–880. doi:10.3762/bjnano.7.79

54. Gareau D., Desrosiers A., and Vallée-Bélisle A. Programmable Quantitative DNA Nanothermometers//Nano Lett. – 2016. – Vol. 16 (7). – P. 3976–3981.
55. Riedinger A., Guardia P., Curcio A. et al., Subnanometer Local Temperature Probing and Remotely Controlled Drug Release Based on Azo-Functionalized Iron Oxide Nanoparticles//Nano Lett. – 2013. – Vol. 13 (6). – P. 2399–2406.
56. Joyce C., Fothergill S. M., Xie F. Recent advances in gold-based metal enhanced fluorescence platforms for diagnosis and imaging in the near-infrared//Materials Today Advances. – 2020. – Vol. 7. – P. 100073.
57. Ángela I. López-Lorente, Recent developments on gold nanostructures for surface enhanced Raman spectroscopy: Particle shape, substrates and analytical applications//A review, Analytica Chimica Acta. – 2021. – Vol. 1168. – P. 338474.
58. Sajid Farooq, Renato E. de Araujo, dentifying high performance gold nanoshells for singlet oxygen generation enhancement//Photodiagnosis and Photodynamic Therapy. – 2021. – Vol. 35. – P. 102466.
59. Seyfollah Toroghi and Pieter G. Kik Cascaded plasmon resonant field enhancement in nanoparticle dimers in the point dipole limit Appl//Phys. Lett. – 2013. – Vol. 100. – P. 183105.
60. Y. R. Davletshin, J. C. Kumaradas, J. Beilstein Nanotechnol. – 2016. – Vol. 7. – P. 869–880. doi:10.3762/bjnano.7.79

PHOTODYNAMIC THERAPY FOR PRECANCER DISEASES AND CERVICAL CANCER (REVIEW OF LITERATURE)

Gilyadova A.V.[1,2], Romanko Yu.S.[1], Ishchenko A.A.[2], Samoilova S.V.[1], Shiryaev A.A.[1], Alekseeva P.M.[3,4], Efendiev K.T.[3,4], Reshetov I.V.[1,5,6]
[1]Sechenov First Moscow State Medical University, Moscow, Russia
[2]Treatment and Rehabilitation Center, Moscow, Russia
[3]Prokhorov General Physics Institute of the Russian Academy of Sciences, Moscow, Russia
[4]National Research Nuclear University MEPhI (Moscow Engineering Physics Institute), Moscow, Russia
[5]Federal Research and Clinical Center of Specialized Medical Care
and Medical Technologies FMBA of Russia, Moscow, Russia
[6]Moscow Witte University, Moscow, Russia

Abstract

The paper presents the results of literature data analysis on the main directions of precancerous diseases of the cervix uteri and cervical cancer treatment. Side effects following surgery or radiation treatment can lead to structural deformities, scarring, hyperpigmentation, systemic side effects, and destruction of normal tissue. In addition, the use of traditional methods of treatment can cause multidrug resistance, which will lead to ineffective treatment and the development of a relapse of the disease. To avoid toxicity and reduce side effects, alternative treatment strategies have been proposed. Photodynamic therapy (PDT) is a promising organ-preserving highly selective method for treating cervical neoplasia, which includes two stages: the introduction of a photosensitizer and local exposure to directed light radiation. A number of studies have demonstrated the high clinical efficacy of this method in the treatment of patients with cervical neoplasia and carriage of human papillomavirus infection without adverse consequences for fertility. The use of PDT contributes to the successful outcome of the treatment of pathological foci on the mucous membrane of the cervix, the effectiveness and safety of the method is ensured by the selective effect on tissues. In the course of treatment, normal surrounding tissues are not damaged, there is no gross scarring and stenosis of the cervical canal, thereby PDT allows maintaining the normal anatomical and functional characteristics of the cervix.

Key words: cervical cancer, cervical dysplasia, human papillomavirus, photodynamic therapy, photosensitizers..

For citations: Gilyadova A.V., Romanko Yu.S., Ishchenko A.A., Samoilova S.V., Shiryaev A.A., Alekseeva P.M., Efendiev K.T., Reshetov I.V. Photodynamic therapy for precancer diseases and cervical cancer (review of literature), *Biomedical Photonics*, 2021, vol. 10, no. 4, pp. 59–67. doi: 10.24931/2413–9432–2021–10-4-59-67

Contacts: Gilyadova A.V., e-mail: aida-benyagueva@mail.ru

ФОТОДИНАМИЧЕСКАЯ ТЕРАПИЯ ПРЕДРАКОВЫХ ЗАБОЛЕВАНИЙ И РАКА ШЕЙКИ МАТКИ (ОБЗОР ЛИТЕРАТУРЫ)

А.В. Гилядова[1,2], Ю.С. Романко[1], А.А. Ищенко[2], С.В. Самойлова[1], А.А. Ширяев[1], П.М. Алексеева[3,4], К.Т. Эфендиев[3,4], И.В. Решетов[1,5,6]
[1]Первый Московский государственный медицинский университет им. И.М. Сеченова, Москва, Россия
[2]Лечебно-реабилитационный центр Минздрава, Москва, Россия
[3]ФИЦ «Институт общей физики им. А.М. Прохорова РАН», Москва, Россия
[4]Национальный исследовательский ядерный университет МИФИ, Москва, Россия
[5]Федеральный научно-клинический центр специализированных видов медицинской помощи и медицинских технологий ФМБА, Москва, Россия
[6]Московский университет им. С.Ю. Витте, Москва, Россия

Резюме

Представлены результаты анализа данных литературы об основных направлениях лечения предраковых заболеваний шейки матки и рака шейки матки. Побочные эффекты после хирургического или лучевого лечения могут привести к структурным деформациям, рубцам, гиперпигментации, системным побочным эффектам и разрушению нормальных тканей. Использование традиционных методов лечения может вызвать множественную лекарственную устойчивость, что приведет к неэффективности лечения и развитию рецидива заболевания. Чтобы избежать токсичности и уменьшить побочные эффекты были предложены альтернативные стратегии лечения. Перспективным органосохраняющим высокоселективным методом лечения неоплазии шейки матки является фотодинамическая терапия (ФДТ), которая включает два этапа: введение фотосенсибилизатора и локальное воздействие направленного светового излучения. В ряде исследований продемонстрирована высокая клиническая эффективность этого метода в лечении пациенток с цервикальной неоплазией и носительством инфекции вируса папилломы человека без неблагоприятных последствий для фертильности. Использование ФДТ способствует успешному результату лечения патологических очагов на слизистой оболочке шейки матки, эффективность и безопасность метода обеспечивается избирательностью воздействия на ткани. В процессе лечения не повреждаются нормальные окружающие ткани, не происходит грубого рубцевания и стеноза цервикального канала, тем самым ФДТ позволяет сохранить нормальные анатомо-функциональные характеристики шейки матки.

Ключевые слова: рак шейки матки, дисплазия шейки матки, вирус папилломы человека, фотодинамическая терапия, фотосенсибилизатор.

Для цитирования: Гилядова А.В., Романко Ю.С., Ищенко А.А., Самойлова С.В., Ширяев А.А., Алексеева П.М., Эфендиев К.Т., Решетов И.В. Фотодинамическая терапия предраковых заболеваний и рака шейки матки (обзор литературы) // Biomedical Photonics. – 2021. – Т. 10, № 4. – С. 59–67. doi: 10.24931/2413–9432–2021–10-4-59-67

Контакты: Гилядова А.В. e-mail: aida-benyagueva@mail.ru

Introduction

Currently, cervical cancer (CC) is one of the most common oncological diseases and is a serious public health problem. In most countries, this disease is the main cause of death for women [1]. According to the International Agency for Research on Cancer, in 2020, 603,863 new cases of cervical cancer were registered in the world, of which 341,680 were fatal. In the structure of oncological mortality in women, cervical cancer is 7.7% [2]. The 5-year survival rate of patients with cervical cancer in 2020 varied in different countries from 37% to 77% [3]. The proposed approaches to the treatment of this disease largely depend on the stage of the disease, the presence of relapses and tumor metastases [4].

Intraepithelial neoplasia of the cervix are precancerous forms of CC. The risk of developing a malignant tumor in patients with squamous intraepithelial neoplasia is 20 times higher than in healthy women [5]. Therefore, timely treatment of cervical intraepithelial neoplasia (CIN) in the early stages is an extremely important task to prevent the development of cervical cancer.

In the vast majority of cases, the human papillomavirus (HPV) acts as the leading etiological factor in the development of squamous intraepithelial lesions of cervical cancer and squamous cervical cancer [6].

Conventional anticancer therapy for cervical cancer includes surgery, radiation therapy, and chemotherapy. However, these methods have obvious disadvantages [7].

Side effects after surgery or radiation treatment can lead to structural deformities, scarring, hyperpigmentation, systemic side effects, and destruction of normal tissues. In addition, the use of traditional therapies can cause multidrug resistance, leading to treatment failure and disease recurrence. Alternative treatment strategies have been proposed to avoid toxicity and reduce side effects. Photodynamic therapy (PDT) is one of the least invasive methods, in which non-toxic photosensitizers (PS) are administered systemically or applied locally, followed by their activation by light of a certain wavelength in the presence of cellular oxygen. PDT is successfully used in clinical practice, in particular, in the treatment of oncological diseases [8, 9, 10]. PDT makes it possible to achieve positive results, avoid the appearance of rough cicatricial tissues, and preserve the patients' quality of life, including in cases where the use of other methods of antitumor therapy was ineffective [11, 12, 13]. Fluorescent diagnostics, also based on the use of PS, is successfully used for the purpose of early diagnosis of neoplasms, as well as to clarify the boundaries of an already detected tumor focus and identify additional foci during surgical treatment in order to more radically remove the tumor and reduce the likelihood of recurrences [14, 15].

After a certain time (from several minutes to several days), the tumor is irradiated with red or near infra-

red light, which excites the PS with the formation of a long-lived triplet state. PS reacts with ambient oxygen to form reactive oxygen species and/or hydroxyl radicals, which kill tumor cells, destroy tumor blood vessels, and lead to tumor regression and necrosis [16].

The aim of the work was to analyze the literature on the effectiveness of PDT for precancerous diseases of the cervix and cervical cancer.

The effectiveness of PDT depends primarily on the accumulation of PS in the affected tissue, as well as on local light delivery. At the same time, the physicochemical properties of PS have a great influence on their effectiveness, pharmacodynamics, and pharmacokinetics [17]. Porphyrins, chlorins, bacteriochlorins, and phthalocyanins have been extensively studied for use in PDT. Several compounds have received clinical approval [18, 19]. For the treatment of large or deep-seated tumors, bacteriochlorophyll a derivatives with intense absorption in the long-wavelength region of the spectrum have recently been studied [20]. Numerous experimental works studying the mechanisms of action, tissue and cellular targets of PS have been performed abroad [21] and in Russia [22, 23].

Results of experimental studies of the effectiveness of PDT

In 2019, Guo W. et al. [7] investigated *in vitro* the antitumor activity of curcumin-containing liposomes against three different cancer cell lines: HeLa, UD-SCC-2, and VX2. Cancer cells in the concentration range from 0 to 100 μmol/l were incubated with liposomes for 4 h, then irradiated with LEDs at a wavelength of 457 nm and an energy density of 1, 3, and 5 J/cm^2. The results showed increased cytotoxicity at a light energy density of 3 J/cm^2, a decrease in the rate of colony formation, cell proliferation and migration. Curcumin-containing liposomes have been proposed as an effective treatment for HPV-associated cancers.

Microencapsulation and targeted delivery of cytotoxic and antibacterial agents during PDT improve the results of cancer treatment. In many cases, loss of potency, poor encapsulation efficiency, and inadequate drug dosing hinder the success of this technology. Therefore, the development of new and reliable microencapsulated dosage forms that provide high therapeutic efficacy is of paramount importance. In the study of Ermakov A.V. et al. [24] a delivery using biodegradable microcapsules assembled from dextran sulfate (DS) and poly-1-arginine (PArg), a choline derivative of zinc phthalocyanine (holosens), a water-soluble cationic preparation for PDT was carried out *in vitro*. The capsules were tested using cervical adenocarcinoma (HeLa) cell lines, normal human diploid fibroblasts (NHDF), and two bacterial strains: Gram-positive Staphylococcus aureus and Gram-negative Escherichia coli. The results of the study provided strong evidence that the encapsulated forms of holosens are effective as PDT preparations. The authors believe that polymer multilayer capsules obtained by sequential self-assembly on the surface of additional naturally occurring biocompatible polyions will outperform the vast majority of nanomaterials in cancer treatment due to their stable structure and safety.

A study of the effect of 5-aminolevulinic acid PDT (5-ALA-PDT) on the endoplasmic reticulum and associated mechanisms of infection with high-risk HPV types showed that 5-ALA-PDT suppressed the viability of HeLa cells *in vitro* and induced autophagy in HeLa cells via the pathway Ca^{2+}-CamKKβ-AMPK. At the same time, 5-ALA-PDT induced apoptosis via activation of caspase 12 [25].

The same authors investigated the effectiveness of combined treatment of HPV infection with 5-ALA-PDT and dihydroartemisinin (DHA). DHA is a derivative of artemisinin, which has an inhibitory effect on cancer cells. HeLa cells were treated with 5-ALA and/or DHA and PDT was performed. Cell viability, proliferation duration, production of reactive oxygen species (ROS), and apoptosis activity were assessed. It was found that the use of DHA can enhance the effect of 5-ALA-PDT on the duration of cell proliferation and viability, the level of ROS production, and apoptosis in HeLa cells. According to the authors, the use of 5-ALA and DHA during PDT is very promising, since DHA enhances the effect of 5-ALA-PDT in the presence of HPV [26].

In the work of J.H. Ha and Y.J. Kim [27] the possibility of using capsules with pheophorbide A (an epitopic analogue of oncoprotein E7, EAE7) as part of polymeric nanoparticles in the combined treatment of HPV infection using PDT and cold plasma treatment of cervical cancer cells was evaluated. The results of *in vitro* analysis of PDT efficiency demonstrated that the use of nanoparticles increases the activity of the method in relation to CaSki cells, which is due to an increase in the targeted effect of radiation. The combined effect, causing increased intracellular formation of reactive oxygen species and apoptotic death of tumor cells, more effectively inhibited the growth of cervical cancer cells.

M. Pola et al. [28] studied the role of oxygen during photodynamic treatment of CC cells of the HeLa line. The effect of PDT was evaluated by adding disulfonated zinc phthalocyanine ($ZnPcS_2$) and tetrasulfonated zinc tetraphenylporphyrin ($ZnTPPS_4$) to the cell culture. Analysis of phototoxicity at various levels of oxygen partial pressure showed dose-dependent cellular responses during PDT. The efficiency of using $ZnPcS_2$ as a PS at the minimum level of oxygen in the atmosphere was noted. It was found that hyperbaric

oxygen therapy did not result in higher PDT efficacy with any of the PSs used in the study. At the same time, both PS can cause a significant decrease in the potential of the mitochondrial membrane, and $ZnPcS_2$ has a more pronounced effect on mitochondrial respiration, which is completely blocked after two short sessions of PDT. In general, the results of the study showed that PDT can be effective even under hypoxic conditions with the selection of the appropriate PS, for example, $ZnPcS_2$.

Z. Li et al. studied the action mechanism of a new PS (TBZPy) and the possibility of its potential use in the treatment of HPV-associated diseases with a high carcinogenic risk. HeLa cells infected with HPV type 18 were subjected to PDT using TBZPy. PDT contributed to the loss of the mitochondrial membrane potential, led to suppression of the expression of anti-apoptotic proteins, increased the expression of pro-apoptotic proteins, stimulated the production of reactive oxygen species, the release of lactate dehydrogenase and apoptosis of HeLa cells *in vitro*, and suppressed cell viability. Photodynamic exposure also suppressed the expression of HPV E6 and E7 proteins, which indicated the possibility of using the new PS in the treatment of diseases etiologically associated with human papillomavirus infection [29].

Results of clinical studies of the effectiveness of PDT of precancerous lesions of cervix and cervical cancer

In clinical trials, PDT has proven to be a promising organ-preserving highly selective treatment for intraepithelial neoplasia of cervical cancer and early invasive cervical cancer. According to the data given in the work of Park Y.K. et al. [30], the frequency of complete remission during PDT of cervical intraepithelial neoplasia was noted in 95% of cases. The authors showed that PDT can be recommended as a new method for the treatment of patients with pre-malignant lesions, as well as carcinoma in situ and early invasive cervical cancer. In the case of more advanced stages of invasive cervical cancer, combined chemo-photodynamic therapy is necessary.

J. Xie et al. [31] assessed the HPV viral load before and after PDT with 5-ALA during a dynamic examination of 111 patients with genital warts. In condyloma cells, induction of the expression of the regulatory proteins LC3II and p62 was observed along with an increase in the regulatory activity of caspase-3. This approach contributed to the inhibition of HeLa cell proliferation in a dose-dependent manner and effectively reduced the HPV viral load by influencing autophagy, apoptosis, Ras/Raf/MEK/ERK and PI3K/AKT/mTOR signaling cascades.

The high clinical efficacy of the PDT method has been demonstrated in the treatment of patients with CIN and carriers of cervical HPV infection without adverse effects on fertility [32].

The effectiveness of PDT with 5-ALA in the treatment of foci of vaginal intraepithelial neoplasia has been shown. H. Cai et al. [33] evaluated the effectiveness of PDT in 6 women aged 49-54 years with a diagnosis of HPV-induced vaginal intraepithelial neoplasia. Treatment included 4 to 8 procedures. Irradiation was carried out 3 h after the introduction of 5-ALA, the power density was 80 mW/cm^2. In 4 out of 6 women, the result of testing for HPV was negative 3-4 months after the end of PDT. There were no signs of relapse during this follow-up period.

The efficacy and safety of PDT in the treatment of cervix neoplasms have also been substantiated in a number of other studies. Tissue selectivity and high safety of the method compared to traditional methods have contributed to the fact that PDT is increasingly being used as an effective alternative approach to the treatment of HPV-associated CIN and preinvasive cancer, especially in young women planning reproductive function [34, 35].

Several types of PS are currently in use, but it should be noted that there are no clinical trial data comparing the efficacy of these PS in the treatment of CIN or cervical HPV infection.

The high efficiency of PDT with the use of PS based on chlorin e6 in the treatment of women with severe squamous intraepithelial damage to cervical cancer (HSIL) [36, 37]. The advantages of these PS are the selectivity of accumulation in tissues, which leads to mild phototoxicity and a low incidence of side effects. The high rate of distribution of water-soluble PS derivatives of chlorin e6 in tumor tissues makes it possible to shorten the interval between drug administration and irradiation. The action mechanism of these PSs is largely based on the accumulation of the drug in the vascular network that feeds the neoplasm, which justifies the effectiveness of PDT [38].

Resistant persistence of HPV is also due to the presence of the virus in the vaginal mucosa, as a result of which re-infection with cervical cancer is possible [39]. Therefore, the actual problem remains the development of treatment methods that allow to achieve the elimination of the virus from all mucous membranes of the genital tract, to which HPV is tropic. Based on this, it is impossible to carry out the destruction and/or ablation of relatively large areas on the surface of the cervix, vagina and vulva at the same time, given the possibility of infection of these anatomical areas. The advantage of PDT is the possibility of influencing all localizations in order to eradicate HPV.

A systematic review and meta-analysis of 168 randomized clinical trials by M.C. Choi et al. demonstrated the effectiveness of PDT in patients with CIN

grades I, II, and III [40]. According to the pooled data, 82% (804 of 980) of patients achieved primary complete remission at the end of the 3-month follow-up period, which was confirmed by cytological and histological data. None of the patients was pregnant at the time of PDT, 6 women became pregnant within 3 months after the end of treatment and gave birth to full-term healthy babies. These results indicate the effectiveness of the method for the treatment of patients with HPV-associated squamous intraepithelial lesions of cervical cancer without any serious adverse effect on fertility.

In another study [36], 15 patients with CIN were able to become pregnant after PDT treatment. Of these, 6 women gave birth to full-term children, 2 required delivery by caesarean section, 1 patient had a dead fetus, 4 who became pregnant within 3 months after PDT had inevitable miscarriage in the early stages of gestation.

In the study of E.V. Grebenkina et al. [41] the experience of PDT treatment of 12 patients diagnosed with CIN II–III and cancer in situ was described. The chlorin PS photolon was administered intravenously at a dose of 0.75–1.15 mg/kg of body weight, after 1.5–2 hours an irradiation session was performed using a polypositional laser exposure technique (the energy density of laser radiation was 150 J/cm^2, the power density – 400–500 mW/cm^2). 30 days after treatment, cervical conization was performed with endocervical curettage. According to the results of the histological study of postoperative material, the effect of treatment in 4 patients was assessed as complete regression, 7 patients had small CIN I foci, and 1 had CIN II foci. In 8 out of 10 HPV-positive patients, complete eradication of HPV was obtained after treatment. No serious adverse events were reported during the irradiation procedure. The authors concluded that the pronounced therapeutic effect, high antiviral activity, and good tolerability make it possible to consider PDT as an alternative organ-preserving treatment for early cervical cancer and precancer.

In the study [42], the purpose of which was to optimize the parameters of PDT with the PS photoditazine in patients with tumor and precancerous pathology of cervical cancer, 52 patients were included, of which 34 were diagnosed with precancerous cervical disease, 11 with cervical cancer, and 7 with chronic cervicitis. PS in the form of a 0.5% gel was applied to the CM in a volume of 1 ml. The results of the study showed that photoditazine accumulates well in pathological tissues. The maximum accumulation of the drug was noted after 30 min, persisted for about 15 min, then the PS level gradually decreased. It was found that the minimum light dose required to activate photochemical reactions is 100 J/cm^2, while the optimal dose that destroys all atypical cells is 250 J/cm^2.

E. V. Filonenko et al. [43] presented the results of a clinical study of the effectiveness of PDT with radachlorin in 30 patients with precancerous and neoplastic cervical pathology. PS was administered once intravenously by means of a 30-minute infusion at a dose of 1.0 mg/kg of body weight 3 hours before irradiation at a power density of 300–350 J/cm^2. The result of treatment in 26 (86.7%) patients was qualified as a complete regression of the tumor, in 4 (13.3%) – as a partial regression. In groups with a clinical diagnosis of cervical erosion, II st. dysplasia and carcinoma in situ complete regression was observed in all cases. After the first course of PDT in the group of patients with stage III dysplasia, complete regression was achieved in 77%, with a diagnosis of cervical cancer Ia. stage – in 75% of observations. Patients with partial regression of the pathological process 3–6 months after the end of the first course of treatment underwent a second course of PDT, which resulted in complete regression. During treatment and during follow-up, no adverse reactions associated with the use of radachlorin or PDT were recorded. The PDT method using radachlorin showed high efficiency in the treatment of cervical cancer pathology.

M.C. Choi et al. [44] reported the frequency of adverse events during PDT at the level of only 13.6%. Adverse reactions were manifested only by a burning sensation and vaginal discharge from mild to moderate severity.

T.G. Ahn and S.J. Han [45] in cervical cancer 1B1 and 1B2 st. in women of childbearing age who wished to preserve fertility, simultaneous chemo-photodynamic therapy (CPDT) was used. 16 months after the cessation of CPDT, 2 out of 3 patients gave birth to full-term babies by caesarean section. 45 months after 1 patient gave birth to twins by caesarean section. Observation for 60 months revealed no cases of recurrence of the disease.

In general, the currently available information on the effectiveness and safety of PDT, as well as the convenience and ease of use of the method, allow us to consider this medical technology as the most promising direction in the treatment of varying degrees of severity of intraepithelial lesions of the cervix, vulva, and vagina [46].

The effectiveness of PDT in the treatment of patients with CIN depends on the PS chemical structure and the method of its administration. At the same time, the maximum efficiency is achieved with systemic (intravenous) administration of PS, while the use of 5-ALA application forms (solutions, gels and ointments) does not lead to high efficiency in the treatment of CIN. The results of studies by various authors confirm the wide possibilities of using PDT in the treatment of patients with CIN, which is

possible due to the presence of a number of advantages of this method compared to existing standard methods of treatment. The main advantages of PDT include minimal toxicity to surrounding normal tissues due to the selective accumulation of PS in pathological tissues, a low risk of a pronounced pain syndrome, minor systemic effects, the absence of mechanisms of primary and acquired resistance, the possibility of an outpatient treatment session, the possibility of combination with other methods of therapeutic exposure, the absence of limiting cumulative doses of PS and light exposure, the possibility of repeating the procedure many times, good cosmetic results, the possibility of implementing an organ-preserving approach [9, 15, 47].

Conclusion

Due to the fact that CC occupies a leading position among malignant tumors in women aged 15 to 39 years, there is a need for adequate timely treatment of precancerous CC and early invasive CC while maintaining the reproductive capabilities of patients. CC is one of the most successfully treatable forms of cancer when the disease is detected at an early stage. Therefore, the development of effective alternative methods for the treatment of HPV-associated squamous intraepithelial lesions of cervical cancer and preinvasive cervical cancer without compromising the patient's fertility is of high relevance.

An analysis of literature data indicates that the use of PDT contributes to the successful treatment of pathological foci on the cervical mucosa. The effectiveness of the method is ensured by the selectivity of the effect of light radiation on pathologically altered tissue areas in this area. When implementing the method, an impact is carried out that does not cause damage to normal surrounding tissues, rough scarring and stenosis of the cervical canal, thereby PDT allows to save the normal anatomical and functional characteristics of the cervix.

REFERENCES

1. Cohen P. A. et al. Cervical cancer. *Lancet*, 2019, vol. 393, no. 10167, pp. 169–182. doi: org/10.1016/S0140–6736 (18)32470-X
2. Sung H. et al. Global cancer statistics 2020: GLOBOCAN Estimates of Incidence and Mortality Worldwide for 36 Cancers in 185 Countries. *CA Cancer J Clin*, 2021, vol. 71, no. 3, pp. 209–249. doi: 10.3322/caac.21660.
3. https://gco.iarc.fr/
4. https://guidelines.esgo.org/cervical-cancer/guidelines/recommendations/
5. Sayed S. A. et al. Cervical Screening Practices and Outcomes for Young Women in Response to Changed Guidelines in Calgary, Canada, 2007–2016, *J Low Genit Tract Dis*, 2021, vol. 25, no. 1, pp. 1–8. doi: 10.1097/LGT.0000000000000574
6. Lyu Z. et al. Human papillomavirus in semen and the risk for male infertility: A systematic review and meta-analysis, *BMC Infect. Dis*, 2017, vol. 17 (1), pp.714. doi: 10.1186/s12879–017–2812-z
7. Guo W. et al. Recent Developments of Nanoparticles in the Treatment of Photodynamic Therapy for Cervical Cancer, *Anticancer Agents Med Chem*, 2019, vol. 19. No. 15, 1809–1819. doi: 10.2174/1871520619666190411121953
8. Ambreen G. et al. Sensitivity of Papilloma Virus-Associated Cell Lines to Photodynamic Therapy with Curcumin-Loaded Liposomes. *Cancers (Basel)*, 2020, vol. 12, no. 5, pp. 3278. doi: 10.3390/cancers12113278
9. Kaprin A. D., Mardinskiy Yu. S., Smirnov V. P., Ivanov S. A., Kostin A. A., Polikhov S. A., Reshetov I. V., Fatianova A. S., Denisenko M. V., Epatova T. V., Korenev S. V., Tereshchenko A. V., Filonenko E. V., Gafarov M. M., Romanko Yu. S. The history of radiation therapy (part I), *Biomedical Photonics*, 2019, vol. 8, no. 1, pp. 52–62. (in Russian) doi: 10.24931/2413–9432–2019–8–1–52–62
10. Filonenko E. V., Grigoryevykh N. I., Ivanova-Radkevich V. I. Photodynamic therapy for facial skin cancer developed in the zone of previous radiotherapy (clinical case), *Biomedical Photonics*, 2021, vol. 10, no. 2, pp. 42–50 (in Russian). doi: 10.24931/2413–9432–2021–10–2–42–50.

ЛИТЕРАТУРА

1. Cohen P. A. et al. Cervical cancer//Lancet. – 2019. – Vol. 393 (10167). – P. 169–182. doi: org/10.1016/S0140–6736 (18)32470-X
2. Sung H. et al. Global cancer statistics 2020: GLOBOCAN Estimates of Incidence and Mortality Worldwide for 36 Cancers in 185 Countries//C. A. Cancer J. Clin. – 2021. – Vol. 71 (3). – P. 209–249. doi: 10.3322/caac.21660
3. https://gco.iarc.fr/
4. https://guidelines.esgo.org/cervical-cancer/guidelines/recommendations/
5. Sayed S. A. et al. Cervical Screening Practices and Outcomes for Young Women in Response to Changed Guidelines in Calgary, Canada, 2007–2016//J. Low Genit. Tract. Dis. – 2021. – Vol. 25 (10). – P. 1–8. doi: 10.1097/LGT.0000000000000574
6. Lyu Z. et al. Human papillomavirus in semen and the risk for male infertility: A systematic review and meta-analysis//BMC Infect. Dis. – 2017. – Vol. 17 (№ 1). – P. 714. doi: 10.1186/s12879–017–2812-z
7. Guo W. et al. Recent Developments of Nanoparticles in the Treatment of Photodynamic Therapy for Cervical Cancer//Anticancer Agents Med. Chem. – 2019. – Vol. 19 (15). – P. 1809–1819. doi: 10.2174/1871520619666190411121953
8. Ambreen G. et al. Sensitivity of Papilloma Virus-Associated Cell Lines to Photodynamic Therapy with Curcumin-Loaded Liposomes//Cancers (Basel). – 2020. – Vol. 12 (11). – P. 3278. doi: 10.3390/cancers12113278
9. Каприн А. Д., Мардынский Ю. С., Смирнов В. П., Иванов С. А., Костин А. А., Полихов С. А., Решетов И. В., Фатьянова А. С., Денисенко М. В., Эпатова Т. В., Коренев С. В., Терещенко А. В., Филоненко Е. В., Гафаров М. М., Романко Ю. С. К истории развития лучевой терапии (часть I)//Biomedical Photonics. – 2019. – Т. 8, № 1. – С. 52–62. doi: 10.24931/2413–9432–2019–8–1–52–62.
10. Филоненко Е. В., Григорьевых Н. И., Иванова-Радкевич В. И. Фотодинамическая терапия при раке кожи лица, развившегося в зоне предшествующей лучевой терапии (клиническое наблюдение)//Biomedical Photonics. – 2021. –

11. Tumanina A. N., Polezhaev A. A., Apanasevich V. A., Gurina L. I., Volkov M. V., Tarasenko A.Yu., Filonenko E. V. Experience of using photodynamic therapy in the treatment of esophageal cancer, *Biomedical Photonics*, 2019, vol. 8, no. 2, pp. 19–24. (in Russian) doi: 10.24931/2413–9432–2019–8–2–19–24
12. Filonenko E. V., Kaprin A. D., Alekseev B.Ya., Apolikhin O. I., Slovokhodov E. K., Ivanova-Radkevich V. I., Urlova A. N. 5-Aminolevulinic acid in intraoperative photodynamic therapy of bladder cancer (results of multicenter trial), *Photodiagnosis and Photodynamic Therapy,* 2016, vol. 16, pp. 106–109. doi: 10.1016/j.pdpdt.2016.09.009
13. Sokolov V. V., Chissov V. I., Filonenko E. V. et al. First clinical results with a new drug for PDT, *Proceedings of SPIE – The International Society for Optical Engineering*, 1995, vol. 2325, pp. 364–366. doi: 10.1117/12.199168
14. Pikin O., Filonenko E., Mironenko D., Vursol D., Amiraliev A. Fluorescence thoracoscopy in the detection of pleural malignancy, *European Journal of Cardio-Thoracic Surgery,* 2012, vol. 41, no. 3, pp. 649–652. doi: 10.1093/ejcts/ezr086
15. Filonenko E. V. The history of development of fluorescence diagnosis and photodynamic therapy and their capabilities in oncology, *Russian Journal of General Chemistry*, 2015, vol. 85 (1), pp. 211–216. doi: 10.1134/S1070363215010399.
16. Hamblin M. R., Abrahamse H. Factors Affecting Photodynamic Therapy and Anti-Tumor Immune Response, *Anticancer Agents Med Chem*, 2021, vol. 21, no. 2, pp. 123–136. doi: 10.2174/1871520620666200318101037
17. Mironov A. F. et al. Synthesis and Investigation of Photophysical and Biological Properties of Novel S-Containing Bacteriopurpurinimides, *J Med Chem*, 2017, vol. 60, no. 24, pp. 10220–10230. doi: 10.1021/acs.jmedchem.7b00577
18. Abrahamse H., Hamblin M. R. New photosensitizers for photodynamic therapy, *Biochem J*, 2016, vol. 473, no. 4, pp. 347–64. doi: 10.1042/BJ20150942
19. Romanko Yu. S. et al. Efficacy of photodynamic therapy for basal cell carcinoma using photosensitizers of different classes, *Voprosy Onkologi*, 2016, vol. 62, no. 3, pp. 447–450.
20. Yuzhakov V. V. et al. Morphofunctional characteristics of rat sarcoma M-1 after photodynamic therapy with the bacteriochlorophyll a derivative, *Biomedical Photonics*, 2016, vol. 5, no. 4, pp. 4–14.
21. Kessel D. Death Pathways Associated with Photodynamic Therapy, *Photochem Photobiol*, 2021, vol. 97, no. 5, pp. 1101–1103. doi: 10.1111/php.13436
22. Romanko Y. S. et al. Effect of photodynamic therapy with photodithazine on morphofunctional parameters of M-1 sarcoma, *Bull Exp Biol Med*, 2004, vol. 138, no. 6, pp. 584–9. doi: 10.1007/s10517–005–0133–5
23. Romanko Y. S. et al. Relationship between antitumor efficiency of photodynamic therapy with photoditasine and photoenergy density, *Bull Exp Biol Med*, 2005, vol. 139, no. 4, pp. 460–464. doi: 10.1007/s10517–005–0322–2
24. Ermakov A. V. et al. In Vitro Bioeffects of Polyelectrolyte Multilayer Microcapsules Post-Loaded with Water-Soluble Cationic Photosensitizer, *Pharmaceutics,* 2020, vol. 12, no. 7, pp. 610. doi: 10.3390/pharmaceutics12070610
25. Li Z. et al. The mechanism of 5-aminolevulinic acid photodynamic therapy in promoting endoplasmic reticulum stress in the treatment of HR-HPV-infected HeLa cells, *Photodermatol. Photoimmunol. Photomed,* 2021, vol. 37, no. 4, pp. 348–359. doi: 10.1111/phpp.12663
26. Li Z. et al. Dihydroartemisinin administration improves the effectiveness of 5-aminolevulinic acid-mediated photodynamic therapy for the treatment of high-risk human papillomavirus infection, *Photodiagnosis Photodyn. Ther*, 2021, no. 33, pp. 102078. doi: 10.1016/j.pdpdt.2020.102078

T. 10, № 2. – C. 42–50. doi: 10.24931/2413–9432–2021–10–2–42–50
11. Туманина А. Н., Полежаев А. А., Апанасевич В. А., Гурина Л. И., Волков М. В., Тарасенко А. Ю., Филоненко Е. В. Опыт применения фотодинамической терапии в лечении рака пищевода//Biomedical Photonics. – 2019. – Т. 8, № 2. – С. 19–24. doi: 10.24931/2413–9432–2019–8–2–19–24
12. Filonenko E. V., Kaprin A. D., Alekseev B.Ya., Apolikhin O. I., Slovokhodov E. K., Ivanova-Radkevich V. I., Urlova A. N. 5-Aminolevulinic acid in intraoperative photodynamic therapy of bladder cancer (results of multicenter trial)//Photodiagnosis and Photodynamic Therapy. – 2016. – Т. 16. – С. 106–109. doi: 10.1016/j.pdpdt.2016.09.009
13. Sokolov V. V., Chissov V. I., Filonenko E. V., Kozlov D. N., Smirnov V. V. First clinical results with a new drug for PDT//Proceedings of SPIE – The International Society for Optical Engineering. – 1995. – Vol. 2325. – P. 364–366. doi: 10.1117/12.199168
14. Pikin O., Filonenko E., Mironenko D., Vursol D., Amiraliev A. Fluorescence thoracoscopy in the detection of pleural malignancy//European Journal of Cardio-Thoracic Surgery. – 2012. – Т. 41, № 3. – С. 649–652. doi: 10.1093/ejcts/ezr086
15. Filonenko E. V. The history of development of fluorescence diagnosis and photodynamic therapy and their capabilities in oncology//Russian Journal of General Chemistry. – 2015. – Vol. 85 (1). – P. 211–216. doi: 10.1134/S1070363215010399
16. Hamblin M. R., Abrahamse H. Factors Affecting Photodynamic Therapy and Anti-Tumor Immune Response//Anticancer Agents Med. Chem. – 2021. – Vol. 21 (2). – P. 123–136. doi: 10.2174/1871520620666200318101037
17. Mironov A. F. et al. Synthesis and Investigation of Photophysical and Biological Properties of Novel S-Containing Bacteriopurpurinimides//J. Med. Chem. – 2017. – Vol. 60 (24). – P. 10220–10230. doi: 10.1021/acs.jmedchem.7b00577
18. Abrahamse H., Hamblin M. R. New photosensitizers for photodynamic therapy//Biochem. J. – 2016. – Vol. 473 (4). – P. 347–364. doi: 10.1042/BJ20150942
19. Романко Ю. С., Каплан М. А., Иванов С. А. и соавт. Эффективность фотодинамической терапии базально-клеточной карциномы с использованием фотосенсибилизаторов различных классов//Вопросы онкологии. – 2016. – Т. 62 (3). – С. 447–450.
20. Южаков В. В., Бурмистрова Н. В., Фомина Н. К. и соавт. Морфофункциональные характеристики саркомы М-1 крыс после фотодинамической терапии с производным бактериохлорофилла а//Biomedical Photonics. – 2016. – Т. 5 (4). – С. 4–14.
21. Kessel D. Death Pathways Associated with Photodynamic Therapy//Photochem. Photobiol. – 2021. – Vol. 97 (5). – P. 1101–1103. doi: 10.1111/php.13436
22. Романко Ю.С., Цыб А.Ф., Каплан М.А., Попучиев В.В. Влияние фотодинамической терапии с фотодитазином на морфофункциональные характеристики саркомы М-!//Бюллетень экспериментальной биологии и медицины. – 2004. – Т. 138 (12). – С. 658–664.
23. Романко Ю. С., Цыб А. Ф., Каплан М. А., Попучиев В. В. Зависимость противоопухолевой эффективности фотодинамической терапии с фотодитазином от плотности световой энергии//Бюллетень экспериментальной биологии и медицины. – 2005. – Т. 139 (3). – С. 456–461.
24. Ermakov A. V. et al. In Vitro Bioeffects of Polyelectrolyte Multilayer Microcapsules Post-Loaded with Water-Soluble Cationic Photosensitizer//Pharmaceutics. – 2020. – Vol. 12 (7). – P. 610. doi: 10.3390/pharmaceutics12070610
25. Li Z. et al. The mechanism of 5-aminolevulinic acid photodynamic therapy in promoting endoplasmic reticulum stress in the treatment of HR-HPV-infected HeLa cells//Photodermatol. Photoimmunol. Photomed. – 2021. – Vol. 37 (4). – P. 348–359. doi: 10.1111/phpp.12663

27. Ha J.H., Kim Y.J. Photodynamic and Cold Atmospheric Plasma Combination Therapy Using Polymeric Nanoparticles for the Synergistic Treatment of Cervical Cancer, *Int J Mol Sci*, 2021, vol. 23, no. 3, pp. 1172. doi: 10.3390/ijms22031172
28. Pola M. et al. Effects of zinc porphyrin and zinc phthalocyanine derivatives in photodynamic anticancer therapy under different partial pressures of oxygen in vitro, *Invest New Drugs*, 2021, vol. 39, no. 1, pp. 89–97. doi: 10.1007/s10637–020–00990–7
29. Li Z. et al. Mechanism of a new photosensitizer (TBZPy) in the treatment of high-risk human papillomavirus-related diseases, *Photodiagnosis Photodyn Ther*, 2021, pp. 102591. doi: 10.1016/j.pdpdt.2021.102591
30. Park Y.K., Park C.H. Clinical efficacy of photodynamic therapy, *Obstet Gynecol Sci*, 2016, vol. 59, no. 6, pp. 479–488. doi: 10.5468/ogs.2016.59.6.479
31. Xie J. et al. 5-aminolevulinic acid photodynamic therapy reduces HPV viral load via autophagy and apoptosis by modulating Ras/Raf/MEK/ERK and PI3K/AKT pathways in HeLa cells, *J. Photochem. Photobiol. B,* 2019, vol. 194, pp. 46–55. doi: 10.1016/j.jphotobiol.2019.03.012
32. Zhang W. et al. Efficacy and safety of photodynamic therapy for cervical intraepithelial neoplasia and human papilloma virus infection: A systematic review and meta-analysis of randomized clinical trials, *Medicine (Baltimore),* 2018, vol. 97, no. 21, pp. 10864. doi: 10.1097/MD.0000000000010864
33. Cai H. et al. Application of 5-aminolevulinic acid photodynamic therapy for vaginal intraepithelial neoplasia, a report of six cases, *Photodiagnosis Photodyn Ther*, 2020, no. 31, pp. 101837. doi: 10.1016/j.pdpdt.2020.101837
34. Shramova E.I. et al. Near-Infrared Activated Cyanine Dyes As Agents for Photothermal Therapy and Diagnosis of Tumors, *Acta Naturae*, 2020, vol. 12, no. 3, pp. 102–113. doi: 10.32607/actanaturae.11028
35. Inada N.M. et al. Long Term Effectiveness of Photodynamic Therapy for CIN Treatment, *Pharmaceuticals (Basel),* 2019, vol. 12, no. 3, pp. 107. doi: 10.3390/ph12030107
36. Istomin Y.P. et al. Photodynamic therapy of cervical intraepithelial neoplasia grades II and III with Photolon, *Photodiagnosis Photodyn Ther*, 2010, no. 7, pp. 144–151.
37. Li D. et al. Treatment of HPV Infection-Associated Low Grade Cervical Intraepithelial Neoplasia with 5-Aminolevulinic Acid-Mediated Photodynamic Therapy, *Photodiagnosis Photodyn. Ther,* 2020, no. 32, pp.101974. doi: 10.1016/j.pdpdt.2020.101974
38. Gomes A.T.P.C. et al. Synthesis, Characterization and Photodynamic Activity against Bladder Cancer Cells of Novel Triazole-Porphyrin Derivatives, *Molecules*, 2020, vol. 25, no. 7, pp.1607. doi: 10.3390/molecules25071607
39. Hoffman S.R. et al. Patterns of persistent HPV infection after treatment for cervical intraepithelial neoplasia (CIN): A systematic review, *Int. J. Cancer*, 2017, no. 141 (1), pp. 8–23. doi: 10.1002/ijc.30623
40. Choi M.C. et al. Photodynamic therapy for management of cervical intraepithelial neoplasia II and III in young patients and obstetric outcomes, *Lasers Surg. Med*, 2013, no. 45 (9), pp. 564–572. doi: 10.1002/lsm.22187
41. Grebenkina E.V. et al. Photodynamic therapy for cervical lesions. *Photodynamic therapy and photodyagnosis,* 2014, no. 3 (2), pp. 12–14. (In Russ.)
42. Aminodova I.P., Aminodov S.A. Adjustment of treatment parameters for photodynamic therapy of cervical pre-cancer and cancer. *Photodynamic therapy and photodyagnosis*, 2015, no. 4 (2), pp. 17–21. (In Russ.) https://doi.org/10.24931/2413–9432–2015–4-2–17–21
43. Filonenko E.V., Serova L.G., Ivanova-Radkevich V.I. Results from phase III clinical trials with radachlorine for photodynamic

26. Li Z. et al. Dihydroartemisinin administration improves the effectiveness of 5-aminolevulinic acid-mediated photodynamic therapy for the treatment of high-risk human papillomavirus infection//Photodiagnosis Photodyn. Ther.– 2021.– Vol. 33.– P. 102078. doi: 10.1016/j.pdpdt.2020.102078
27. Ha J.H., Kim Y.J. Photodynamic and Cold Atmospheric Plasma Combination Therapy Using Polymeric Nanoparticles for the Synergistic Treatment of Cervical Cancer//Int. J. Mol. Sci.– 2021.– Vol. 22 (3).– P. 1172. doi: 10.3390/ijms22031172
28. Pola M. et al. Effects of zinc porphyrin and zinc phthalocyanine derivatives in photodynamic anticancer therapy under different partial pressures of oxygen in vitro//Invest New Drugs.– 2021.– Vol. 39 (1).– P. 89–97. doi: 10.1007/s10637–020–00990–7
29. Li Z. et al. Mechanism of a new photosensitizer (TBZPy) in the treatment of high-risk human papillomavirus-related diseases//Photodiagnosis Photodyn. Ther.– 2021.– Vol. 17.– P. 102591. doi: 10.1016/j.pdpdt.2021.102591
30. Park Y.K., Park C.H. Clinical efficacy of photodynamic therapy//Obstet. Gynecol. Sci.– 2016.– Vol. 59 (6).– P. 479–488. doi: 10.5468/ogs.2016.59.6.479
31. Xie J. et al. 5-aminolevulinic acid photodynamic therapy reduces HPV viral load via autophagy and apoptosis by modulating Ras/Raf/MEK/ERK and PI3K/AKT pathways in HeLa cells//J. Photochem. Photobiol. B.– 2019.– Vol. 194.– P. 46–55. doi: 10.1016/j.jphotobiol.2019.03.012
32. Zhang W. et al. Efficacy and safety of photodynamic therapy for cervical intraepithelial neoplasia and human papilloma virus infection: A systematic review and meta-analysis of randomized clinical trials//Medicine (Baltimore).– 2018.– Vol. 97 (21).– P. 10864. doi: 10.1097/MD.0000000000010864
33. Cai H. et al. Application of 5-aminolevulinic acid photodynamic therapy for vaginal intraepithelial neoplasia, a report of six cases//Photodiagnosis Photodyn. Ther.– 2020.– Vol. 31.– P. 101837. doi: 10.1016/j.pdpdt.2020.101837
34. Shramova E.I. et al. Near-Infrared Activated Cyanine Dyes As Agents for Photothermal Therapy and Diagnosis of Tumors//Acta Naturae.– 2020.– Vol. 12 (3).– P. 102–113. doi: 10.32607/actanaturae.11028.
35. Inada N.M. et al. Long Term Effectiveness of Photodynamic Therapy for CIN Treatment//Pharmaceuticals (Basel).– 2019.– Vol. 12 (3).– P. 107. doi: 10.3390/ph12030107
36. Istomin Y.P. et al. Photodynamic therapy of cervical intraepithelial neoplasia grades II and III with Photolon//Photodiagnosis Photodyn. Ther.– 2010.– Vol. 7.– P. 144–151.
37. Li D. et al. Treatment of HPV Infection-Associated Low Grade Cervical Intraepithelial Neoplasia with 5-Aminolevulinic Acid-Mediated Photodynamic Therapy//Photodiagnosis Photodyn. Ther.– 2020.– Vol. 32.– P. 101974. doi: 10.1016/j.pdpdt.2020.101974
38. Gomes A.T.P.C. et al. Synthesis, Characterization and Photodynamic Activity against Bladder Cancer Cells of Novel Triazole-Porphyrin Derivatives//Molecules.– 2020.– Vol. 25.– № 7.– P. 1607. doi: 10.3390/molecules25071607
39. Hoffman S.R. et al. Patterns of persistent HPV infection after treatment for cervical intraepithelial neoplasia (CIN): A systematic review//Int. J. Cancer.– 2017.– Vol. 141 (1).– P. 8–23. doi: 10.1002/ijc.30623
40. Choi M.C. et al. Photodynamic therapy for management of cervical intraepithelial neoplasia II and III in young patients and obstetric outcomes//Lasers Surg. Med.– 2013.– Vol. 45 (9).– P. 564–572. doi: 10.1002/lsm.22187
41. Гребёнкина Е.В., Гамаюнов С.В., Кузнецов С.С. и соавт. Фотодинамическая терапия заболеваний шейки матки//Фотодинамическая терапия и фотодиагностика.– 2014.– № 2.– С. 12–14.
42. Аминодова И.П., Аминодов С.А. Оптимизация параметров лечения при фотодинамической терапии предрака и рака шейки матки//Фотодинамическая терапия и фотодиагности-

therapy of pre-cancer and early cancer of cervix. *Biomedical Photonics*, 2015, no. 4 (3), pp. 36–42. (In Russ.) https://doi.org/10.24931/2413–9432–2015–4-3–36–42

44. Choi M. C. et al. Photodynamic therapy for management of cervical intraepithelial neoplasia II and III in young patients and obstetric outcomes, *Lasers Surg. Med*, 2013, no. 45 (9), pp. 564–572. doi: 10.1002/lsm.22187
45. Ahn T. G., Han S. J. The clinical experiences of Concurrent Chemo-Photodynamic Therapy (CCPDT) in the uterine cervical cancer staged 1B1 and 1B2, especially young women desiring fertility, *Photodiagnosis Photodyn. Ther*, 2011, no. 8, pp. 217. doi.org/10.1016/j.pdpdt.2011.03.307
46. Filonenko E. V., Trushina O. I., Novikova E. G., Zarochentseva N. V., Rovinskaya O. V., Ivanova-Radkevich V. I., Kaprin A. D. Photodynamic therapy in the treatment of intraepithelial neoplasia of the cervix, vulva and vagina, *Biomedical Photonics*, 2020, no. 9 (4), pp. 31–39. (In Russ.) https://doi.org/10.24931/2413–9432–2020–9-4–31–39
47. Tzerkovsky D. A., Dunaevskaya V. V. Laser technologies in treatment of cervical intraepithelial neoplasia (review). *Biomedical Photonics*, 2020, no. 9 (3), pp. 30–39. (In Russ.) https://doi.org/10.24931/2413–9432–2020–9-3–30–39

ка. – 2015. – № 2. – С. 17–21. https://doi.org/10.24931/2413–9432–2015–4-2–17–21

43. Филоненко Е. В., Серова Л. Г., Иванова-Радкевич В. И. Результаты III фазы клинических исследований препарата радахлорин для фотодинамической терапии предрака и начального рака райки матки//Biomedical photonics. – 2015. – № 3. – С. 36–42. https://doi.org/10.24931/2413–9432–2015–4-3–36–42
44. Choi M. C. et al. Photodynamic therapy for management of cervical intraepithelial neoplasia II and III in young patients and obstetric outcomes//Lasers Surg. Med. – 2013. – Vol. 45 (9). – P. 564–572. doi: 10.1002/lsm.22187
45. Ahn T. G., Han S. J. The clinical experiences of Concurrent Chemo-Photodynamic Therapy (CCPDT) in the uterine cervical cancer staged 1B1 and 1B2, especially young women desiring fertility//Photodiagnosis Photodyn. Ther. – 2011. – Vol. 8. – P. 217. doi.org/10.1016/j.pdpdt.2011.03.307
46. Филоненко Е. В., Трушина О. И., Новикова Е. Г., Зарочинцева Н. В., Ровинская О. В., Иванова-Радкевич В. И., Каприн А. Д. Фотодинамическая терапия в лечении интраэпителиальных неоплазий шейки матки, вульвы и влагалища//Biomedical Photonics. – 2020. – Т. 9 (4). – С. 31–39. doi: 10.24931/2413–9432–2020–9–4–31–39.
47. Церковский Д. А., Дунаевская В. В. Лазерные технологии в лечении цервикальной интраэпителиальной неоплазии (обзор литературы)//Biomedical Photonics. – 2020. – Т. 9 (3). – С. 30–39. doi: 10.24931/2413–9432–2020–9–3–30–39.

CASE REPORTS

PHOTODYNAMIC THERAPY OF A PATIENT WITH BASAL CELL SKIN CANCER OF THE EAR STAGE T3N0M0 (CLINICAL CASE)

Filonenko E.V.[1], Grigoryevykh N.I.[1], Ivanova-Radkevich V.I.[2]
[1]P.A. Herzen Moscow Oncology Research Center – branch of FSBI NMRRC of the Ministry of Health of the Russian Federation, Moscow, Russia
[2]Peoples' Friendship University of Russia (RUDN University), Moscow, Russia

Abstract

The article presents a clinical observation. The patient, 72 years old, applied to the MNII them. P.A. Herzen with complaints about the presence of an ulcerated tumor of the left ear. After further examination, a diagnosis was made – basal cell carcinoma of the ear skin with spread to the skin of the parotid region T3N0M0. On July 9, 2021, the patient underwent a course of photodynamic therapy (PDT) using a photosensitizer based on chlorin e6 and a diode laser with a wavelength of 662 nm. After one course of PDT, complete regression of the tumor was recorded.

Key words: basal cell skin cancer, photodynamic therapy, photosensitizer, chlorin e6.

For citations: Filonenko E.V., Grigoryevykh N.I., Ivanova-Radkevich V.I. Photodynamic therapy of a patient with basal cell skin cancer of the ear stage T3N0M0 (clinical case), *Biomedical Photonics*, 2021, vol. 10, no. 4, pp. 68–70. doi: 10.24931/2413–9432–2021–10-4-68-70

Contacts: Filonenko E.V., e-mail: derkul23@yandex.ru

ФОТОДИНАМИЧЕСКАЯ ТЕРАПИЯ БОЛЬНОГО БАЗАЛЬНОКЛЕТОЧНЫМ РАКОМ КОЖИ УШНОЙ РАКОВИНЫ СТАДИИ T3N0M0 (КЛИНИЧЕСКОЕ НАБЛЮДЕНИЕ)

Е.В. Филоненко[1], Н.И. Григорьевых[1], В.И. Иванова-Радкевич[2]
[1]«Московский научно-исследовательский онкологический институт им. П.А. Герцена – филиал ФГБУ «Национальный медицинский исследовательский центр радиологии» Министерства здравоохранения Российской Федерации, Москва, Россия
[2]Российский Университет дружбы народов, Москва, Россия

Резюме

В статье представлено клиническое наблюдение. Больной, 72 лет, обратился в МНИОИ им. П.А. Герцена с жалобами на наличие изъязвленной опухоли левого уха. После дообследования поставлен диагноз – базальноклеточный рак кожи уха с распространением на кожу околоушной области T3N0M0. Больному 09.07.2021 был выполнен курс фотодинамической терапии (ФДТ) с использованием фотосенсибилизатора на основе хлорина е6 и диодного лазера с длиной волны 662 нм. После проведения одного курса ФДТ была зарегистрирована полная регрессия опухоли.

Ключевые слова: базальноклеточный рак кожи, фотодинамическая терапия, фотосенсибилизатор, хлорин е6.

Для цитирования: Филоненко Е.В., Григорьевых Н.И, Иванова-Радкевич В.И. Фотодинамическая терапия больного базальноклеточным раком кожи ушной раковины стадии T3N0M0 (клиническое наблюдение) // Biomedical Photonics. – 2021. – Т. 10, № 4. – С. 68–70. doi: 10.24931/2413–9432–2021–10-4-68-70

Контакты: Филоненко Е.В., e-mail: derkul23@yandex.ru

Photodynamic therapy (PDT) in patients with basal cell skin cancer has been successfully used in clinical practice in Russia for several decades [1-4]. In some works, there is still a statement that this method can be effective only in superficial forms of this disease. Many years of experience in the treatment of patients in this category indicates that, with the use of appropriate techniques, PDT is effective not only in superficial forms of basal cell skin cancer, but also in locally advanced tumors. At the P. A. Hertsen Moscow Scientific and Research Oncological Institute effective methods of PDT have been developed that make it possible to remove foci of basal cell skin cancer even with invasive tumor growth into the subcutaneous fat or in the presence of a pronounced exophytic component. We carry out a clinical observation.

Patient P., born in 1949, turned to P. A. Hertsen Moscow Scientific and Research Oncological Institute with complaints of a bleeding ulcer in the region of the left ear. The patient about 10 years ago noted for the first time the appearance of a formation in the form of a "small superficial" wound in the region of the left auricle, he did not go to the doctors, was not treated. Since 2020, the formation began to rapidly increase in size, began to bleed. In May 2021, the patient independently applied to P. A. Hertsen Moscow Scientific and Research Oncological Institute When examined on the skin of the left auricle, there is a tumor infiltration in the

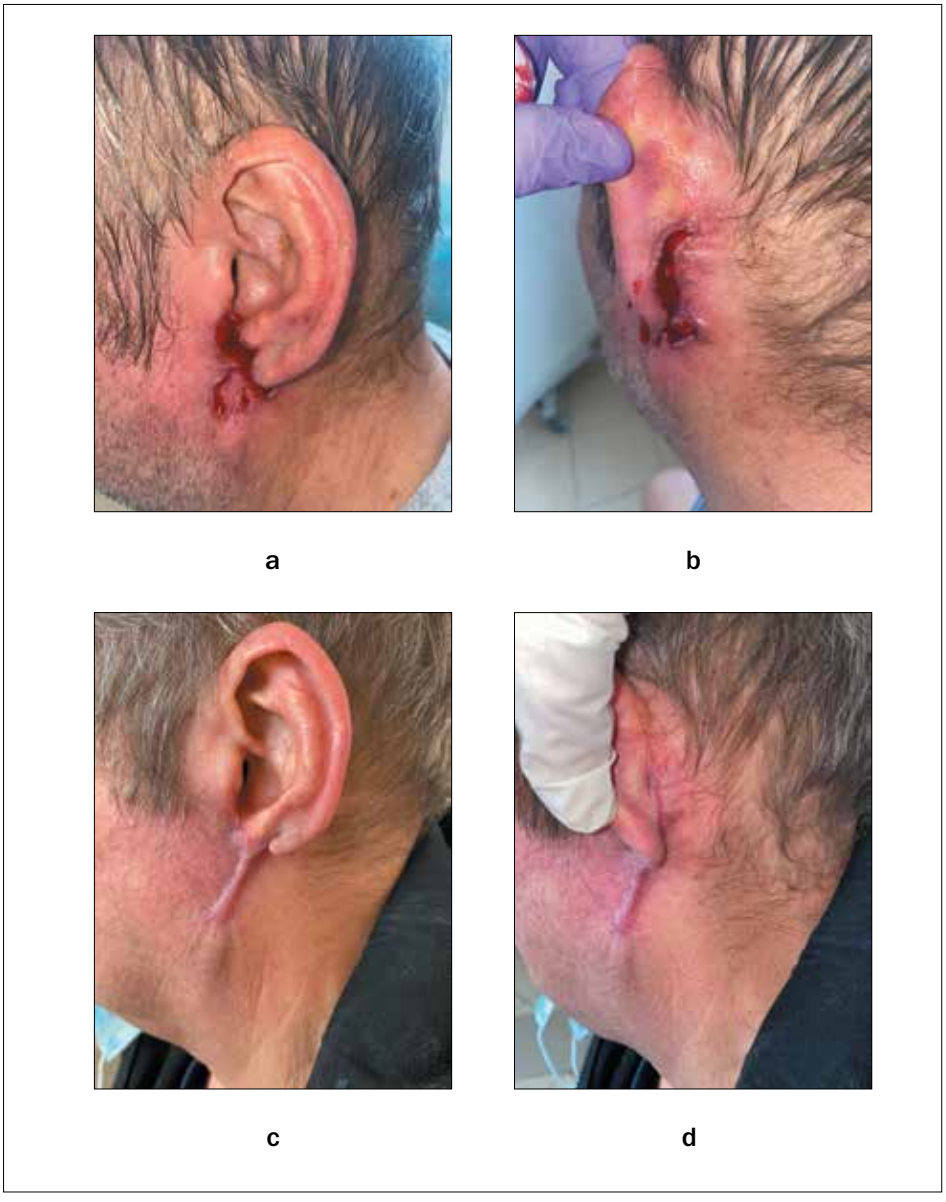

Рис. Базальноклеточный рак кожи левого уха: a, b – опухоль до лечения; c, d – полная регрессия опухоли, контрольный осмотр через 6 мес после ФДТ.
Fig. Basal cell skin cancer of the left ear: a, b – tumor before treatment; c, d – complete regression of the tumor, follow-up examination 6 months after PDT.

region of the lower third of the tragus, intertragus notch, antitragus, earlobe with its partial destruction in the lower part and posterior surface of the ear in the projection of the shell. Tumor infiltration extends to the skin of the parotid region anteriorly (3.1x2.5 cm in size) and posteriorly (4.5x1.5 cm in size). There is ulceration in the area of the tumor. A cytological study was performed, according to which (No. 2717/2021) basal cell carcinoma was diagnosed.

Additional examination is carried out. According to CT scan of the facial area with intravenous contrast: in the parotid region on the left, a zone of skin ulceration is determined, with signs of thickening of the fiber, up to 7 mm deep, anterior-posterior size up to 25 mm, without convincing signs of infiltration into the surrounding structures, the distance to the parotid salivary gland is 3 mm. According to the ultrasound of the left parotid region and regional zones: in the soft tissues of the parotid region on the left, an ulcerous defect with dimensions of 24x32 mm is detected with complete destruction of the dermis and tumor spread into the subcutaneous fat to a depth of 6.4 mm. The edges of the ulcer are undermined. It does not grow into the parotid salivary gland. Along the vessels of the neck, moderately hyperplastic lymph nodes are determined on both sides, in the submandibular region and in the supraclavicular regions – no altered lymph nodes were detected. There are no focal formations and free fluid in the abdominal cavity.

The clinical situation was discussed at an extended consultation. Given the prevalence of the tumor process, the stage of the disease – T3N0M0, the patient was recommended to undergo surgical treatment, which the patient categorically refused, given its volume. As an alternative treatment option, it was decided to perform PDT.

On July 9, 2021, a course of PDT was performed with a photosensitizer based on chlorin e6.

After PDT, the patient came for follow-up examinations in accordance with the terms of observation. 3 months and 6 months after treatment, complete regression of the tumor was registered (Fig.), moderately pronounced cicatricial deformity in the PDT area. The patient remains under strict dynamic supervision.

Conclusion

The above clinical observation demonstrates the effectiveness of the developed original PDT technique even in the case of local prevalence of basal cell skin carcinoma corresponding to T3N0M0. Achieving complete regression in such clinical situations is possible only with strict adherence to the recommended standardized PDT technology. Under these conditions, a high oncological result was obtained with the achievement of complete regression of the tumor, the absence of significant complications and a good cosmetic effect.

REFERENCES

1. Sokolov V.V., Chissov V.I., Filonenko E.V. et al. Photodynamic therapy of cancer with the photosensitizer PHOTOGEM, *Proceedings of SPIE – The International Society for Optical Engineering*, 1995, vol. 2325, pp. 367–374. doi: 10.1117/12.199169
2. Sokolov V.V., Chissov V.I., Yakubovskya R.I. et al. Photodynamic therapy (PDT) of malignant tumors by photosensitzer photosens: results of 45 clinical cases. *Proceedings of SPIE – The International Society for Optical Engineering,* 1996, vol. 2625, pp. 281–287.
3. Sokolov V.V., Chissov V.I., Filonenko E.V. et al. First clinical results with a new drug for PDT, *Proceedings of SPIE – The International Society for Optical Engineering*, 1995, vol. 2325, pp. 364–366. doi: 10.1117/12.199168
4. Filonenko E.V. The history of development of fluorescence diagnosis and photodynamic therapy and their capabilities in oncology, *Russian Journal of General Chemistry*, 2015, vol. 85 (1), pp. 211–216. doi: 10.1134/S1070363215010399

ЛИТЕРАТУРА

1. Sokolov V.V., Chissov V.I., Filonenko E.V., Kozlov D.N., Smirnov V.V. Photodynamic therapy of cancer with the photosensitizer PHOTOGEM//Proceedings of SPIE – The International Society for Optical Engineering. – 1995. – Vol. 2325. – P. 367–374. doi: 10.1117/12.199169
2. Sokolov V.V., Chissov V.I., Yakubovskya R.I., Smirnov V.V., Zhitkova M.B. Photodynamic therapy (PDT) of malignant tumors by photosensitzer photosens: results of 45 clinical cases//Proceedings of SPIE – The International Society for Optical Engineering. – 1996. – Vol. 2625. – P. 281–287.
3. Sokolov V.V., Chissov V.I., Filonenko E.V., Kozlov D.N., Smirnov V.V. First clinical results with a new drug for PDT//Proceedings of SPIE – The International Society for Optical Engineering. – 1995. – Vol. 2325. – P. 364–366. doi: 10.1117/12.199168
4. Filonenko E.V. The history of development of fluorescence diagnosis and photodynamic therapy and their capabilities in oncology//Russian Journal of General Chemistry. – 2015. – Vol. 85 (1). – P. 211–216. doi: 10.1134/S1070363215010399